

Supplementary Information

**Stille Type P–C Coupling Polycondensation towards Phosphorus-
Crosslinked Polythiophenes with P-Regulated Photocatalytic Hydrogen
Evolution**

Zhikai Zhang,^[+,a] Boyang Zhang,^[+,a] Xue Han,^[+,a] Hongyi Chen,^[a] Cece Xue,^[a] Min Peng,^[a] Guijun Ma,^{[a]*} and Yi Ren^{[a]*}

^a School of Physical Science and Technology, ShanghaiTech University, 201210 Shanghai, People's Republic of China

⁺ These authors contributed equally to this work.

Correspondence to: renyi@shanghaitech.edu.cn
magj@shanghaitech.edu.cn

Table of Content

1. Materials and methods.....	2
2. Preparation of substrates	4
3. Reaction condition optimization	11
4. Substrate scopes of P-C coupling reactions	12
5. Theoretical calculation	20
6. Solid state NMR (ssNMR) characterization of polymers.....	21
7. Fourier transform infrared (FT-IR) spectra of polymers	23
8. XPS data of polymers.....	26
9. Mott–Schottky measurements	29
10. Thermogravimetric analysis (TGA) of polymers	30
11. Contact angle measurements	31
12. NMR spectra.....	32
13. References	67

1. Materials and methods

All reagents were purchased from Shanghai Titan Scientific Co. Ltd. (Adamas-beta[®] reagents), Energy Chemical Co. Ltd., Bide Pharmatech Ltd., TCI (Shanghai) Development Co. Ltd. Chloroform-*d* was purchased from J&K Scientific Co. Ltd. Solvents were further purified by standard methods recorded in Purification of Laboratory Chemicals.^{S1} Trichlorophosphane is used after re-distilling under moisture- and oxygen-free conditions. Except specially instructed above, all reagents are used as-received. All reactions and manipulations involving moisture- or oxygen-sensitive compounds were performed using standard Schlenk techniques under dry nitrogen atmosphere or in a nitrogen atmosphere glovebox with O₂<0.5 ppm and H₂O<0.02 ppm.

Solution-state nuclear magnetic resonance (NMR) spectroscopy: ¹H-NMR, ¹³C{¹H}-NMR, ³¹P{¹H}-NMR and ¹⁹F{¹H}-NMR were recorded on Bruker AVANCE NEO 400 or AVANCE III HD 500 MHz spectrometers at 25 °C. Tetramethylsilane (TMS) or the peaks of solvents in the deuterated reagent were used as internal standards for ¹H-NMR and ¹³C-NMR spectra. 85% phosphoric acid was used as external standard for ³¹P-NMR. Quantitative ³¹P{¹H}-NMR spectra were recorded by a zgig pulse sequence with a recycle delay of 10 s. Triphenylphosphine oxide (O=PPh₃, 0.02783 g, 0.1 mmol) was added to serve as an internal standard and about 1 mg Cr(acac)₃ was added to serve as a relaxation reagent to ensure all excited nucleus relaxed completely.

Solid-state nuclear magnetic resonance (ssNMR) spectroscopy: All ssNMR experiments were performed on a Bruker wide-bore 9.4 T ($\nu_0(^1\text{H})=400$ MHz) NMR spectrometer equipped with a Bruker Avance III HD console and a Bruker 3.2 broadband HX MAS probe. All samples were prepared for NMR measurement by packing into a 3.2 mm Bruker zirconia rotor with Kel-F turbine caps in a nitrogen atmosphere glovebox (O₂<0.5 ppm and H₂O<0.02 ppm). Magic angle spinning (MAS) was used to collect high-resolution NMR spectra at 15 kHz spinning rate for all experiments. The ¹H-¹³C cross-polarization (CP) experiment was used in all ¹³C NMR experiment. An initial ¹H $\pi/2$ excitation pulse of 3.12 μs , a Hartmann-Hahn contact period of 5 ms and a recycle delay of 2 s were used throughout. All ¹³C chemical shifts were referenced to the primary reference of TMS via the secondary reference of solid adamantane at 29.9 ppm. For ³¹P NMR experiments, a high-power decoupling (HPDEC) experiment was used employing a ³¹P $\pi/2$ excitation pulse of 2.27 μs and a recycle delay of 10 s. All ³¹P chemical shifts are referenced to ammonium dihydrogen phosphate (ADP) solid at 0.81 ppm. ¹⁹F NMR spectra were acquired using a single-pulse experiment, and ¹⁹F chemical shifts are referenced to trifluoroacetic acid at 76.2 ppm. All spectra were analyzed or simulated using the Bruker Topspin 4.1.1 software.

Fourier transform infrared (FT-IR) spectroscopy: The FT-IR spectra were recorded on the Perkin Elmer Spectrum Frontier with attenuated total reflection (ATR) accessories.

X-ray photoelectron spectroscopy (XPS) measurements were carried out on a Thermo Fisher Scientific ESCALAB 250Xi spectrometer. Samples were loaded into alumina crucibles in a glovebox (O₂<0.5 ppm and H₂O<0.02 ppm) and transferred using a portable sample transfer chamber. Data was analyzed using Advantage software.

Thermogravimetric analysis (TGA): The TGA were carried out on a Perkin Elmer TGA 4000 under 100 mL/min N₂ flow, ramping at 10 °C/min from 30 °C to 800 °C. Ultrahigh-purity-grade N₂ was used for TGA measurements.

UV-Vis diffuse reflectance spectroscopy (DRS) spectra were acquired using an Agilent Cary 5000

UV-Vis-NIR spectrometer with an integrating sphere annex. Samples were measured in solid state.

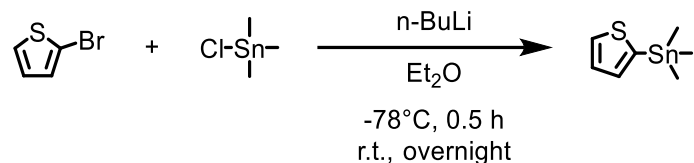
Mott-Schottky curves were obtained using a Zahner electrochemical workstation in a three-electrode system. A Pt plate and an Ag/AgCl electrode (saturated KCl) were used as a counter and reference electrode, respectively. 0.2 M Na₂SO₄ solution (pH = 6.8) was chosen as electrolyte, which was purged with Ar flow for 30 min before testing. The working electrode was prepared by dropcasting method. Typically, 3 mg sample powder was dispersed in *i*-PrOH and dropped on a clean FTO glass (1 mg/cm²) as a work electrode. Mott-Schottky curves were obtained under dark condition at a frequency of 1 kHz, 5 kHz and 10 kHz with an AC amplitude of 5 mV. The evaluated flat-band potential (E_{fb}) was regarded as Fermi level (EF) of the semiconductor sample.

Static water contact angles were measured with the sessile drop method using a drop-shape analysis apparatus at room temperature on a KRÜSS DSA25 instrument. The samples were measured using pressed pellets. The contact angles were fitted by an ellipse fitting method.

The photocatalytic hydrogen production experiments were carried out in a Pyrex vessel connected to a closed glass circulation system (Beijing Perfectlight, Labsolar-6A) under top irradiation from a 300 W Xe lamp (R300-3J) equipped with a chilled mirror and a cut-off filter (HOYA L-42, $\lambda > 420$ nm). For a typical trial, 20 mg catalyst was ultrasonicated to be well dispersed in 100 mL 0.1 M ascorbic acid aqueous solution. 2 wt % Pt was photo-deposited as co-catalyst from H₂PtCl₆ solution. The system was evacuated several times to completely remove the air at first and then appropriate amount of Ar gas was introduced into system, keeping the background pressure at 5 kPa. The temperature of reaction suspension was maintained at 288 K by circulated cooling water. The amounts of evolved gases were measured by an on-line gas chromatograph (SHIMADZU, GC-2014C with a TCD detector, JN. 5Å columns and Ar carrier gas).

2. Preparation of substrates

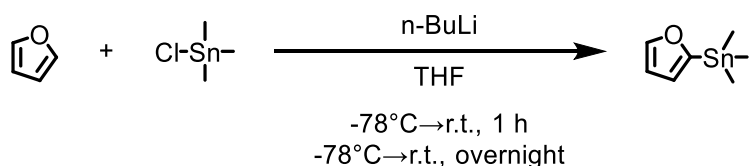
2.1. Trimethyl(thiophen-2-yl)stannane



Scheme S1. Synthesis of trimethyl(thiophen-2-yl)stannane.

Trimethyl(thiophen-2-yl)stannane was synthesized according to the previously reported literature^{S2} with slight modification. To a solution of 2-bromothiophene (8.67 g, 53.1 mmol) in Et₂O (140 mL) was added n-butyllithium (1.6 M in hexane, 36.5 mL, 58.5 mmol) dropwise at -78 °C. After the resulting mixture was stirred at -78 °C for 0.5 h, chlorotrimethylstannane (12.71 g, 63.8 mmol) dissolved in Et₂O (10 mL) was slowly added to the reaction at -78 °C. The resulting solution was slowly warmed to room temperature and stirred overnight. The mixture was washed with water and extracted with DCM. The organic layer was dried with Na₂SO₄. The organic solvent was removed under vacuum. Distillation under reduced pressure gave a colorless liquid (10.81 g, 82 % yield). ¹H NMR (400 MHz, CDCl₃) δ 7.66 (d, *J* = 4.4 Hz, 1H), 7.26 (dd, *J* = 3.3, 4.5 Hz, 1H), 7.23 (dd, *J* = 0.8, 3.3 Hz, 1H), 0.38 (s, 9H) ppm. ¹³C{¹H} NMR (101 MHz, CDCl₃) δ 137.3, 135.1, 130.9, 128.1, -8.1 ppm.

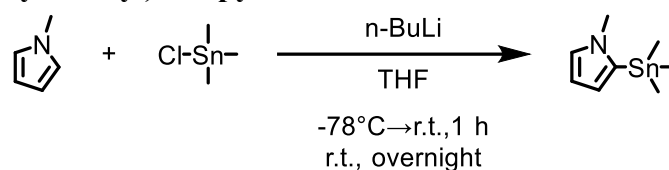
2.2. Furan-2-yltrimethylstannane



Scheme S2. Synthesis of furan-2-yltrimethylstannane.

Furan-2-yltrimethylstannane was synthesized according to the previously reported literature^{S3} with slight modification. To a solution of furan (1.934 g, 28.4 mmol) in THF (60 mL) was added n-butyllithium (1.6 M in hexane, 18.7 mL, 18.7 mmol) dropwise at -78 °C. After the resulting mixture was stirred at -78 °C for 0.5 h, the mixture was slowly warmed to room temperature for another 1 h. Then chlorotrimethylstannane (6.23 g, 31.3 mmol) dissolved in THF (10 mL) was slowly added to the reaction at -78 °C. The resulting solution was slowly warmed to room temperature and stirred overnight. The mixture was washed with water and extracted with DCM. The organic layer was dried with Na₂SO₄. The organic solvent was removed under vacuum. Distillation under reduced pressure gave a colorless liquid (4.92 g, 75 % yield). ¹H NMR (400 MHz, CDCl₃) δ 7.72 (d, *J* = 1.7 Hz, 1H), 6.58 (t, *J* = 3.2 Hz, 1H), 6.42 (dd, *J* = 1.7, 3.1 Hz, 1H), 0.33 (s, 9H). ¹³C{¹H} NMR (101 MHz, CDCl₃) δ 160.7, 147.1, 120.8, 109.3, 109.2, 77.5, 77.2, 76.8, -9.1 ppm.

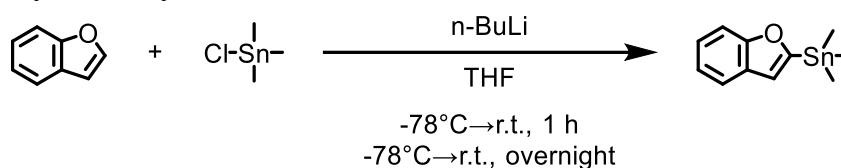
2.3. 1-methyl-2-(trimethylstannyl)-1H-pyrrole



Scheme S3. Synthesis of 1-methyl-2-(trimethylstannyl)-1H-pyrrole.

1-methyl-2-(trimethylstannyl)-1H-pyrrole was synthesized according to the previously reported literature^{S4} with slight modification. To a solution of 1-methyl-1H-pyrrole (0.92 g, 11.4 mmol) in THF (50 mL) was added n-butyllithium (1.6 M in hexane, 7.5 mL, 11.9 mmol) dropwise at -78°C. After the resulting mixture was warmed up to room temperature for an hour and placed into -78°C again. Then chlorotrimethylstannane (2.49 g, 12.5 mmol) dissolved in THF (10 mL) was slowly added. Then the solution was warmed slowly to room temperature and stirred overnight. The mixture was washed with water and extracted with DCM. After that the organic layer was dried with Na₂SO₄. The solution was filtered, and the solvent was removed under vacuum. Distillation under reduced pressure gave a colorless liquid (1.07 g, 39 % yield). ¹H NMR (400 MHz, CDCl₃) δ 6.86 (t, *J* = 1.6 Hz, 1H), 6.29 (dd, *J* = 1.5, 3.3 Hz, 1H), 6.23 (t, *J* = 3.2 Hz, 1H), 3.71 (s, 3H), 0.32 (s, 9H) ppm. ¹³C{¹H} NMR (101 MHz, CDCl₃) δ 132.8, 126.0, 119.0, 108.7, 38.0, -8.6 ppm.

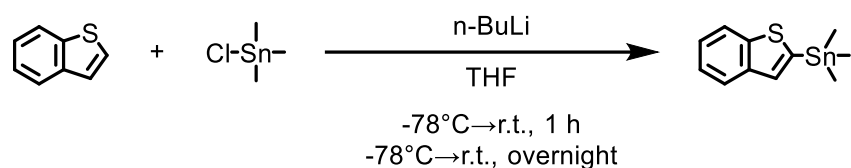
2.4. Benzofuran-2-yltrimethylstannane



Scheme S4. Synthesis of benzofuran-2-yltrimethylstannane.

Benzofuran-2-yltrimethylstannane was synthesized according to the previously reported literature^{S5} with slight modification. To a solution of benzofuran (1.06 g, 9.0 mmol) in THF (50 mL) was added n-butyllithium (1.6 M in hexane, 6.2 mL, 9.9 mmol) dropwise at -78°C. After the resulting mixture was warmed up to room temperature for an hour and placed into -78°C again. Then chlorotrimethylstannane (2.2 g, 10.8 mmol) dissolved in THF (15 mL) was slowly added. Then the solution was warmed slowly to room temperature and stirred overnight. The mixture was washed with water and extracted with DCM. After that the organic layer was dried with Na₂SO₄. The solution was filtered, and the solvent was removed under vacuum. Distillation under reduced pressure gave a colorless liquid (2.9 g, 91 % yield). ¹H NMR (400 MHz, CDCl₃) δ 7.56 (dd, *J* = 0.9, 7.5 Hz, 1H), 7.50 (dd, *J* = 1.1, 8.0 Hz, 1H), 7.23 (td, *J* = 1.4, 8.1 Hz, 1H), 7.19 (td, *J* = 1.2, 7.3 Hz, 1H), 6.93 (d, *J* = 0.7 Hz, 1H), 0.41 (s, 9H) ppm. ¹³C{¹H} NMR (101 MHz, CDCl₃) δ 165.2, 158.7, 128.1, 123.7, 122.3, 120.5, 117.7, 111.1, -9.1 ppm.

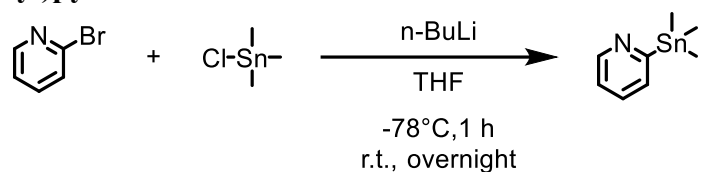
2.5. Benzo[b]thiophen-2-yltrimethylstannane



Scheme S5. Synthesis of benzo[b]thiophen-2-yltrimethylstannane.

Benzo[b]thiophen-2-yltrimethylstannane was synthesized according to the previously reported literature^{S6} with slight modification. To a solution of benzo[b]thiophene (1.94 g, 14.5 mmol) in THF (60 mL) was added n-butyllithium (1.6 M in hexane, 10.0 mL, 16.0 mmol) dropwise at -78 °C. After the resulting mixture was warmed up to room temperature for an hour and placed into -78 °C again. Then chlorotrimethylstannane (3.47 g, 17.4 mmol) dissolved in THF (15 mL) was slowly added. Then the solution was warmed slowly to room temperature and stirred overnight. The mixture was washed with water and extracted with DCM. After that the organic layer was dried with Na₂SO₄. The solution was filtered, and the solvent was removed in vacuo, leaving a yellow liquid. Distillation under reduced pressure gave a colorless liquid (4.09 g, 95 % yield). ¹H NMR (400 MHz, CDCl₃) δ 7.90 (d, *J* = 8.3 Hz, 1H), 7.82 (d, *J* = 8.1 Hz, 1H), 7.44 (s, 1H), 7.34 (ddd, *J* = 1.3, 7.1, 7.9 Hz, 1H), 7.29 (ddd, *J* = 1.4, 7.1, 8.3 Hz, 1H), 0.44 (s, 9H) ppm. ¹³C{¹H} NMR (101 MHz, CDCl₃) δ 144.3, 141.1, 140.5, 132.03, 124.0, 123.7, 122.9, 122.1, -8.2 ppm.

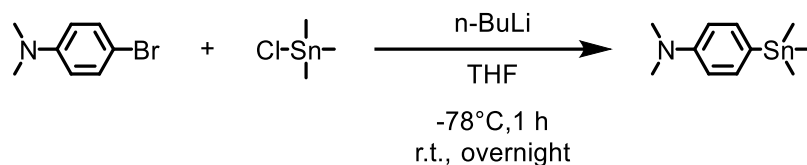
2.6. 2-(trimethylstannyl)pyridine



Scheme S6. Synthesis of 2-(trimethylstannyl)pyridine.

2-(trimethylstannyl)pyridine was synthesized according to the previously reported literature^{S6} with slight modification. To a solution of 2-bromopyridine (0.99 g, 6.3 mmol) in THF (50 mL) was added n-butyllithium (1.6 M in hexane, 4.15 mL, 6.64 mmol) dropwise at -78 °C. After the resulting mixture had been stirred for 1 h at -78 °C, chlorotrimethylstannane (1.39 g, 7.0 mmol) dissolved in THF (10 mL) was slowly added. Then the solution was warmed slowly to room temperature and stirred overnight. The mixture was washed with water and extracted with DCM. After that the organic layer was dried with Na₂SO₄. The solution was filtered, and the organic solvent was removed under vacuum. Distillation under reduced pressure gave a colorless liquid (1.26 g, 83 % yield). ¹H NMR (400 MHz, CDCl₃) δ 8.74 (ddd, *J* = 1.1, 1.9, 5.0 Hz, 1H), 7.52 (td, *J* = 1.8, 7.5 Hz, 1H), 7.45 (dt, *J* = 1.4, 7.5 Hz, 1H), 7.14 (ddd, *J* = 1.5, 4.9, 7.5 Hz, 1H), 0.34 (s, 9H) ppm. ¹³C{¹H} NMR (101 MHz, CDCl₃) δ 173.7, 150.7, 133.7, 131.8, 122.5, -9.3 ppm.

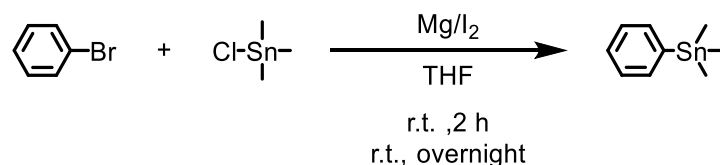
2.7. N,N-dimethyl-4-(trimethylstannyl)aniline



Scheme S7. Synthesis of N,N-dimethyl-4-(trimethylstannyl)aniline.

N,N-dimethyl-4-(trimethylstannyl)aniline was synthesized according to the previously reported literature with slight modification. To a solution of 4-bromo-N,N-dimethylaniline (0.50 g, 2.5 mmol) in THF (30 mL) was added n-butyllithium (1.6 M in hexane, 1.65 mL, 2.6 mmol) dropwise at -78 °C. After the resulting mixture had been stirred for 1 h at -78 °C, chlorotrimethylstannane (0.5480 g, 2.75 mmol) dissolved in THF (10 mL) was slowly added. Then the solution was warmed slowly to room temperature and stirred overnight. The mixture was washed with water and extracted with DCM. After that the organic layer was dried with Na₂SO₄. The solution was filtered, and the organic solvent was removed under vacuum. Distillation under reduced pressure gave a colorless liquid (0.57 g, 81 % yield). ¹H NMR (400 MHz, CDCl₃) δ 7.36 (d, *J* = 8.5 Hz, 2H), 6.76 (d, *J* = 8.5 Hz, 2H), 2.94 (s, 6H), 0.24 (s, 9H) ppm. ¹³C{¹H} NMR (101 MHz, CDCl₃) δ 150.9, 136.7, 127.0, 112.9, 40.5, -9.4 ppm.

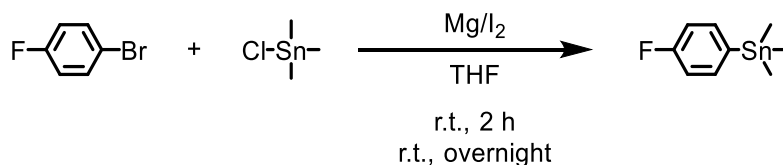
2.8. Trimethyl(phenyl)stannane



Scheme S8. Synthesis of trimethyl(phenyl)stannane.

Trimethyl(phenyl)stannane was synthesized according to the previously reported literature^{S7} with slight modification. Bromobenzene (3.11 g, 20 mmol) was added dropwise to magnesium metal (0.53 g, 22 mmol) in dry THF (5 mL), initiated by a grain of iodine. After vigorously stirred at room temperature for 2 h, chlorotrimethylstannane (4.34 g, 22 mmol) dissolved in THF (10 mL) was slowly added and stirred overnight. Then the mixture was treated with saturated NH₄Cl and extracted with DCM. After that the organic layer was dried with Na₂SO₄, the solution was filtered, and the solvent was removed in vacuo. Distillation under reduced pressure gave a colorless liquid (4.38 g, 76 % yield). ¹H NMR (400 MHz, CDCl₃) δ 7.50 (dd, *J* = 1.9, 7.4 Hz, 2H), 7.38 – 7.29 (m, 3H), 0.29 (s, 9H) ppm. ¹³C{¹H} NMR (101 MHz, CDCl₃) δ 142.5, 136.0, 128.4, 128.2, -9.5 ppm.

2.9. (4-fluorophenyl)trimethylstannane

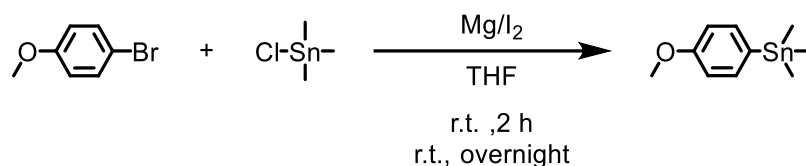


Scheme S9. Synthesis of (4-fluorophenyl)trimethylstannane.

(4-fluorophenyl)trimethylstannane was synthesized according to the previously reported literature^{S8} with slight modification. 1-bromo-4-fluorobenzene (1.65 mL, 15 mmol) was added

dropwise to magnesium metal (0.40 g, 16.5 mmol) in dry THF (5 mL), initiated by a grain of iodine. After vigorously stirred at room temperature for 2 h, chlorotrimethylstannane (3.29 g, 16.5 mmol) dissolved in THF (10 mL) was slowly added and stirred overnight. Then the mixture was treated with saturated NH₄Cl and extracted with DCM. After that the organic layer was dried with Na₂SO₄, the solution was filtered, and the solvent was removed in vacuo. Distillation under reduced pressure gave a colorless liquid (2.37 g, 61 % yield). ¹H NMR (400 MHz, CDCl₃) δ 7.44 (dd, *J* = 6.4, 8.3 Hz, 2H), 7.05 (dd, *J* = 8.4, 9.6 Hz, 2H), 0.29 (s, 9H). ¹³C{¹H} NMR (101 MHz, CDCl₃) δ 163.5 (d, *J* = 246.5 Hz), 137.4 (d, *J* = 6.6 Hz), 137.3, 115.3 (d, *J* = 19.1 Hz), -9.3 ppm. ¹⁹F{¹H} NMR (376 MHz, CDCl₃) δ -113.3 ppm.

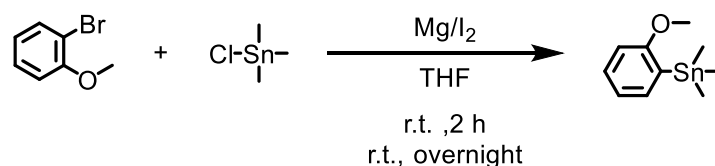
2.10. (4-methoxyphenyl)trimethylstannane



Scheme S10. Synthesis of (4-methoxyphenyl)trimethylstannane.

(4-methoxyphenyl)trimethylstannane was synthesized according to the previously reported literature^{S7} with slight modification. 1-bromo-4-methoxybenzene (1.25 mL, 10 mmol) was added dropwise to magnesium metal (2.19 g, 11 mmol) in dry THF (5 mL), initiated by a grain of iodine. After vigorously stirred at room temperature for 2 h, chlorotrimethylstannane (2.19 g, 11 mmol) dissolved in THF (10 mL) was slowly added and stirred overnight. Then the mixture was treated with saturated NH₄Cl and extracted with DCM. After that the organic layer was dried with Na₂SO₄, the solution was filtered, and the solvent was removed in vacuo. Distillation under reduced pressure gave a colorless liquid (2.32 g, 86 % yield). ¹H NMR (400 MHz, CDCl₃) δ 7.41 (d, *J* = 8.6 Hz, 2H), 6.93 (d, *J* = 8.5 Hz, 1H), 3.81 (s, 3H), 0.27 (s, 9H) ppm. ¹³C{¹H} NMR (101 MHz, CDCl₃) δ 160.1, 137.3, 137.0, 136.8, 132.6, 114.4, 114.2, 113.9, 55.2, -9.4 ppm.

2.11. (2-methoxyphenyl)trimethylstannane

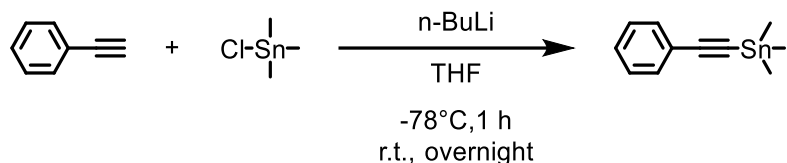


Scheme S11. Synthesis of (2-methoxyphenyl)trimethylstannane.

(2-methoxyphenyl)trimethylstannane was synthesized according to the previously reported literature^{S9} with slight modification. 1-bromo-2-methoxybenzene (1.87 mL, 15 mmol) was added dropwise to magnesium metal (0.40 g, 16.5 mmol) in dry THF (5 mL), initiated by a grain of iodine. After vigorously stirred at room temperature for 2 h, chlorotrimethylstannane (3.29 g, 16.5 mmol) dissolved in THF (10 mL) was slowly added and stirred overnight. Then the mixture was treated with saturated NH₄Cl and extracted with DCM. After that the organic layer was dried with Na₂SO₄, the solution was filtered, and the solvent was removed in vacuo. Distillation under reduced pressure gave a colorless liquid (3.37 g, 83 % yield). ¹H NMR (400 MHz, CDCl₃) δ 7.38 (dd, *J* = 1.8, 7.0 Hz, 1H),

7.32 (ddd, $J = 1.8, 7.4, 8.3$ Hz, 1H), 6.98 (td, $J = 0.9, 7.2$ Hz, 1H), 6.83 (d, $J = 8.4$ Hz, 1H), 3.79 (s, 3H), 0.26 (s, 9H) ppm. $^{13}\text{C}\{^1\text{H}\}$ NMR (101 MHz, CDCl_3) δ 164.0, 136.5, 130.4, 130.2, 121.1, 109.4, 55.5, -9.1 ppm.

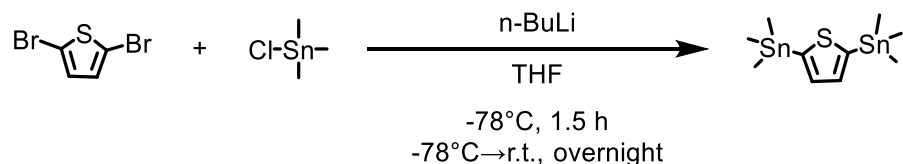
2.12. Trimethyl(phenylethynyl)stannane



Scheme S12. Synthesis of trimethyl(phenylethynyl)stannane.

Trimethyl(phenylethynyl)stannane was synthesized according to the previously reported literature^{S10} with slight modification. To a solution of ethynylbenzene (1.02 g, 10 mmol) in THF (25 mL) was added n-butyllithium (1.6 M in hexane, 10.5 mL, 6.6 mmol) dropwise at -78°C . After the resulting mixture was stirred at -78°C for 1 h, chlorotrimethylstannane (2.19 g, 11 mmol) dissolved in THF (5 mL) was slowly added to the reaction at -78°C . The resulting solution was slowly warmed to room temperature and stirred overnight. The mixture was washed with water and extracted with DCM. The organic layer was dried with Na_2SO_4 . The organic solvent was removed under vacuum. Distillation under reduced pressure to give a colorless liquid (2.13 g, 80 % yield). ^1H NMR (400 MHz, CDCl_3) δ 7.50 – 7.41 (m, 2H), 7.33 – 7.26 (m, 3H), 0.36 (s, 9H) ppm. $^{13}\text{C}\{^1\text{H}\}$ NMR (101 MHz, CDCl_3) δ 132.1, 128.3, 128.2, 123.7, 109.1, 93.5, -7.5 ppm.

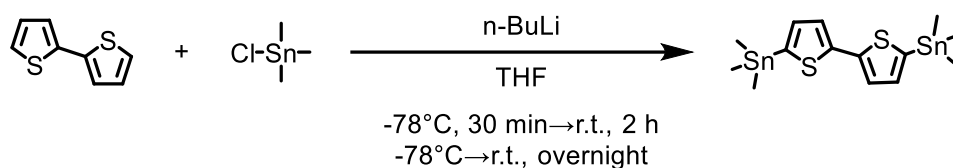
2.13. 2,5-bis(trimethylstannyl)thiophene (B1)



Scheme S13. Synthesis of **B1**.

2,5-bis(trimethylstannyl)thiophene (**B1**) was synthesized according to the previously reported literature^{S11} with slight modification. To a solution of 2,5-dibromothiophene (3.98 g, 16.4 mmol) in THF (120 mL) was added n-butyllithium (1.6 M in hexane, 21.6 mL, 34.6 mmol) dropwise at -78°C . After the resulting mixture was stirred at -78°C for 1.5 h. Then chlorotrimethylstannane (7.26 g, 36.43 mmol) dissolved in THF (10 mL) was slowly added to the reaction at -78°C . The resulting solution was slowly warmed to room temperature and stirred overnight. The mixture was poured into water and extracted with DCM. The organic layer was dried with Na_2SO_4 . The organic solvent was removed under vacuum. The crude product was further washed by large amount of water to provide pale-white solid (6.30 g, 93 % yield). ^1H NMR (400 MHz, CDCl_3) δ 7.38 (s, 2H), 0.37 (s, 18H) ppm. ^{13}C NMR (101 MHz, CDCl_3) δ 143.2, 136.0, -8.0 ppm.

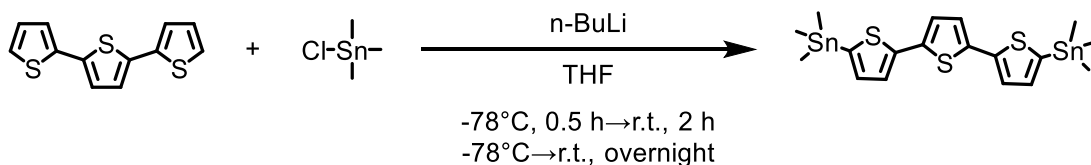
2.14. 5,5'-bis(trimethylstannyl)-2,2'-bithiophene (**B2**)



Scheme S14. Synthesis **B2**.

5,5'-bis(trimethylstannyl)-2,2'-bithiophene (**B2**) was synthesized according to the previously reported literature^{S11} with slight modification. To a solution of 2,2'-bithiophene (2.49 g, 15 mmol) in THF (60 mL) was added n-butyllithium (1.6 M in hexane, 21.5 mL, 34.5 mmol) dropwise at -78 °C. After the resulting mixture was stirred at -78 °C for 0.5 h, the mixture was slowly warmed to room temperature for another 2 h. Then chlorotrimethylstannane (7.47 g, 37.5 mmol) dissolved in THF (10 mL) was slowly added to the reaction at -78 °C. The resulting solution was slowly warmed to room temperature and stirred overnight. The mixture was washed with water and extracted with DCM. The organic layer was dried with Na₂SO₄. The organic solvent was removed under vacuum. The crude product was further washed by large amount of water to provide white solid. (6.99 g, 95 % yield). ¹H NMR (400 MHz, CDCl₃) δ 7.27 (d, *J* = 3.3 Hz, 2H), 7.08 (d, *J* = 3.4 Hz, 2H), 0.38 (s, 18H) ppm. ¹³C {¹H} NMR (101 MHz, CDCl₃) δ 143.2, 137.2, 136.0, 125.0, -8.1 ppm.

2.15. 5,5''-bis(trimethylstannyl)-2,2':5',2''-terthiophene (**B3**)



Scheme S15. Synthesis of **B3**.

5,5''-bis(trimethylstannyl)-2,2':5',2''-terthiophene (**B3**) was synthesized according to the previously reported literature^{S12} with slight modification. To a solution of 2,2':5',2''-terthiophene (2.48 g, 10 mmol) in THF (80 mL) was added n-butyllithium (1.6 M in hexane, 15.6 mL, 25 mmol) dropwise at -78 °C. After 0.5 h, the resulting mixture was warmed up to room temperature for 2 h. Then chlorotrimethylstannane (5.98 g, 30 mmol) dissolved in THF (20 mL) was slowly added. Then the solution was slowly warmed to room temperature and stirred overnight. The mixture was washed with water and extracted with DCM. After that the organic layer was dried with Na₂SO₄. The solution was filtered, and the solvent was removed under vacuum. The crude product was further washed by methanol to provide light yellow solid. (5.08 g, 88 % yield). ¹H NMR (400 MHz, CDCl₃) δ 7.27 (d, 2H), 7.09 (d, *J* = 3.4 Hz, 2H), 7.06 (s, 2H), 0.39 (s, 18H) ppm. ¹³C {¹H} NMR (101 MHz, CDCl₃) δ 142.9, 137.7, 136.2, 136.1, 124.9, 124.3, -8.1 ppm.

3. Reaction condition optimization

General procedure for reaction condition optimization:

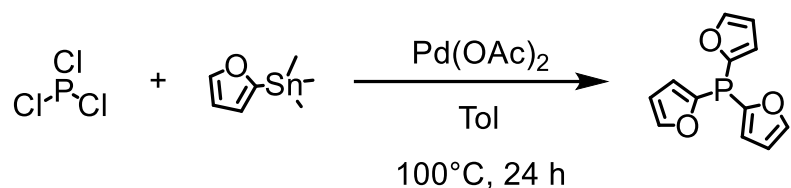
0.5 mL toluene (Tol) was added to a 20 mL oven-dried Schlenk tube to dissolve catalyst (0.025 mmol, 5 mol%). Then trichlorophosphane (0.44 mL 10 times diluted in Tol, 0.5 mmol, 1 eqv.) was added. Then trimethyl(thiophen-2-yl)stannane (0.463 g, 1.875 mmol, 3.75 eqv.) in 0.5 mL Tol was added. The reaction was placed to oil bath under corresponding temperature. After 24 h, the reaction was cooled to room temperature. The crude product was purified by silica gel chromatography with petroleum ether (PE) as eluent to afford colorless liquid. The NMR spectra of compound are in good agreement with the literature^{S13}. ¹H NMR (400 MHz, CDCl₃) δ 7.58 (dd, *J* = 1.1, 5.0 Hz, 1H), 7.36 (ddd, *J* = 1.1, 3.5, 6.3 Hz, 1H), 7.09 (ddd, *J* = 1.4, 3.5, 4.9 Hz, 1H) ppm. ¹³C{¹H} NMR (101 MHz, CDCl₃) δ 135.5 (d, *J* = 27.6 Hz), 132.0, 128.1 (d, *J* = 8.3 Hz) ppm. ³¹P{¹H} NMR (162 MHz, CDCl₃) δ -46.3 ppm.

4. Substrate scopes of P-C coupling reactions

General procedure:

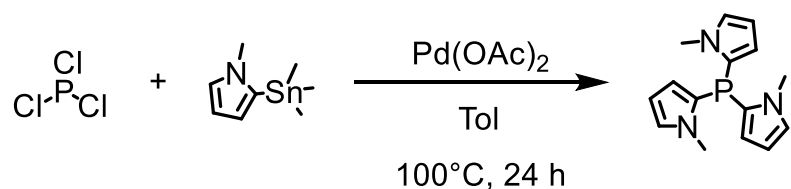
0.5 mL Tol was added to a 20 mL oven-dried Schlenk tube to dissolve Pd(OAc)₂ (0.0056 g, 0.025 mmol, 0.05 eqv.) Then trichlorophosphane (0.44 mL 10 times diluted in Tol, 0.5 mmol, 1 eqv.) was added. Then arylstannane (1.87 mmol, 3.75 eqv.) in 0.5 mL Tol was added. The reaction was placed to 100 °C oil bath. After 24 h, the reaction was cooled to room temperature. The crude product was isolated by silica gel column.

Tri(furan-2-yl)phosphane (2)



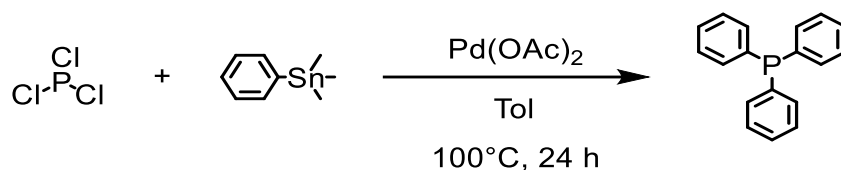
NMR yield was calculated to be 75% (tri(furan-2-yl)phosphine oxide included) according to quantitative ³¹P{¹H}-NMR spectrum with O=PPh₃ (0.0278 g, 0.1 mmol) as an internal standard. The crude product was purified by silica gel chromatography with PE as eluent to afford white solid (0.156 g, 73 % yield). The NMR spectra of compound are in good agreement with the literature^{S14}. ¹H NMR (400 MHz, CDCl₃) δ 7.66 (d, *J* = 1.7 Hz, 3H), 6.80 (ddd, *J* = 0.7, 1.9, 3.1 Hz, 3H), 6.41 (dt, *J* = 1.8, 3.4 Hz, 3H) ppm. ¹³C{¹H} NMR (101 MHz, CDCl₃) δ 98.0, 97.7, 90.0 (d, *J* = 7.5 Hz), 87.0 (d, *J* = 1.9 Hz) ppm. ³¹P{¹H} NMR (162 MHz, CDCl₃) δ -77.8 ppm.

Tris(1-methyl-1H-pyrrol-2-yl)phosphane (3)



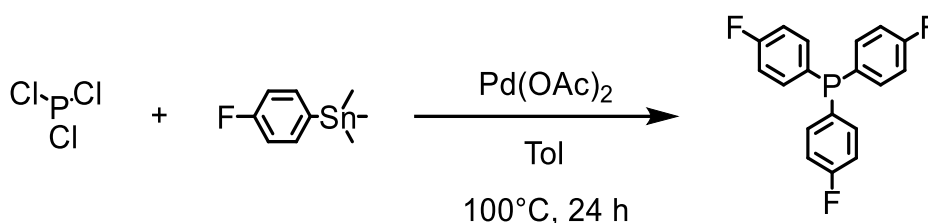
NMR yield was calculated to be 44% according to quantitative ³¹P{¹H}-NMR spectrum with O=PPh₃ (0.0278 g, 0.1 mmol) as an internal standard. The crude product was purified by silica gel chromatography with PE:DCM (dichloromethane) =3:1 as eluent to afford white solid (0.042 g, 31 % yield). The NMR spectra of compound are in good agreement with the literature^{S15}. ¹H NMR (400 MHz, CDCl₃) δ 6.82 (q, *J* = 2.4 Hz, 3H), 6.14 (ddd, *J* = 1.0, 2.6, 3.6 Hz, 3H), 5.98 (ddd, *J* = 0.9, 1.8, 3.6 Hz, 3H), 3.62 (s, 9H) ppm. ¹³C{¹H} NMR (101 MHz, CDCl₃) δ 126.6 (d, *J* = 3.0 Hz), 125.6 (d, *J* = 10.2 Hz), 118.3 (d, *J* = 5.0 Hz), 108.5 (d, *J* = 3.7 Hz), 35.2 (d, *J* = 12.3 Hz) ppm. ³¹P{¹H} NMR (162 MHz, CDCl₃) δ -73.0 ppm.

Triphenylphosphine (4)



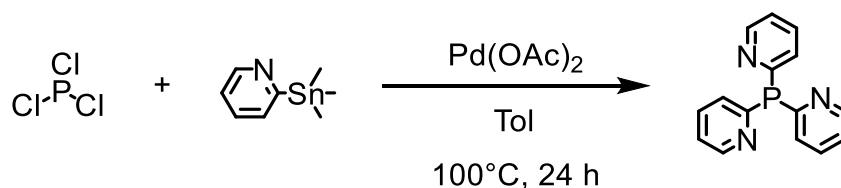
The target compound was observed in the crude product, which is consistent with NMR spectra reported in the literature^{S16}. NMR yield was calculated to be 0.4 % according to quantitative $^{31}\text{P}\{^1\text{H}\}$ -NMR spectrum with $\text{O}=\text{PPh}_3$ (0.0278 g, 0.1 mmol) as an internal standard.

Tris(4-fluorophenyl)phosphane (5)



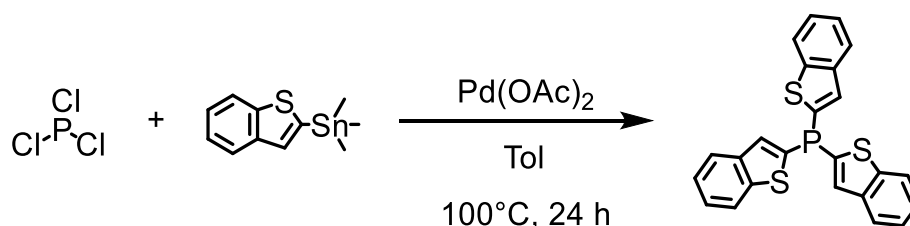
NMR yield was calculated to be 12 % according to quantitative $^{31}\text{P}\{^1\text{H}\}$ -NMR spectrum with $\text{O}=\text{PPh}_3$ (0.0278 g, 0.1 mmol) as an internal standard. The crude product was purified by silica gel chromatography with PE as eluent to afford white solid (0.0099 g, 6 % yield). The NMR spectra of compound are in good agreement with the literature^{S16}. ^1H NMR (400 MHz, CDCl_3) δ 7.25 (ddt, 6H), 7.06 (ddt, $J = 8.9, 6.8, 1.8$ Hz, 6H) ppm. $^{13}\text{C}\{^1\text{H}\}$ NMR (101 MHz, CDCl_3) δ 163.6 (d, $J = 249.4$ Hz), 135.6 (dd, $J = 21.3, 8.1$ Hz), 132.6 (d, $J = 11.4$ Hz), 116.1 (dd, $J = 20.9, 7.7$ Hz) ppm. $^{31}\text{P}\{^1\text{H}\}$ NMR (162 MHz, CDCl_3) δ -9.1 (d, $J = 5.2$ Hz) ppm. $^{19}\text{F}\{^1\text{H}\}$ NMR (376 MHz, CDCl_3) δ -111.9 (d, $J = 4.7$ Hz) ppm.

Tri(pyridin-2-yl)phosphane (6)



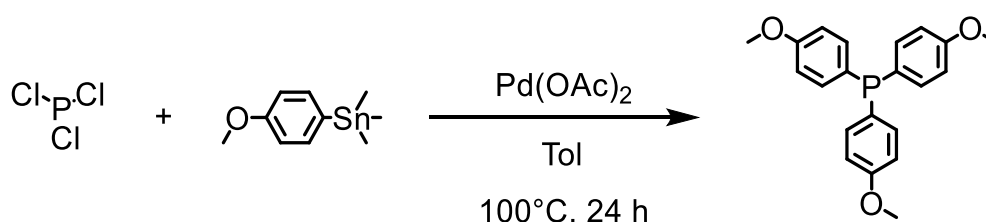
NMR yield was calculated to be 56 % according to quantitative $^{31}\text{P}\{^1\text{H}\}$ -NMR spectrum with $\text{O}=\text{PPh}_3$ (0.0278 g, 0.1 mmol) as an internal standard. The crude product was purified by silica gel chromatography with DCM:MeOH=20:1 as eluent to afford white solid (0.0747 g, 56 % yield). The NMR spectra of compound are in good agreement with the literature^{S17}. ^1H NMR (400 MHz, CDCl_3) δ 8.72 (dt, $J = 1.4, 4.8$ Hz, 3H), 7.62 (tt, $J = 2.0, 7.7$ Hz, 3H), 7.41 (ddt, $J = 1.1, 2.1, 7.8$ Hz, 3H), 7.22 (ddt, $J = 1.2, 4.8, 7.5$ Hz, 3H) ppm. $^{13}\text{C}\{^1\text{H}\}$ NMR (101 MHz, CDCl_3) δ 162.0, 150.6 (d, $J = 11.9$ Hz), 136.1, 129.4 (d, $J = 20.0$ Hz), 123.0 ppm. $^{31}\text{P}\{^1\text{H}\}$ NMR (162 MHz, CDCl_3) δ -0.7 ppm.

Tris(benzo[b]thiophen-2-yl)phosphane (7)



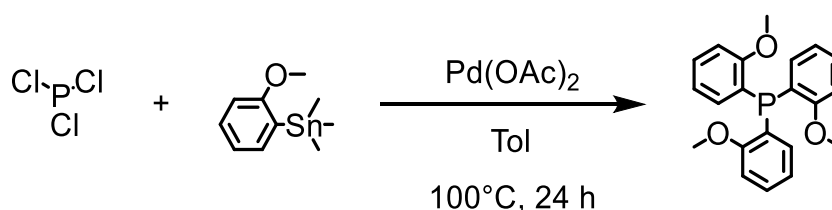
NMR yield was calculated to be 70 % according to quantitative $^{31}\text{P}\{^1\text{H}\}$ -NMR spectrum with $\text{O}=\text{PPh}_3$ (0.0278 g, 0.1 mmol) as an internal standard. The crude product was purified by silica gel chromatography with PE as eluent to afford white solid (0.1561 g, 73 % yield). The NMR spectra of compound are in good agreement with the literature^{S18}. ^1H NMR (400 MHz, CDCl_3) δ 7.87 – 7.74 (m, 6H), 7.70 (dd, $J = 7.3, 0.8$ Hz, 3H), 7.42 – 7.30 (m, 6H) ppm. $^{13}\text{C}\{^1\text{H}\}$ NMR (101 MHz, CDCl_3) δ 144.0, 140.1 (d, $J = 9.4$ Hz), 138.8 (d, $J = 23.7$ Hz), 133.3 (d, $J = 28.2$ Hz), 125.4, 124.7, 124.3, 122.5 ppm. $^{31}\text{P}\{^1\text{H}\}$ NMR (162 MHz, CDCl_3) δ -38.7 ppm.

Tris(4-methoxyphenyl)phosphane (8)



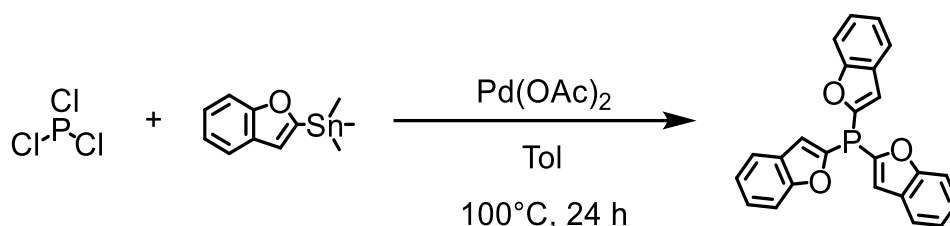
NMR yield was calculated to be 12 % according to quantitative $^{31}\text{P}\{^1\text{H}\}$ -NMR spectrum with $\text{O}=\text{PPh}_3$ (0.0278 g, 0.1 mmol) as an internal standard. The crude product was purified by silica gel chromatography with PE as eluent to afford white solid (0.0171 g, 10 % yield). The NMR spectra of compound are in good agreement with the literature^{S16}. ^1H NMR (400 MHz, CDCl_3) δ 7.23 (dd, $J = 8.7, 1.4$ Hz, 6H), 6.88 (dd, $J = 8.7, 1.0$ Hz, 6H), 3.80 (s, 9H) ppm. $^{13}\text{C}\{^1\text{H}\}$ NMR (101 MHz, CDCl_3) δ 160.2, 135.8 (d, $J = 20.8$ Hz), 128.9, 114.3 (d, $J = 7.7$ Hz), 55.3 ppm. $^{31}\text{P}\{^1\text{H}\}$ NMR (162 MHz, CDCl_3) δ -10.2 ppm.

Tris(2-methoxyphenyl)phosphane (9)



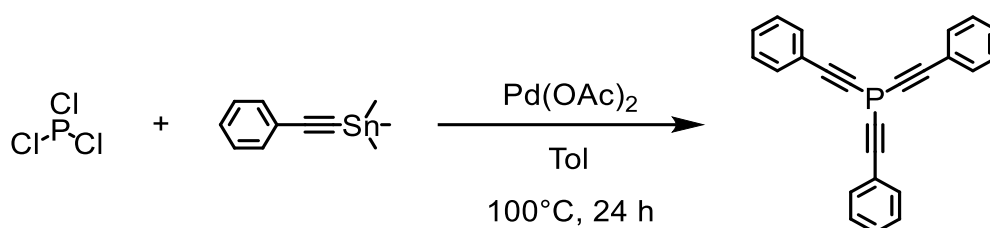
No targeted product was observed in quantitative $^{31}\text{P}\{^1\text{H}\}$ -NMR spectrum with $\text{O}=\text{PPh}_3$ (0.0278 g, 0.1 mmol) as an internal standard. No target compound was isolated.

Tri(benzofuran-2-yl)phosphane (10)



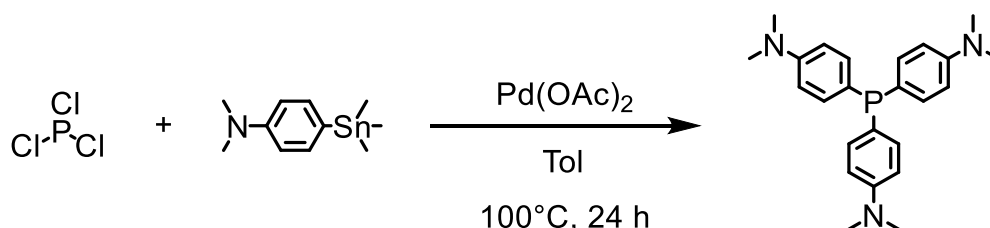
NMR yield was calculated to be 55 % according to quantitative $^{31}\text{P}\{^1\text{H}\}$ -NMR spectrum with $\text{O}=\text{PPh}_3$ (0.0278 g, 0.1 mmol) as an internal standard. The crude product was purified by silica gel chromatography with PE as eluent to afford white solid (0.0985 g, 52 % yield). The NMR spectra of compound are in good agreement with the literature^{S14}. ^1H NMR (500 MHz, CDCl_3) δ 7.58 (dd, $J = 1.2, 7.7$ Hz, 3H), 7.54 (d, $J = 8.3$ Hz, 3H), 7.33 (ddd, $J = 1.3, 7.1, 8.4$ Hz, 3H), 7.28 – 7.26 (m, 3H), 7.24 (t, $J = 7.4$ Hz, 3H) ppm. $^{13}\text{C}\{^1\text{H}\}$ NMR (126 MHz, CDCl_3) δ 158.3 (d, $J = 3.2$ Hz), 151.0 (d, $J = 4.8$ Hz), 128.0 (d, $J = 6.5$ Hz), 125.7, 123.2, 121.6, 118.5 (d, $J = 22.6$ Hz), 111.9 ppm. $^{31}\text{P}\{^1\text{H}\}$ NMR (202 MHz, CDCl_3) δ -67.7 ppm.

Tris(phenylethynyl)phosphane (11)



NMR yield was calculated to be 63 % according to quantitative $^{31}\text{P}\{^1\text{H}\}$ -NMR spectrum with $\text{O}=\text{PPh}_3$ (0.0278 g, 0.1 mmol) as an internal standard. The crude product was purified by silica gel chromatography with PE as eluent to afford white solid (0.1039 g, 62 % yield). The NMR spectra of compound are in good agreement with the literature^{S20}. ^1H NMR (400 MHz, CDCl_3) δ 7.59 – 7.53 (m, 6H), 7.40 – 7.30 (m, 9H) ppm. $^{13}\text{C}\{^1\text{H}\}$ NMR (101 MHz, CDCl_3) δ 132.3 (d, $J = 2.0$ Hz), 129.6, 128.5, 122.2, 105.8 (d, $J = 11.4$ Hz), 79.5 (d, $J = 6.7$ Hz) ppm. $^{31}\text{P}\{^1\text{H}\}$ NMR (162 MHz, CDCl_3) δ -88.3 ppm.

Tris(4-(dimethylamino)phenyl)phosphine (12)

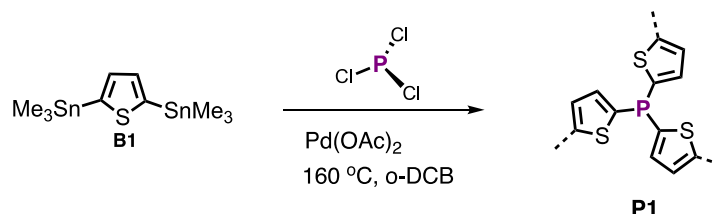


NMR yield was calculated to be 16% according to quantitative $^{31}\text{P}\{^1\text{H}\}$ -NMR spectrum with $\text{O}=\text{PPh}_3$ (0.0278 g, 0.1 mmol) as an internal standard. The target compound was observed in the crude product according to the ^{31}P chemical shift reported in the literature^{S21}. The crude product was oxidized during purification. Oxide compound tris(4-(dimethylamino)phenyl)phosphine oxide was obtained as white solid by silica gel chromatography with $\text{DCM}:\text{MeOH}=20:1$ as eluent. The NMR spectra of compound are in good agreement with the literature^{S21}. ^1H NMR (400 MHz, CDCl_3) δ 7.47 (dd, $J = 11.3, 8.9$ Hz, 6H), 6.67 (dd, $J = 8.9, 2.2$ Hz, 6H), 2.98 (s, 18H) ppm. $^{13}\text{C}\{^1\text{H}\}$ NMR (101 MHz, CDCl_3)

δ 152.2, 133.5 (d, $J = 11.1$ Hz), 119.5 (d, $J = 114.7$ Hz), 111.3 (d, $J = 12.7$ Hz), 40.2 ppm. $^{31}\text{P}\{^1\text{H}\}$ NMR (162 MHz, CDCl_3) δ 30.5 ppm.

Synthesis of polymers

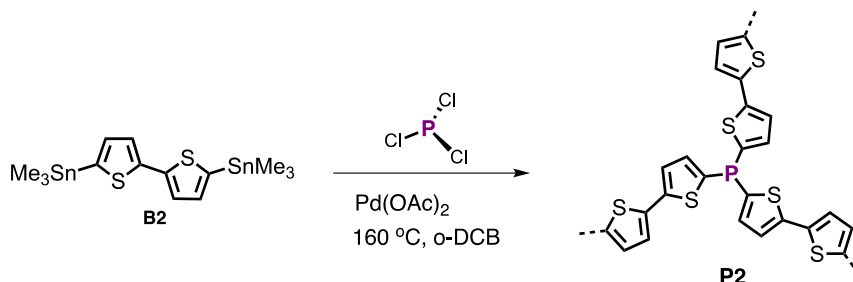
4.1. Synthesis of P1



Scheme S16. Synthesis of **P1**.

Pd(OAc)₂ (0.02 g, 0.1 mmol) in 10 mL o-DCB (1,2-dichlorobenzene) was added to a 100 mL Schlenk tube charged with trichlorophosphane (0.18 mL, 2 mmol) and 2,5-bis(trimethylstannyl)thiophene (**B1**) (1.27 g, 3.1 mmol) in 30 mL o-DCB. The reaction was placed into 160 °C oil bath. After 3 days, the mixture was filtered in the glovebox and wash with DCM until no other impurity peaks were observed in liquid ¹H-NMR spectrum. Brown solid (0.289 g, 109 % yield) was finally obtained after drying under high vacuum at room temperature.

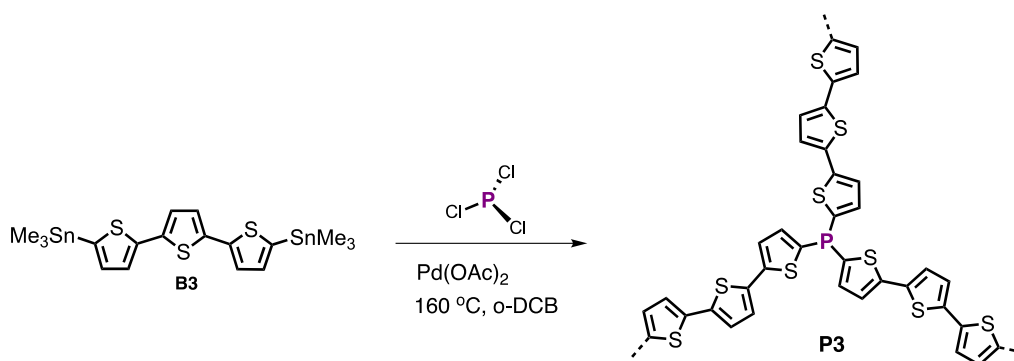
4.2. Synthesis of P2



Scheme S17. Synthesis of **P2**.

Pd(OAc)₂ (0.02 g, 0.1 mmol) in 10 mL o-DCB was added to a 100 mL Schlenk tube charged with trichlorophosphane (0.18 mL, 2 mmol) and 5,5'-bis(trimethylstannyl)-2,2'-bithiophene (**B2**) (1.52 g, 3.1 mmol) in 30 mL o-DCB. The reaction solution was placed to 160 °C oil bath. After 3 days, the mixture was filtered in the glovebox and wash with DCM until no other impurity peaks were observed in liquid ¹H-NMR spectrum. Orange solid (0.54 g, 98% yield) was finally obtained after drying under high vacuum at room temperature.

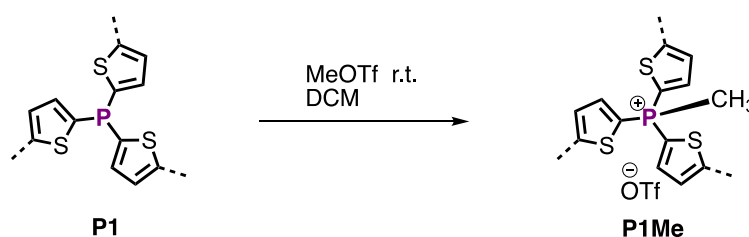
4.3. Synthesis of P3



Scheme S18. Synthesis of **P3**.

$\text{Pd}(\text{OAc})_2$ (0.01 g, 0.05 mmol) in 5 mL *o*-DCB was added to a 100 mL Schlenk tube charged with trichlorophosphane (0.09 mL, 1 mmol) and 5,5''-bis(trimethylstannyl)-2,2':5',2''-terthiophene (**B3**) (0.89 g, 1.55 mmol) in 15 mL *o*-DCB. The reaction was placed into 160 °C oil bath. After 3 days, the mixture was filtered in the glovebox and wash with DCM until no other impurity peaks were observed in liquid $^1\text{H-NMR}$ spectrum. Brown solid (0.42 g, 105% yield) was finally obtained after drying under high vacuum at room temperature.

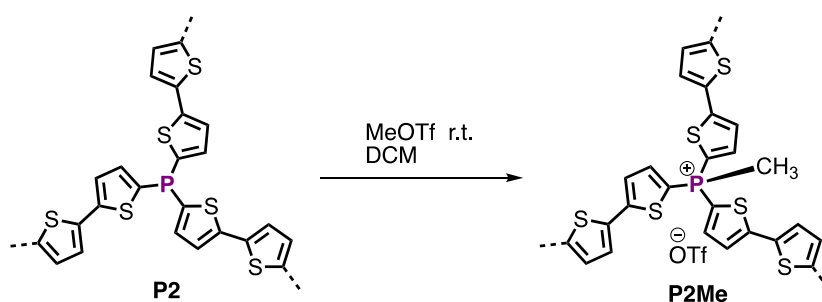
4.4. Synthesis of P1Me



Scheme S19. Synthesis of **P1Me**.

The **P1** solid (0.08 g, 0.55 mmol P atoms in theory) was dispersed in 5 mL DCM and then trifluoromethanesulfonate (MeOTf) (0.23 mL, 2 mmol) was added. The mixture was stirred at room temperature for 3 days, then 50 °C for 30 days. After that, the mixture was filtered and washed with DCM until no other impurity peaks were observed in liquid $^1\text{H-NMR}$ spectrum. Yellow solid (0.1694 g, 91% yield) was finally obtained after drying under high vacuum at room temperature.

4.5. Synthesis of P2Me

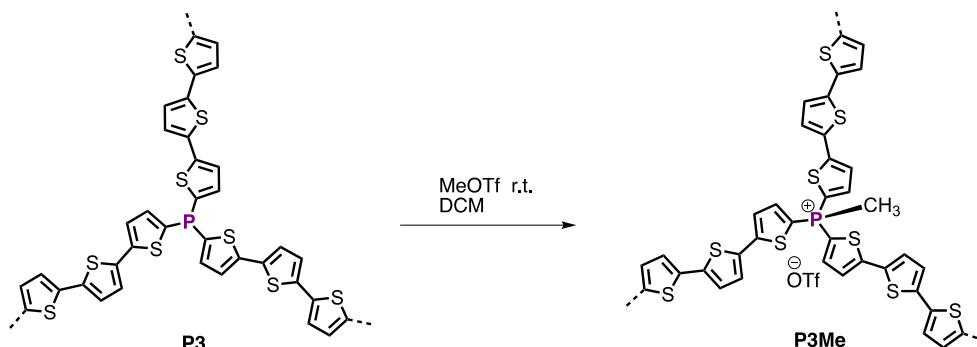


Scheme S20. Synthesis of **P2Me**.

The **P2** solid (0.14 g, 0.5 mmol P atoms in theory) was dispersed in 5 mL DCM and then

trifluoromethanesulfonate (MeOTf) (0.23 mL, 2 mmol) was added. The mixture was stirred at room temperature for 3 days. After that, the mixture was filtered and washed with DCM until no other impurity peaks were observed in liquid $^1\text{H-NMR}$ spectrum. Brown solid (0.20 g, 89% yield) was finally obtained after drying under high vacuum at room temperature.

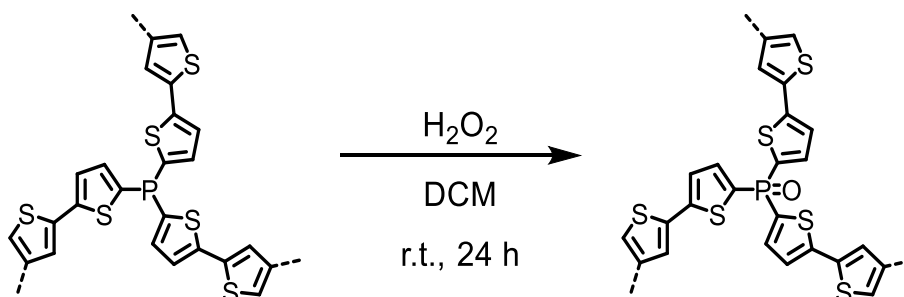
4.6. Synthesis of P3Me



Scheme S21. Synthesis of **P3Me**.

The **P3** solid (0.19 g, 0.47 mmol P atoms in theory) was dispersed in 5 mL DCM and then trifluoromethanesulfonate (MeOTf) (0.23 mL, 2 mmol) was added. The mixture was stirred at room temperature for 3 days. After that, the mixture was filtered and washed with DCM until no other impurity peaks were observed in liquid $^1\text{H-NMR}$ spectrum. Orange solid (0.26 g, 97% yield) was finally obtained after drying under high vacuum at room temperature.

4.7. Synthesis of P2O



Scheme S22. Synthesis of **P2O**.

The **P2** solid (0.18 g, 0.5 mmol P atoms in theory) was dissolved in 5 mL DCM and then 5 drops of H_2O_2 (33%, excess) were added. The mixture was stirred at room temperature. After 24 h, the mixture was filtered and washed with DCM until no other impurity peaks were observed in liquid $^1\text{H-NMR}$ spectrum. Orange solid (0.19 g, 99% yield) was finally obtained after drying under high vacuum at room temperature.

4.8. Synthesis of model compounds

Tri(thiophen-2-yl)phosphine was synthesized in the reaction condition optimization section. $^1\text{H-NMR}$ (400 MHz, CDCl_3) δ 7.58 (dd, $J = 1.1, 5.0$ Hz, 1H), 7.36 (ddd, $J = 1.1, 3.5, 6.3$ Hz, 1H), 7.09 (ddd, $J = 1.4, 3.5, 4.9$ Hz, 1H) ppm. $^{13}\text{C}\{^1\text{H}\}$ NMR (101 MHz, CDCl_3) δ 135.5 (d, $J = 27.6$ Hz), 132.0, 128.1 (d, $J = 8.3$ Hz) ppm. $^{31}\text{P}\{^1\text{H}\}$ NMR (162 MHz, CDCl_3) δ -46.3 ppm.

Tri(thiophen-2-yl)phosphine oxide was obtained by treating tri(thiophen-2-yl)phosphine with hydrogen peroxide. The compound data was in good agreement with the literature^{S22}. ¹H NMR (400 MHz, CDCl₃) δ 7.77 (dt, *J* = 4.7, 2.9 Hz, 3H), 7.61 (dd, *J* = 8.0, 3.6 Hz, 3H), 7.21 (ddd, *J* = 5.4, 3.5, 2.0 Hz, 3H) ppm. ¹³C{¹H} NMR (101 MHz, CDCl₃) δ 137.1 (d, *J* = 11.2 Hz), 134.6 (d, *J* = 128.2 Hz), 134.5 (d, *J* = 5.9 Hz), 128.5 (d, *J* = 15.2 Hz) ppm. ³¹P{¹H} NMR (162 MHz, CDCl₃) δ 6.8 ppm.

Methyl-tri(2-thienyl)phosphonium triflate was obtained by treating tri(thiophen-2-yl)phosphine with stoichiometric methyl triflate. ¹H NMR (400 MHz, CDCl₃) δ 8.14 (td, *J* = 4.9, 1.1 Hz, 3H), 7.98 (ddd, *J* = 8.7, 3.9, 1.1 Hz, 3H), 7.42 (ddd, *J* = 4.9, 3.8, 2.3 Hz, 3H), 2.99 (d, *J* = 14.0 Hz, 3H) ppm. ¹³C{¹H} NMR (101 MHz, CDCl₃) δ 142.0 (d, *J* = 12.7 Hz), 139.8 (d, *J* = 6.4 Hz), 130.9 (d, *J* = 16.2 Hz), 120.9 (q, *J* = 319.6 Hz), 119.0 (d, *J* = 112.6 Hz), 15.0 (d, *J* = 63.6 Hz) ppm. ³¹P{¹H} NMR (162 MHz, CDCl₃) δ 3.1 ppm. ¹⁹F{¹H} NMR (376 MHz, CDCl₃) δ -78.2 ppm.

5. Theoretical calculation

All density functional theory (DFT) calculations were performed using Gaussian09 packages^{S23} supported by supercomputer cluster in HPC platform of ShanghaiTech University. Geometry optimizations were carried out with B3LYP/g-31g(d) level^{S24-S26} in gas-phase, using the SDD (Stuttgart/Dresden)^{S27-S28} effective core potential for Pd and Sn, and the double- ζ quality plus polarization 6-31G(d) basis set for all other elements.

Single-point calculations on the gas-phase-optimized geometries were performed to estimate the change in the Gibbs energies in the presence of toluene as solvent using the triple- ζ quality 6-311+G(d) basis set including the SDD for Pd and Sn. Solvents effects were taken into account using the solvation model based on density (SMD). Gibbs free energies were calculated by Shermo software.^{S29}

Frequency analysis was also performed at the same level of theory as geometry optimization to confirm optimized stationary points were either local minimum or transition state, as well as to evaluate zero-point vibrational energies and thermal corrections for enthalpies and free energies at 298.15 K. The intrinsic reaction coordinate (IRC) calculations were performed for all transition states at the same level to confirm that each transition state links the corresponding reactant and product well.

For models molecules, all the calculations were performed using Gaussian09 Packages^{S23} by supercomputer cluster supported by HPC Platform of ShanghaiTech University. Geometry optimizations were carried out with RCAM-B3LYP/g-31g(d) level. Single point calculations at TD RCAM-B3LYP/6-31(g) scrf = (solvent = dichloromethane) level were performed to reevaluate the energy of optimized structures. Structures were generated using GaussView 6.0^{S24} program.

Table S3. TD-DFT data of model molecules at the level of rcam-b3lyp/6-31+g(d) scrf=(solvent=dichloromethane).

Compound	LUMO [eV]	HOMO [eV]	S ₀ -S ₁ Wavelength (nm) Energy gap (eV)	S ₀ -S ₁ Oscillator strength
M	-0.37	-6.83	310.2 nm 4.00 eV	1.07
MO	-0.48	-7.25	301.3 nm 4.11 eV	1.11
MMe	-3.43	-9.78	320.6 nm 3.88 eV	1.15
M2	-0.63	-6.76	330.6 nm 3.75 eV	1.98
M2O	-0.85	-7.26	313.1 nm 3.96 eV	2.02
M2Me	-2.21	-8.00	329.9 nm 3.76 eV	0.01

6. Solid state NMR (ssNMR) characterization of polymers

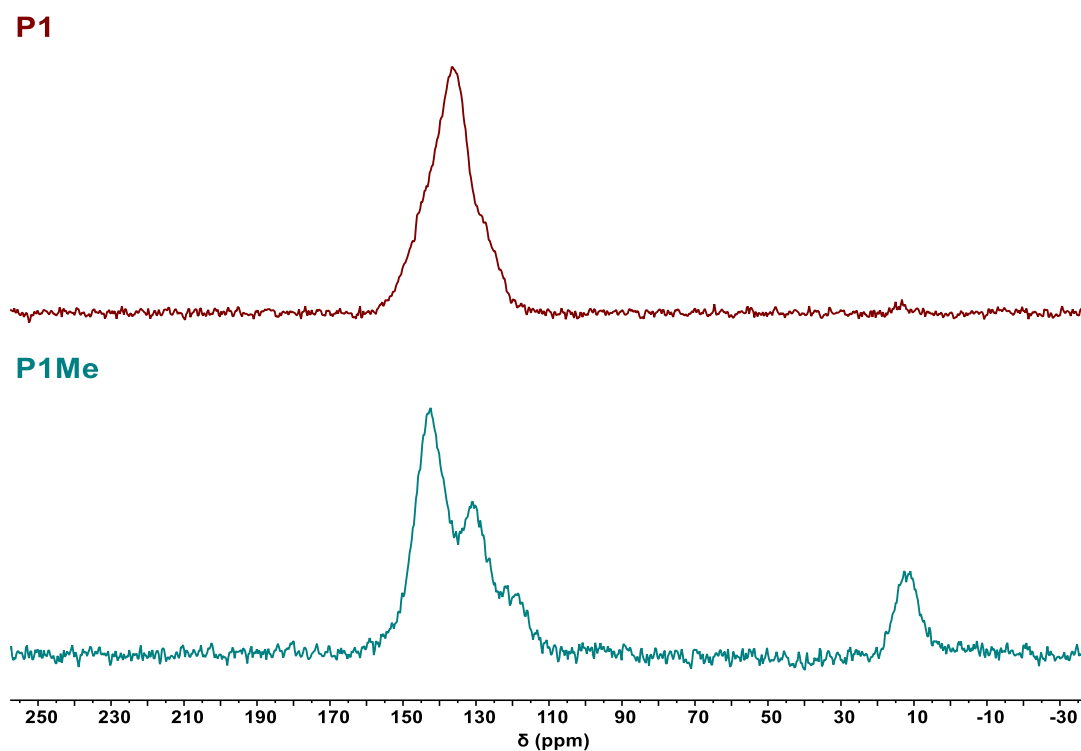


Figure S1. $^{13}\text{C}\{^1\text{H}\}$ CP/MAS NMR spectra (101 MHz, 298 K) of **P1** and **P1Me**.

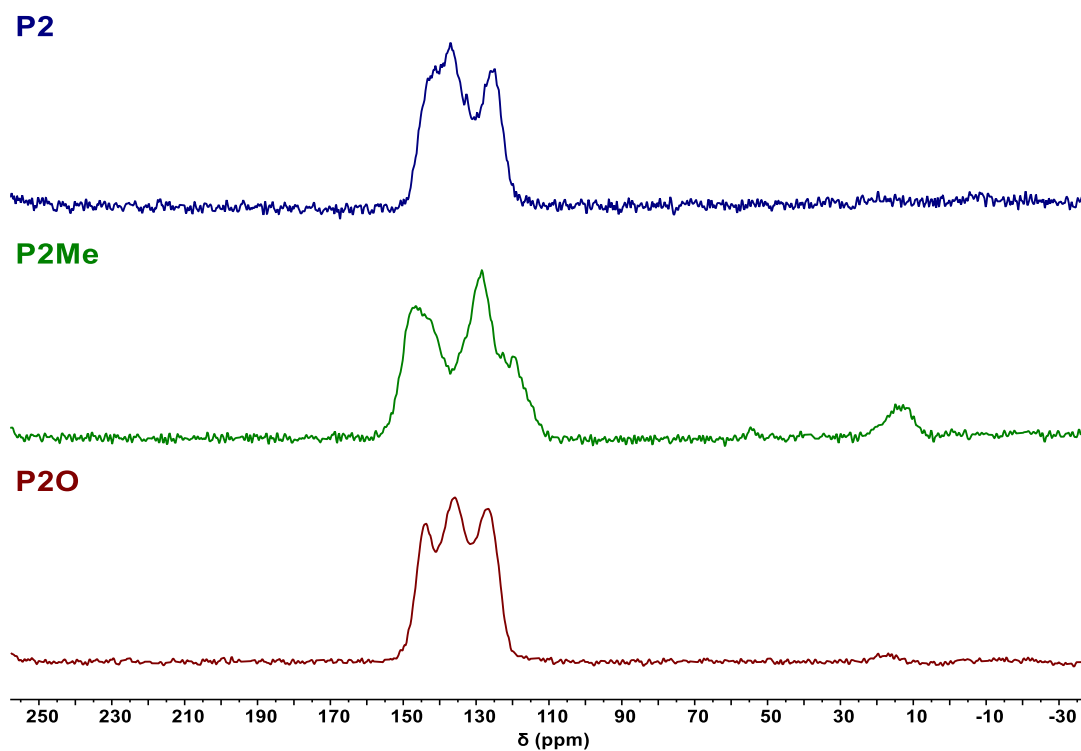


Figure S2. $^{13}\text{C}\{^1\text{H}\}$ CP/MAS NMR spectra (101 MHz, 298 K) of **P2**, **P2Me** and **P2O**.

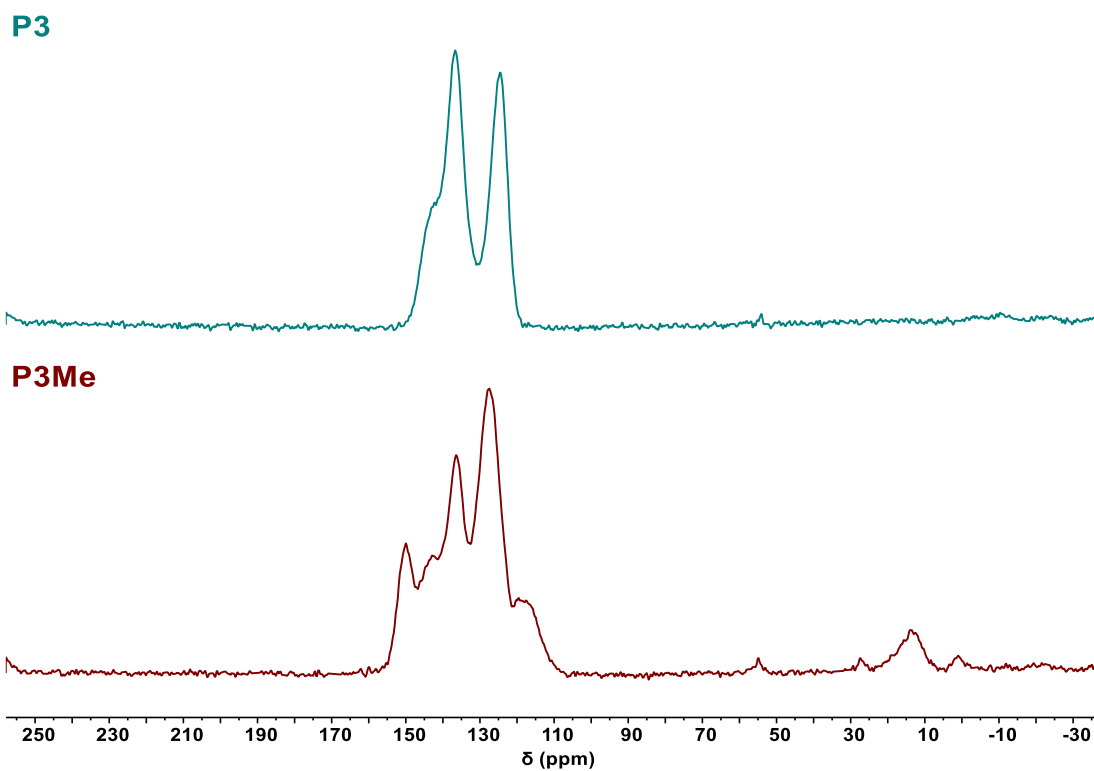


Figure S3. $^{13}\text{C}\{^1\text{H}\}$ CP/MAS NMR spectra (101 MHz, 298 K) of **P3** and **P3Me**.

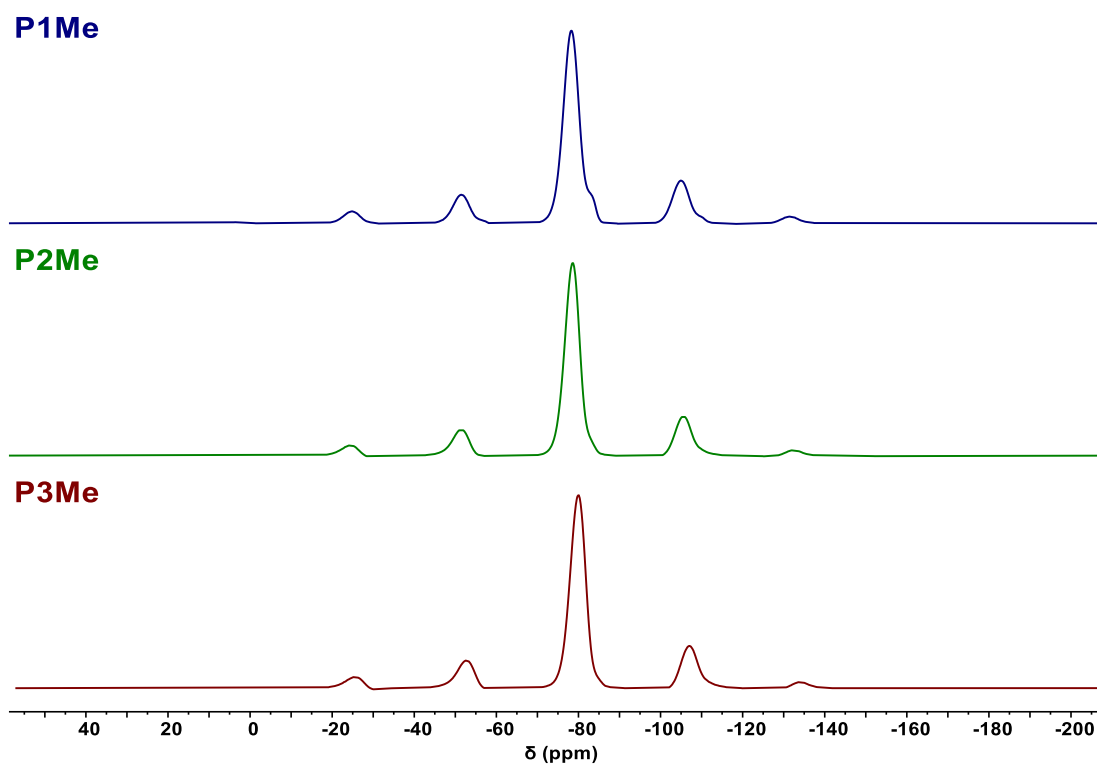


Figure S4. ^{19}F MAS NMR spectra (376 MHz, 298 K) of **P1Me**, **P2Me** and **P3Me**.

7. Fourier transform infrared (FT-IR) spectra of polymers

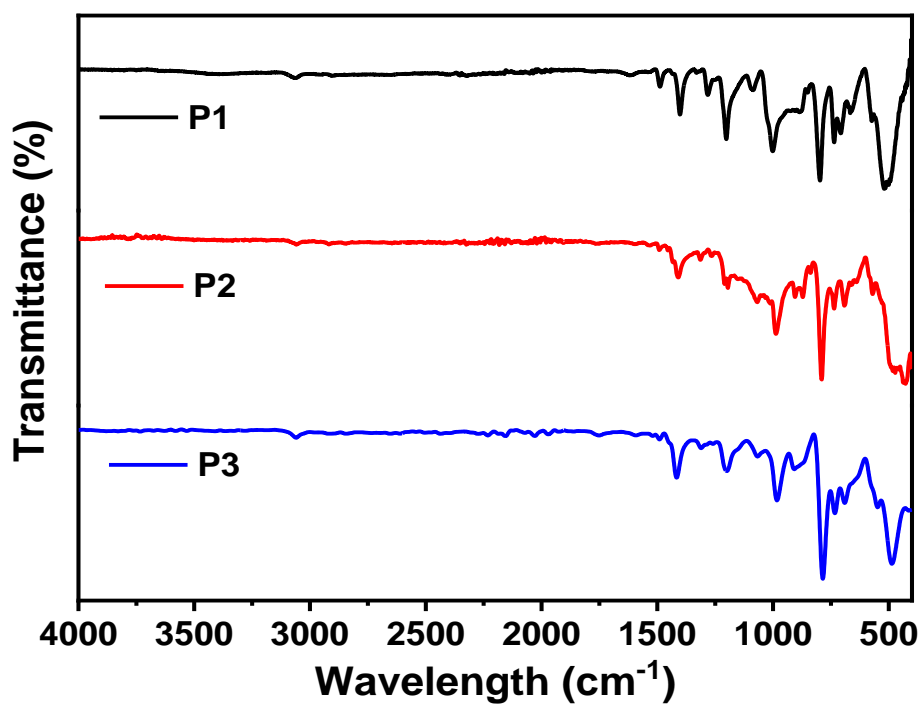


Figure S5. FT-IR spectra of P1, P2 and P3.

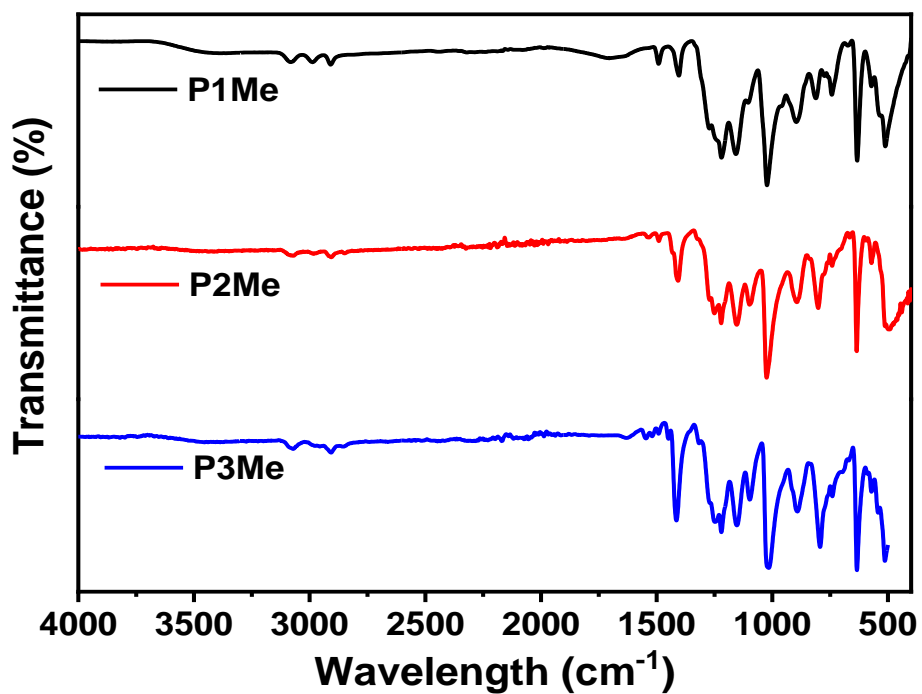


Figure S6. FT-IR spectra of P1Me, P2Me and P3Me.

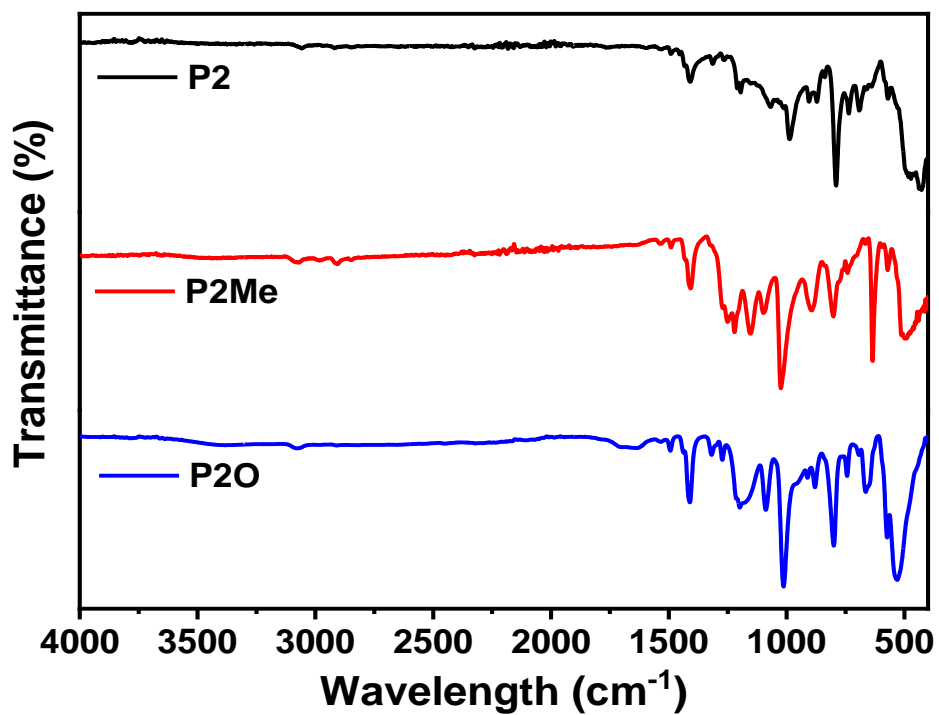


Figure S7. FT-IR spectra of P2, P2Me and P2O.

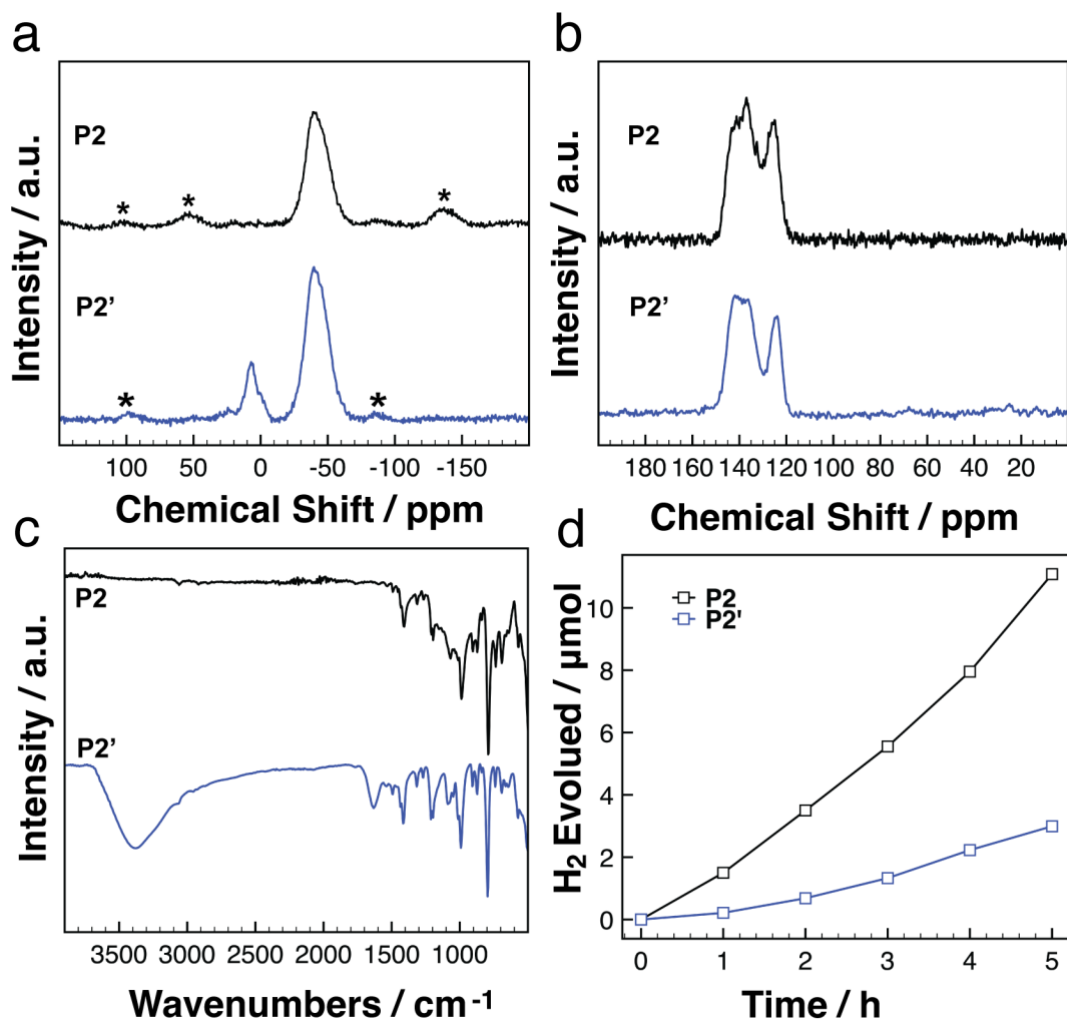


Figure S8. (a) ^{31}P HPDEC/MAS NMR spectra, (b) $^{13}\text{C}\{^1\text{H}\}$ CP/MAS NMR spectra (101 MHz, 298 K), and (c) FT-IR spectra of **P2** and **P2'**. (d) Time course for photocatalytic H_2 evolution under full-arc and (b) $\lambda > 420$ nm light illumination using 20 mg photocatalysts of **P2** and **P2'**.

8. XPS data of polymers

Table S4. Element ratio of polymers.

Sample	Calculated element ratio	XPS found element ratio
	C : P : S : (F : O)	C : P : S : (F : O) : Pd
P1	4 : 1 : 1	5.34 : 1 : 1.33 : 0.038
P2	8 : 1 : 2	12.55 : 1 : 2.92 : 0.039
P3	12 : 1 : 3	15.34 : 1 : 4.34 : 0.063
P1Me	6 : 1 : 1 : (3 : 3)	6.57 : 1 : 1.6 : (2.40 : 2.75) : 0.032
P2Me	10 : 1 : 3 : (3 : 3)	14.42 : 1 : 3.99 : (4.19 : 8.11) : 0.044
P3Me	14 : 1 : 4 : (3 : 3)	18.32 : 1 : 5.35 : (3.54 : 3.42) : 0.047
P2O	8 : 1 : 2 : (0 : 1)	9.76 : 1 : 2.45 : (0 : 1.99) : 0.029

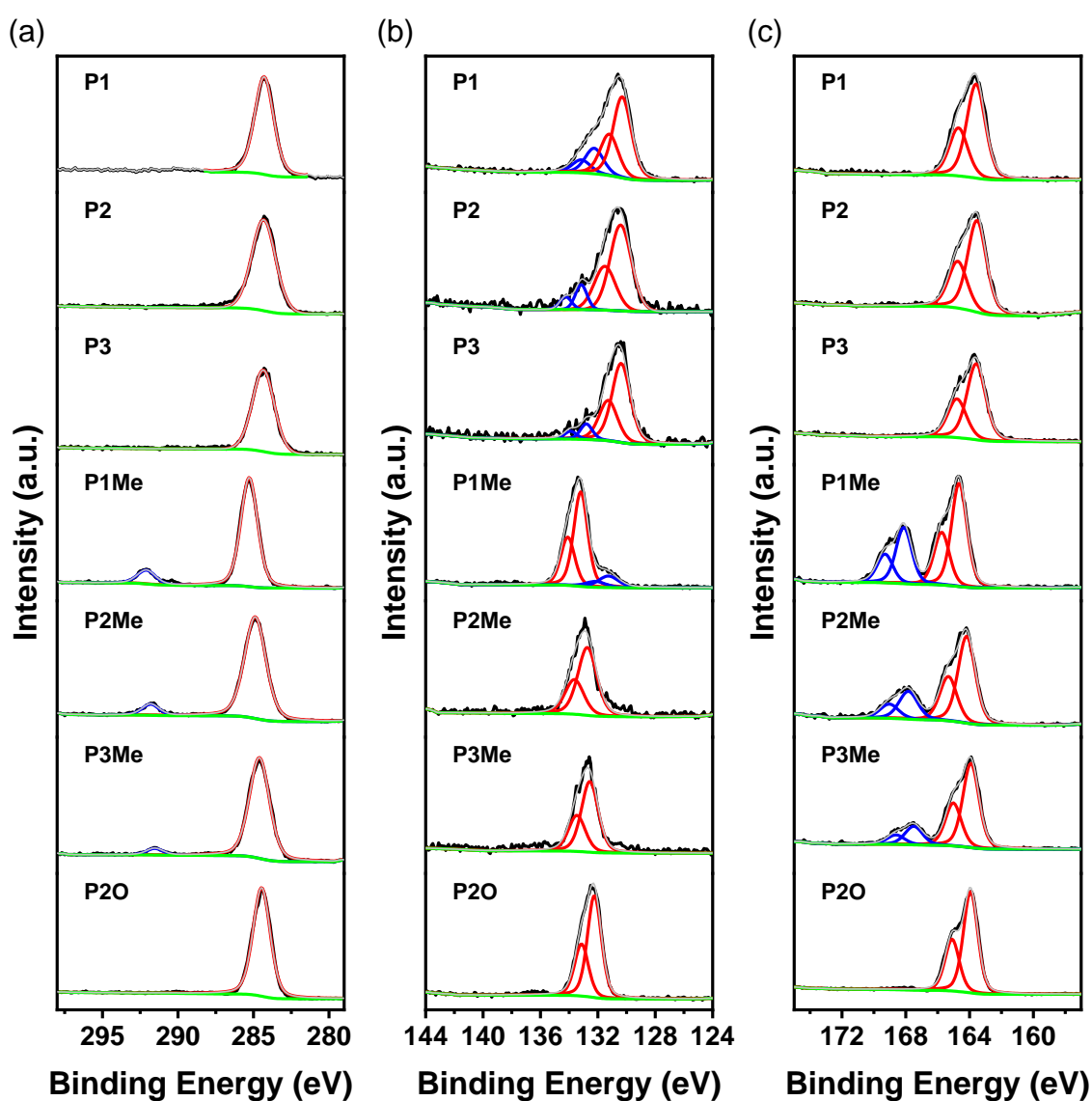


Figure S9. XPS spectra of polymers in the region of (a) C 1s, (b) P 2p, and (c) S 2p.

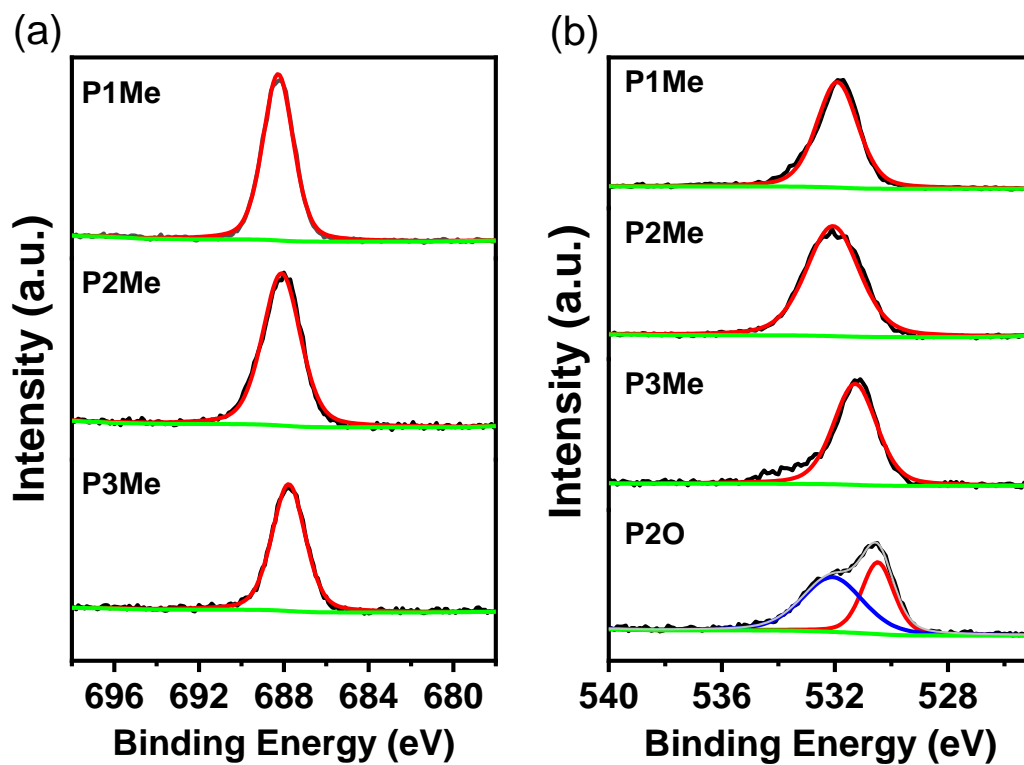


Figure S1. XPS spectra of P1Me, P2Me, P3Me and P2O in the region of (a) F 1s and (b) O 1s.

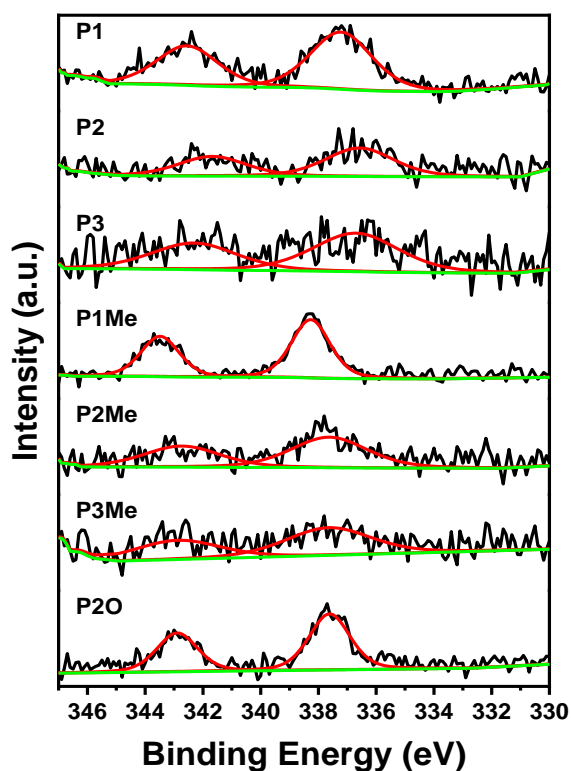


Figure S11. XPS spectra of the residual Pd in polymers in the region of Pd 3d.

Table S5. XPS peak analysis results of polymers.

Peak	P1	P2	P3	P1Me	P2Me	P3Me	P2O
C 1s (CH)	284.30	284.33	284.35	285.28	284.88	284.61	284.46
C 1s (CF ₃)	-	-	-	292.09	291.81	291.53	-
P 2p ₃ (PR ₃)	130.30	130.41	130.38	131.27	-	-	-
P 2p ₁ (PR ₃)	131.20	131.51	131.28	132.17	-	-	-
P 2p ₃ (MePR ₃)	-	-	-	133.20	132.73	132.56	-
P 2p ₁ (MePR ₃)	-	-	-	134.10	133.63	133.46	-
P 2p ₃ (O=PR ₃)	132.26	133.16	132.80	-	-	-	132.24
P 2p ₁ (O=PR ₃)	133.16	134.24	133.90	-	-	-	133.14
S 2p ₃ (Th)	163.59	163.53	163.58	164.65	164.18	163.92	163.94
S 2p ₁ (Th)	164.69	164.74	164.67	165.75	165.33	165.02	165.09
S 2p (SO ₃)	-	-	-	168.12	167.84	167.50	-
S 2p (SO ₃)	-	-	-	169.31	169.04	168.62	-
F 1s (CF ₃)	-	-	-	688.27	688.11	687.77	-
O 1s (SO ₃)	-	-	-	531.91	532.07	531.28	-
O 1s (P=O)	-	-	-	-	-	-	530.48
Pd 3d ₅	337.22	336.58	336.71	338.27	337.62	337.65	337.62
Pd 3d ₃	345.22	341.68	342.31	343.48	342.74	342.88	342.89

9. Mott–Schottky measurements

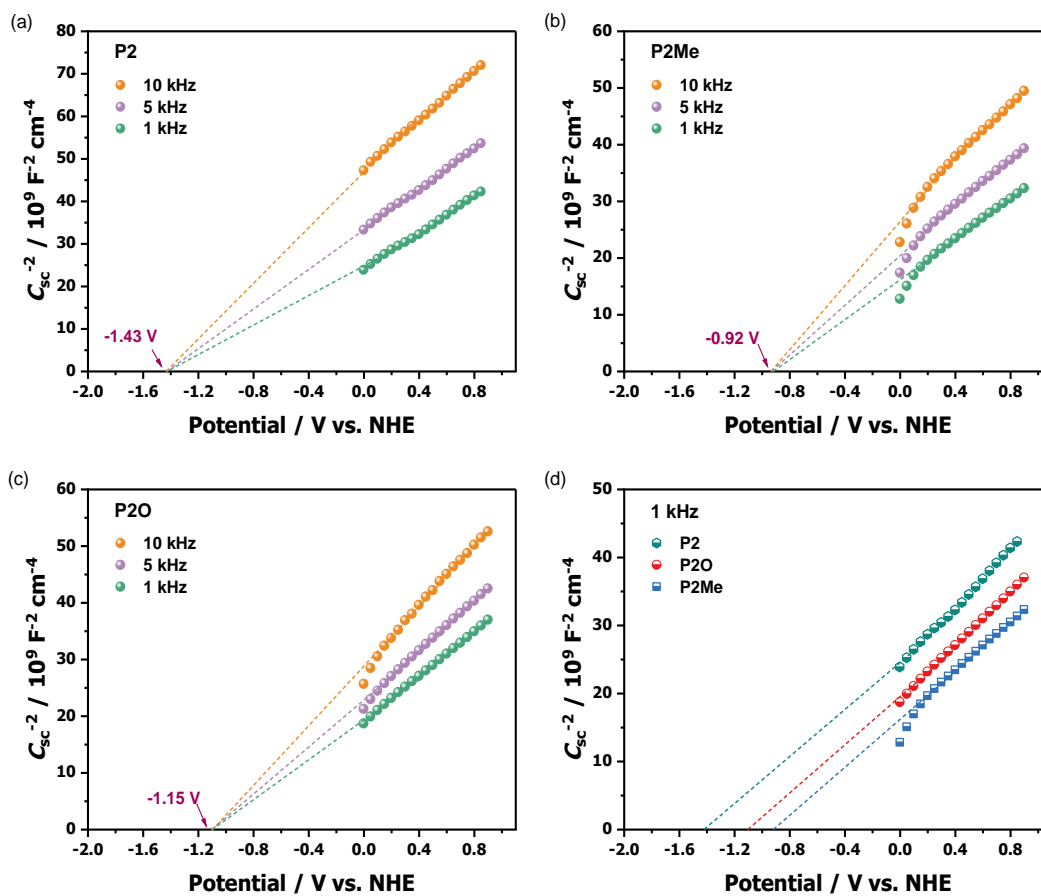


Figure S2. Mott–Schottky curves of (a) **P2**, (b) **P2Me**, (c) **P2O** and (d) comparison measured at 1 kHz.

10. Thermogravimetric analysis (TGA) of polymers

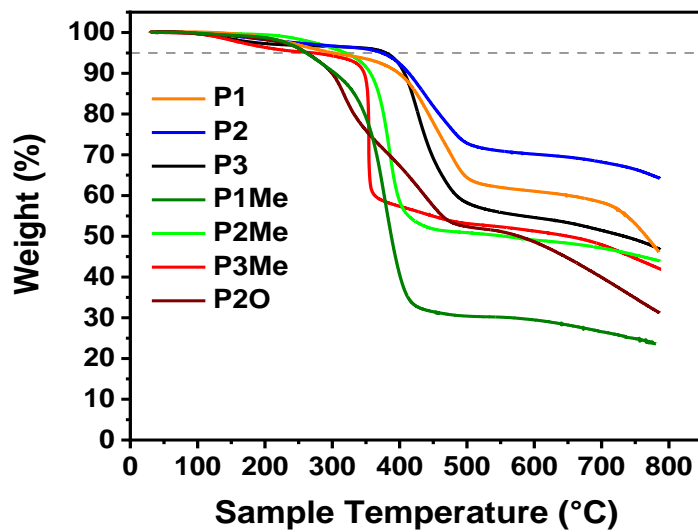


Figure S3. TGA curves of polymers.

11. Contact angle measurements

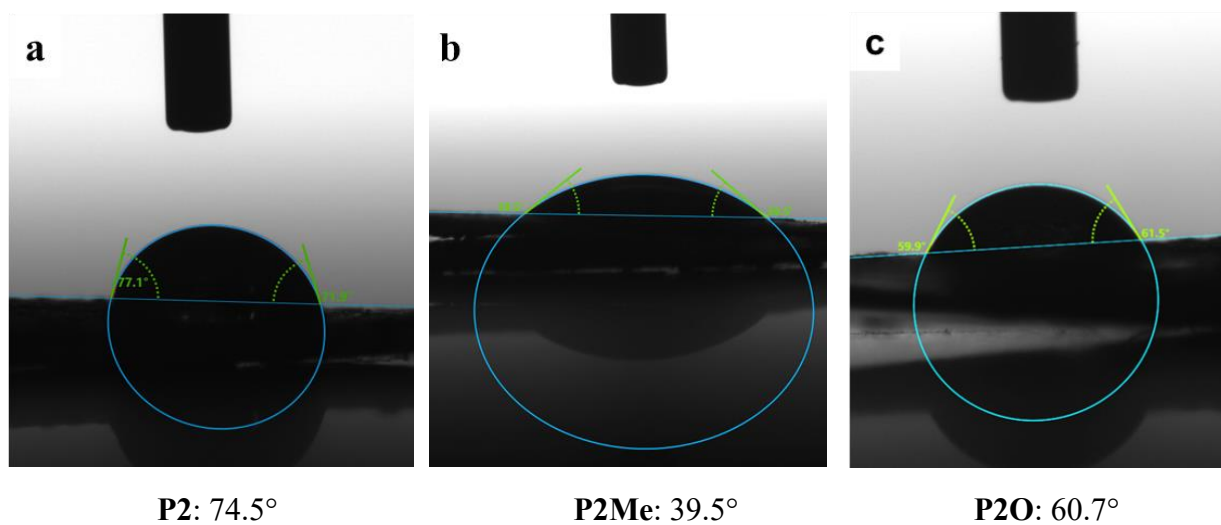


Figure S4. Water contact angles for pressed pellets of (a) **P2**, (b) **P2Me**, and (c) **P2O** at room temperature in air.

12. NMR spectra

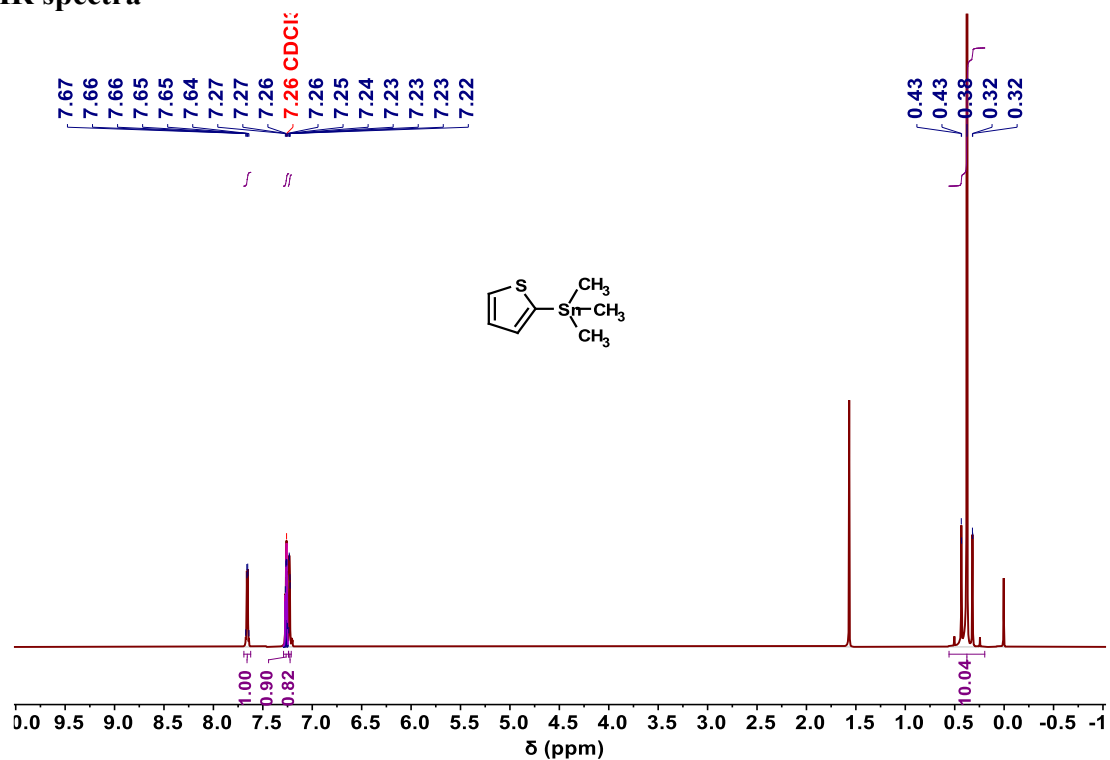


Figure S15. ¹H-NMR spectrum (400 MHz, 298 K, CDCl₃) of trimethyl(thiophen-2-yl)stannane.

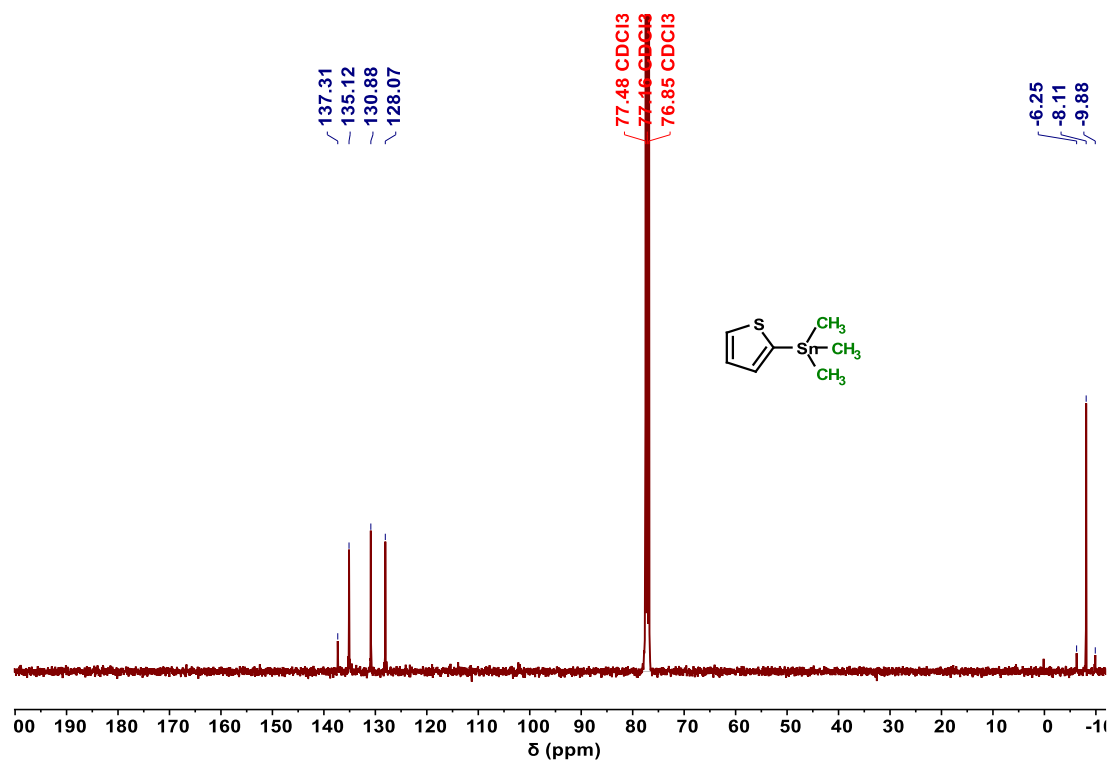


Figure S16. ¹³C{¹H}-NMR spectrum (101 MHz, 298 K, CDCl₃) of trimethyl(thiophen-2-yl)stannane.

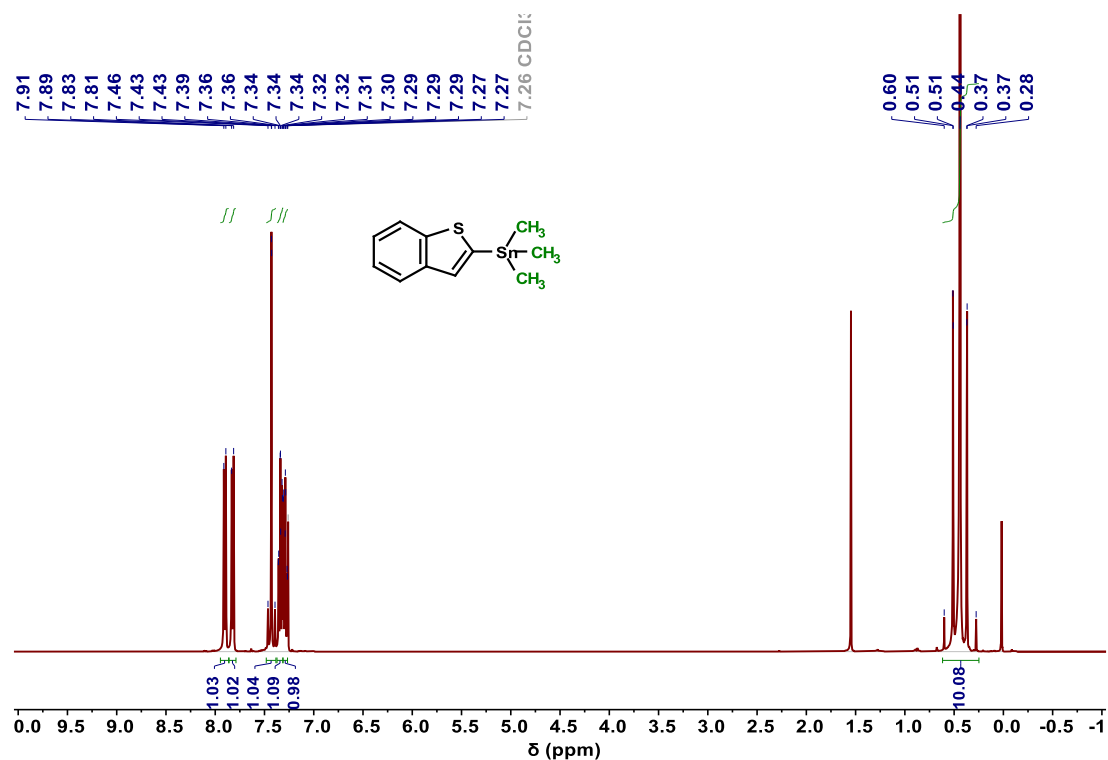


Figure S17. ^1H -NMR spectrum (400 MHz, 298 K, CDCl_3) of benzo[*b*]thiophen-2-yltrimethylstannane.

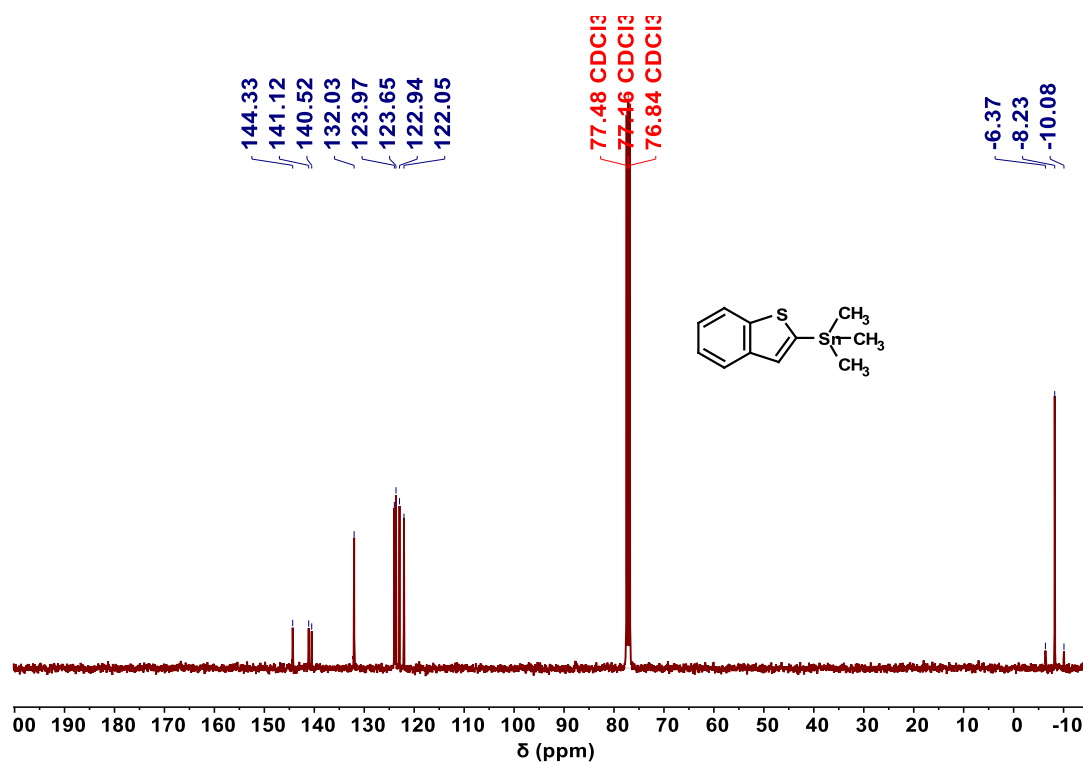


Figure S18. $^{13}\text{C}\{^1\text{H}\}$ -NMR spectrum (101 MHz, 298 K, CDCl_3) of benzo[*b*]thiophen-2-yltrimethylstannane.

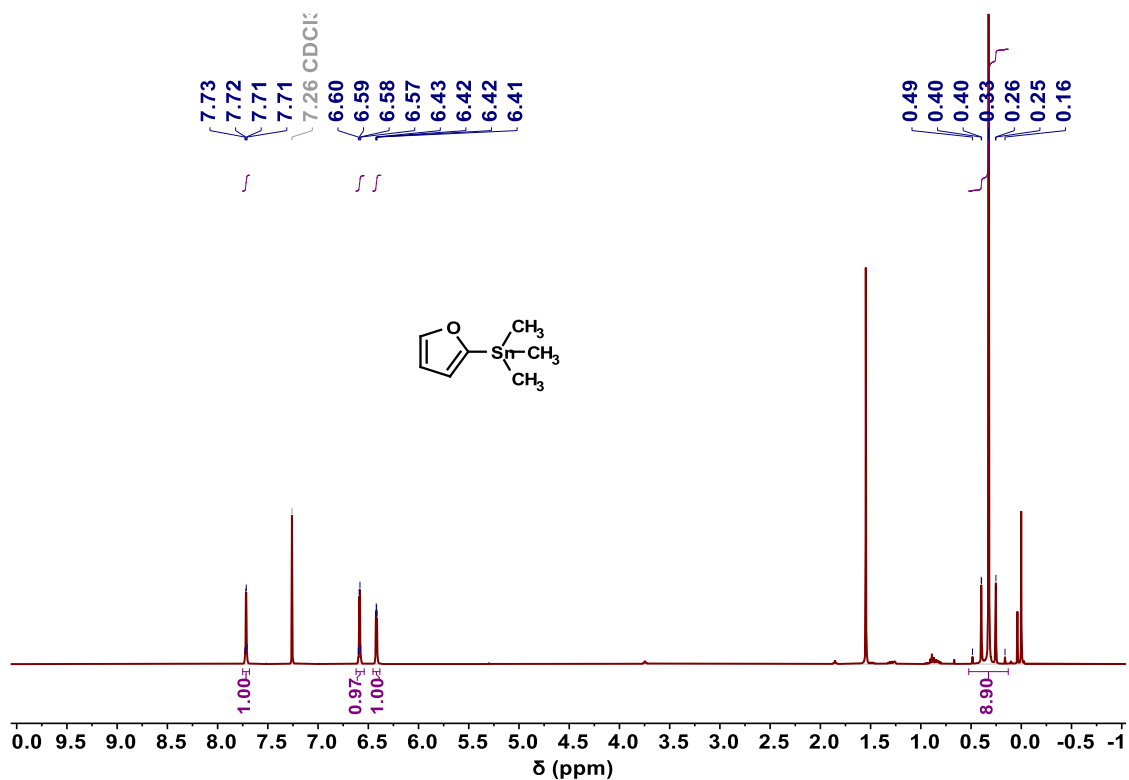


Figure S19. ¹H-NMR spectrum (400 MHz, 298 K, CDCl₃) of furan-2-yltrimethylstannane.

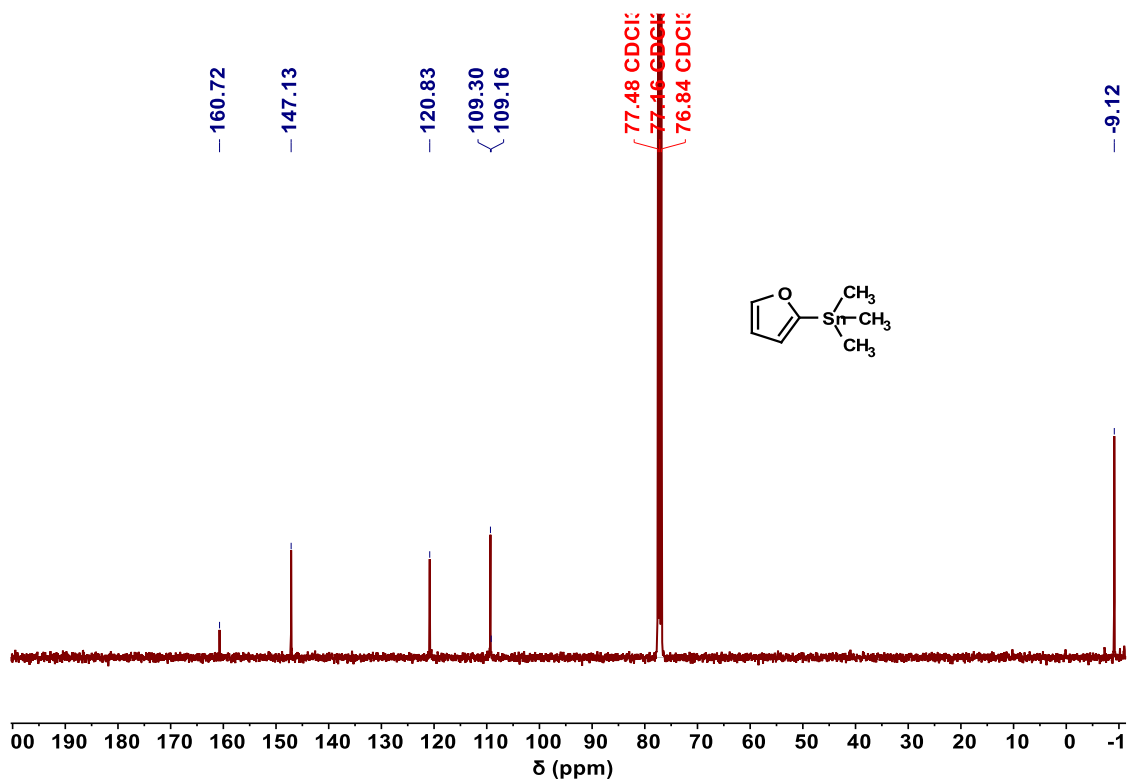


Figure S20. ¹³C{¹H}-NMR spectrum (101 MHz, 298 K, CDCl₃) of furan-2-yltrimethylstannane.

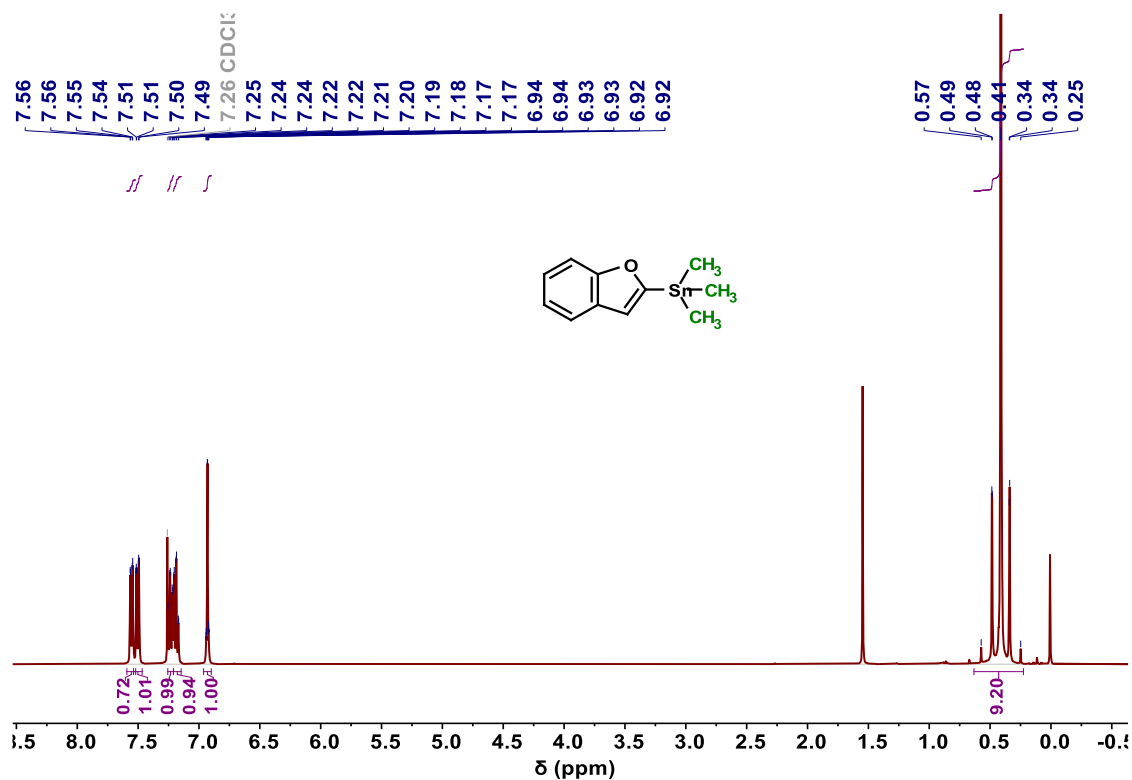


Figure S21. ^1H -NMR spectrum (400 MHz, 298 K, CDCl_3) of benzofuran-2-yltrimethylstannane.

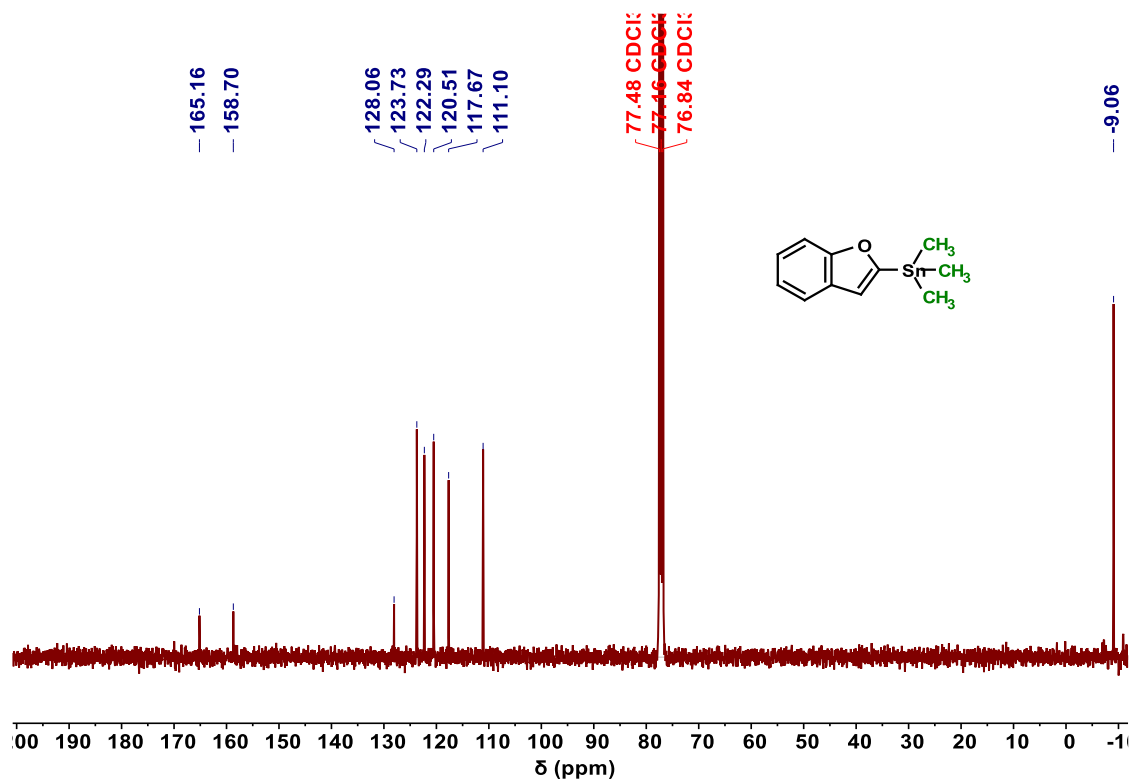
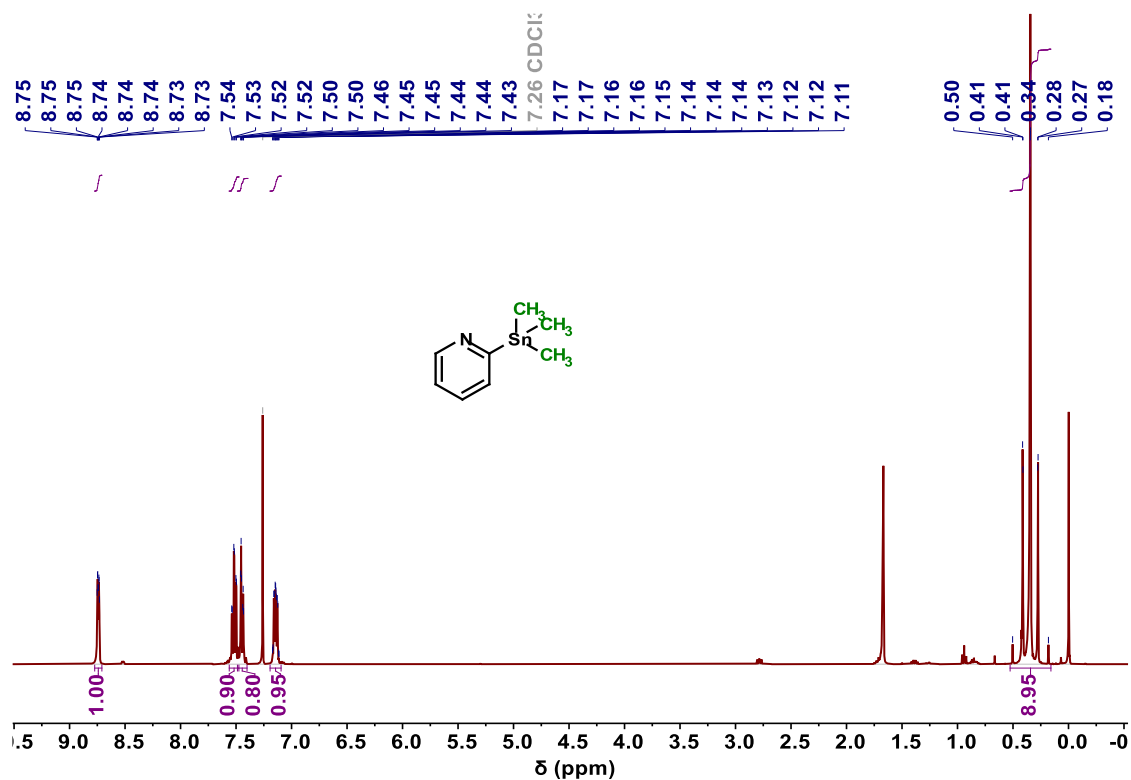


Figure S22. $^{13}\text{C}\{^1\text{H}\}$ -NMR spectrum (101 MHz, 298 K, CDCl_3) of benzofuran-2-yltrimethylstannane.



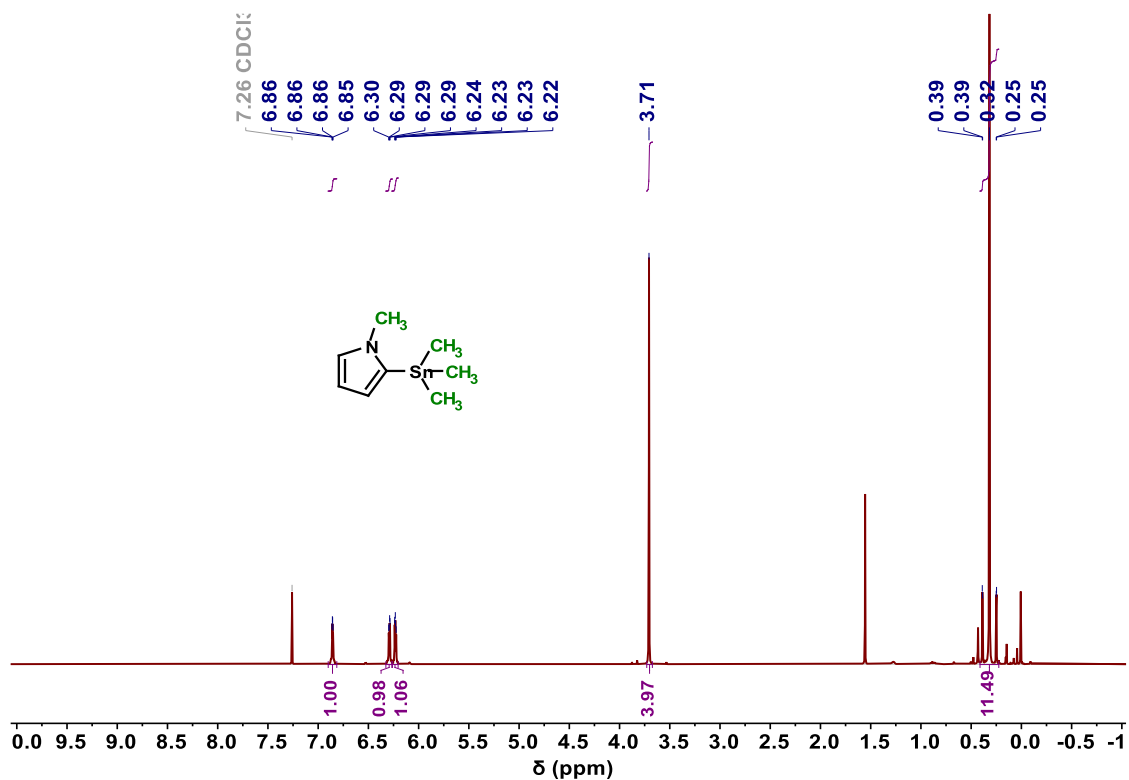


Figure S25. ^1H -NMR spectrum (400 MHz, 298 K, CDCl_3) of 1-methyl-2-(trimethylstannyl)-1H-pyrrole.

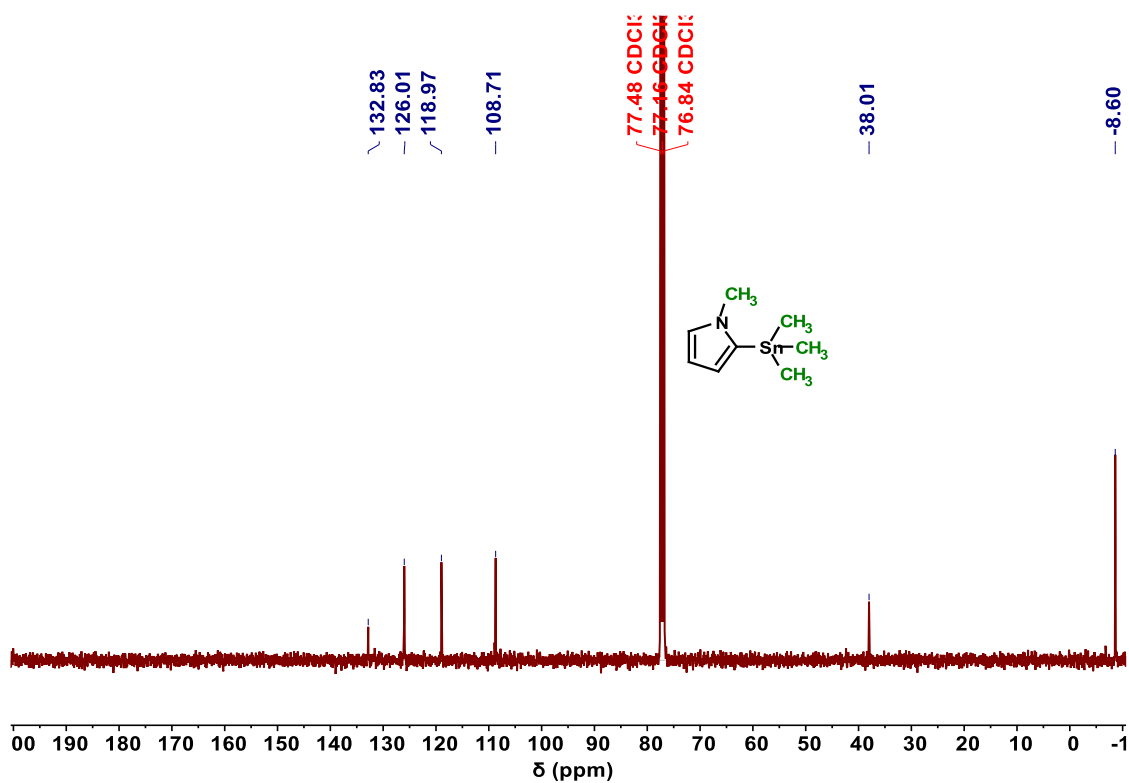


Figure S26. $^{13}\text{C}\{^1\text{H}\}$ -NMR spectrum (101 MHz, 298 K, CDCl_3) of 1-methyl-2-(trimethylstannyl)-1H-pyrrole.

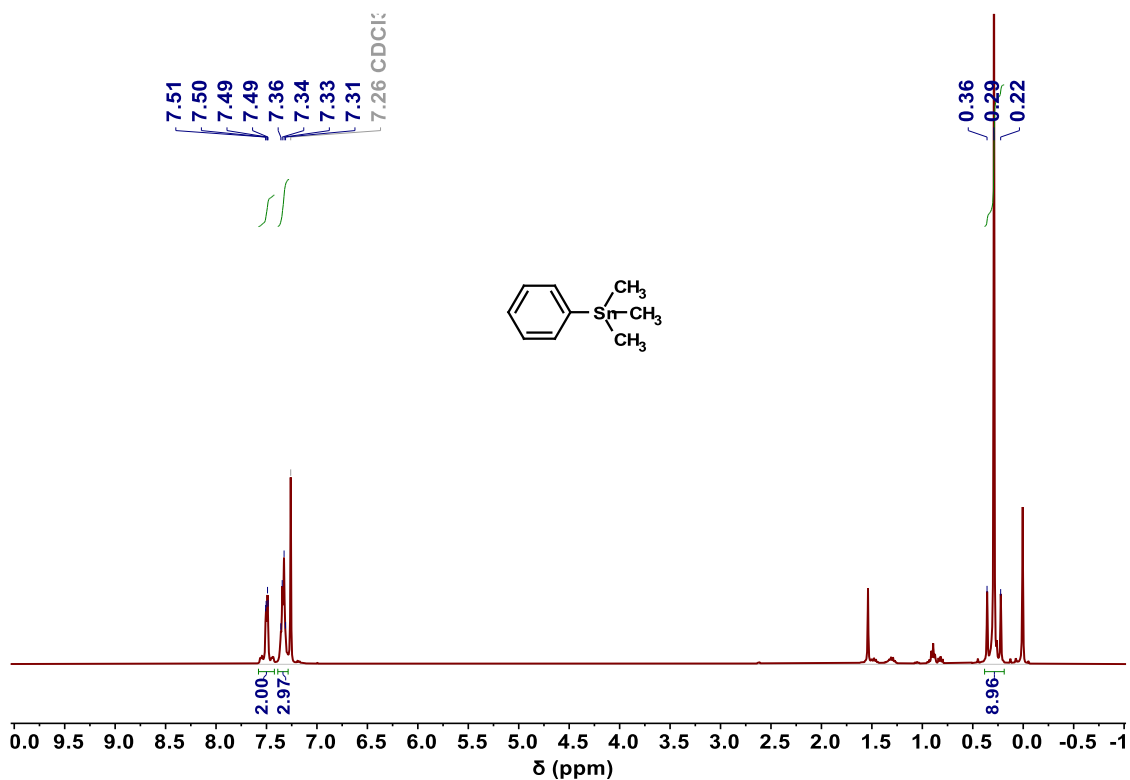


Figure S27. ^1H -NMR spectrum (400 MHz, 298 K, CDCl_3) of trimethyl(phenyl)stannane.

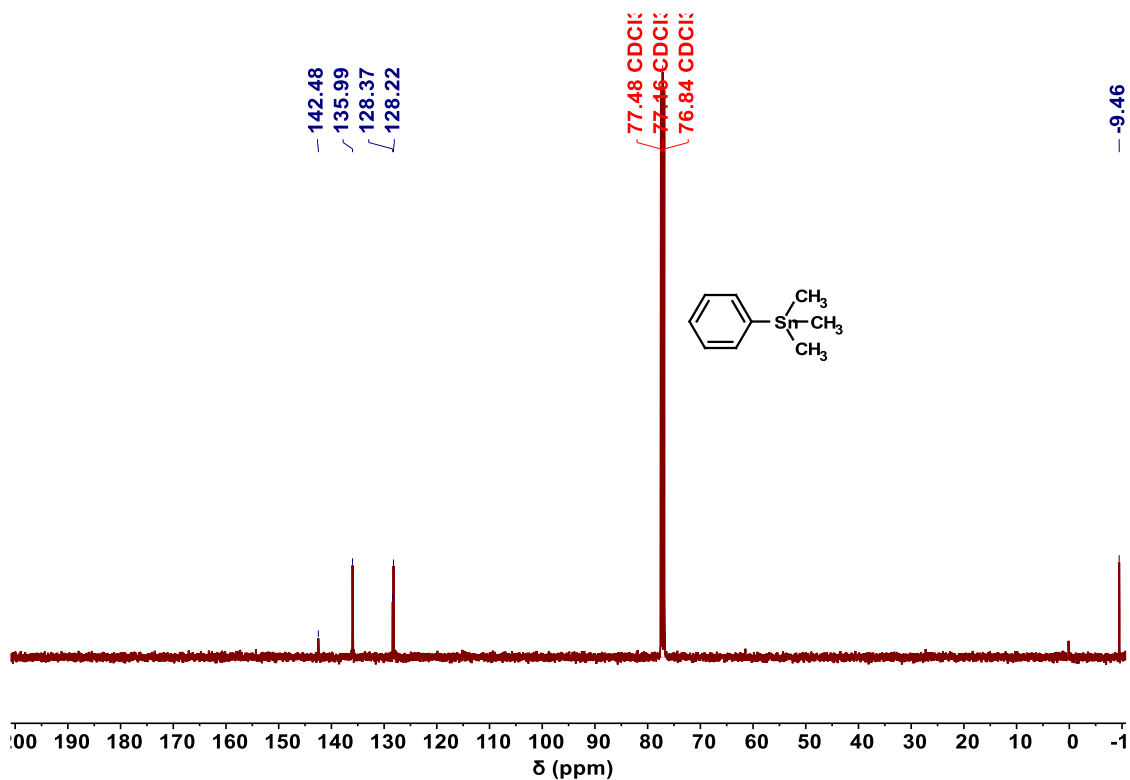


Figure S28. $^{13}\text{C}\{^1\text{H}\}$ -NMR spectrum (101 MHz, 298 K, CDCl_3) of trimethyl(phenyl)stannane.

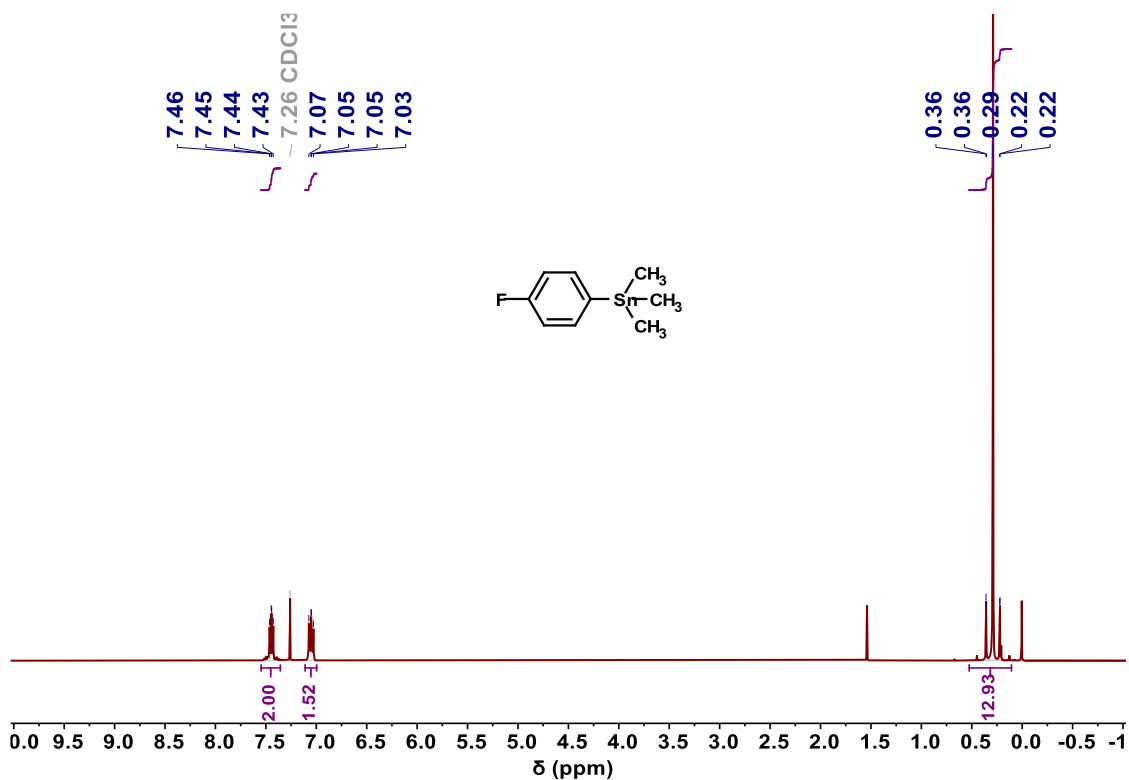


Figure S5. ¹H-NMR spectrum (400 MHz, 298 K, CDCl₃) of (4-fluorophenyl)trimethylstannane.

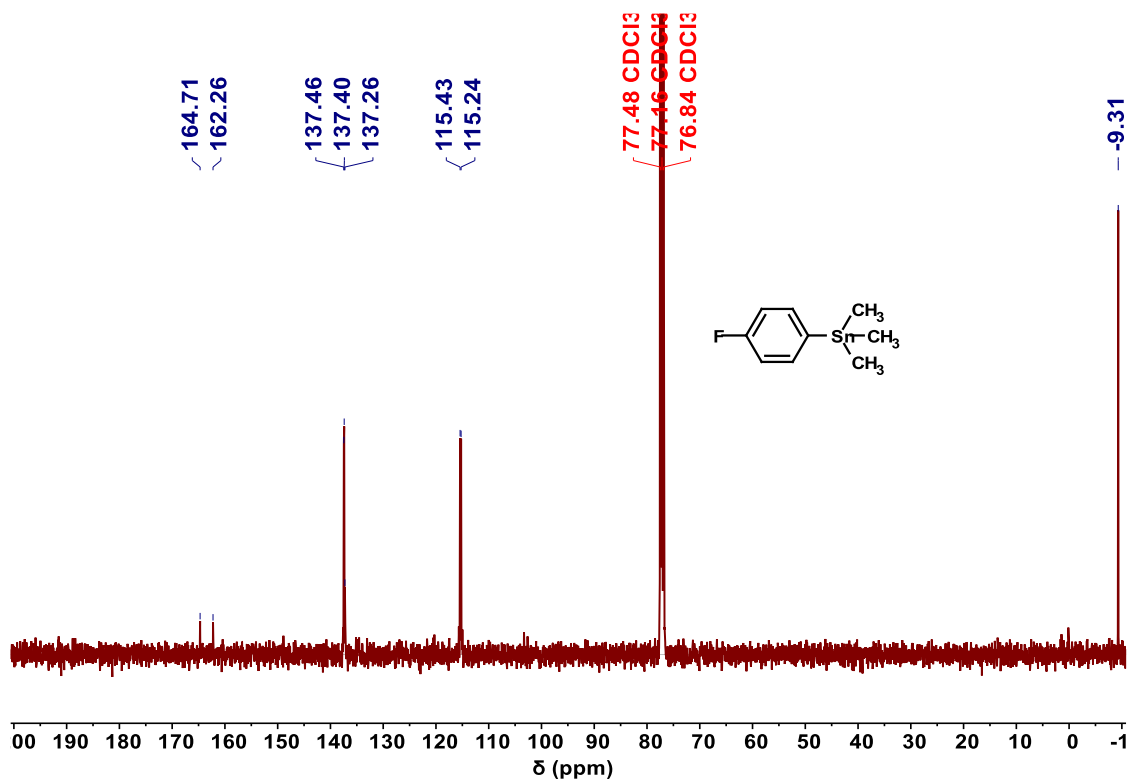


Figure S30. ¹³C{¹H}-NMR spectrum (101 MHz, 298 K, CDCl₃) of (4-fluorophenyl)trimethylstannane.

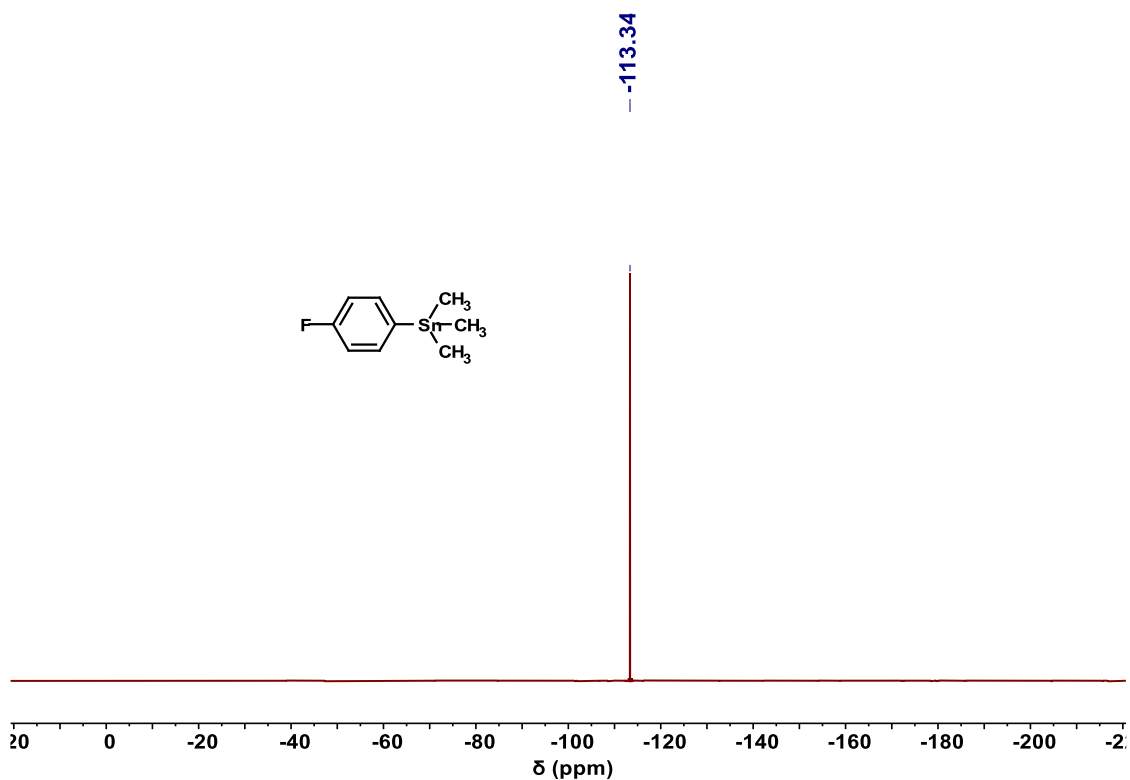


Figure S31. $^{19}\text{F}\{^1\text{H}\}$ -NMR spectrum (376 MHz, 298 K, CDCl_3) of (4-fluorophenyl)trimethylstannane.

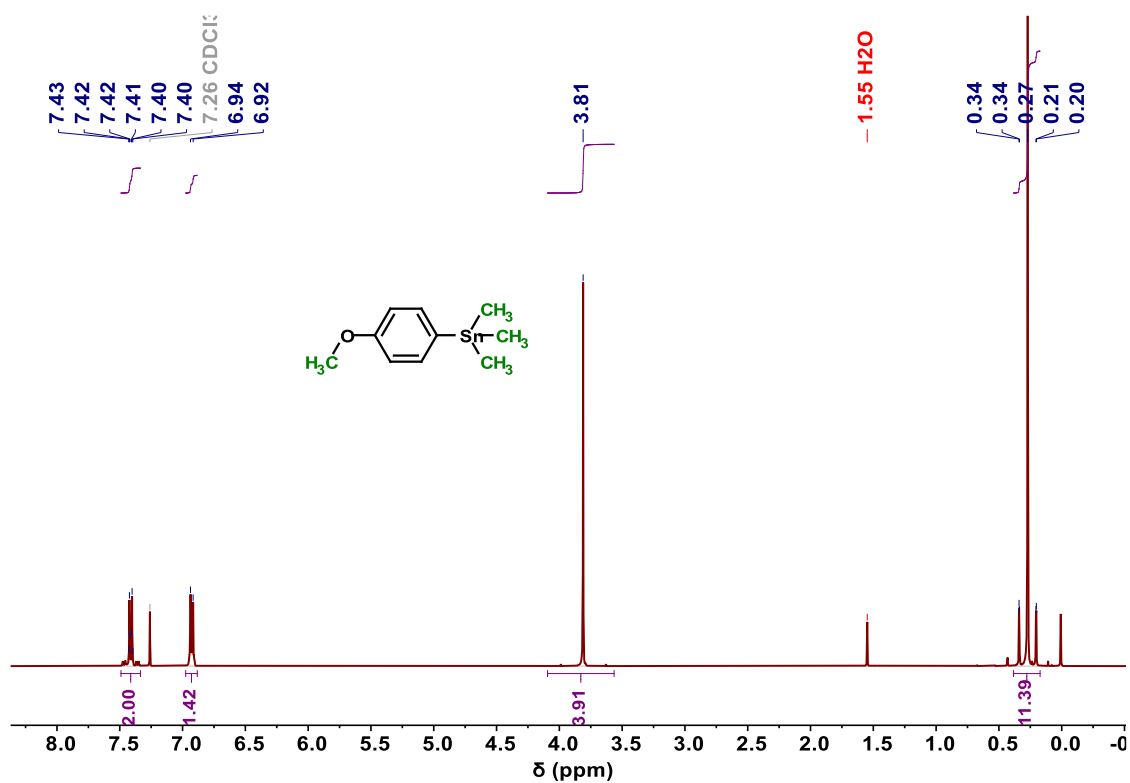


Figure S32. ^1H -NMR spectrum (400 MHz, 298 K, CDCl_3) of (4-methoxyphenyl)trimethylstannane.

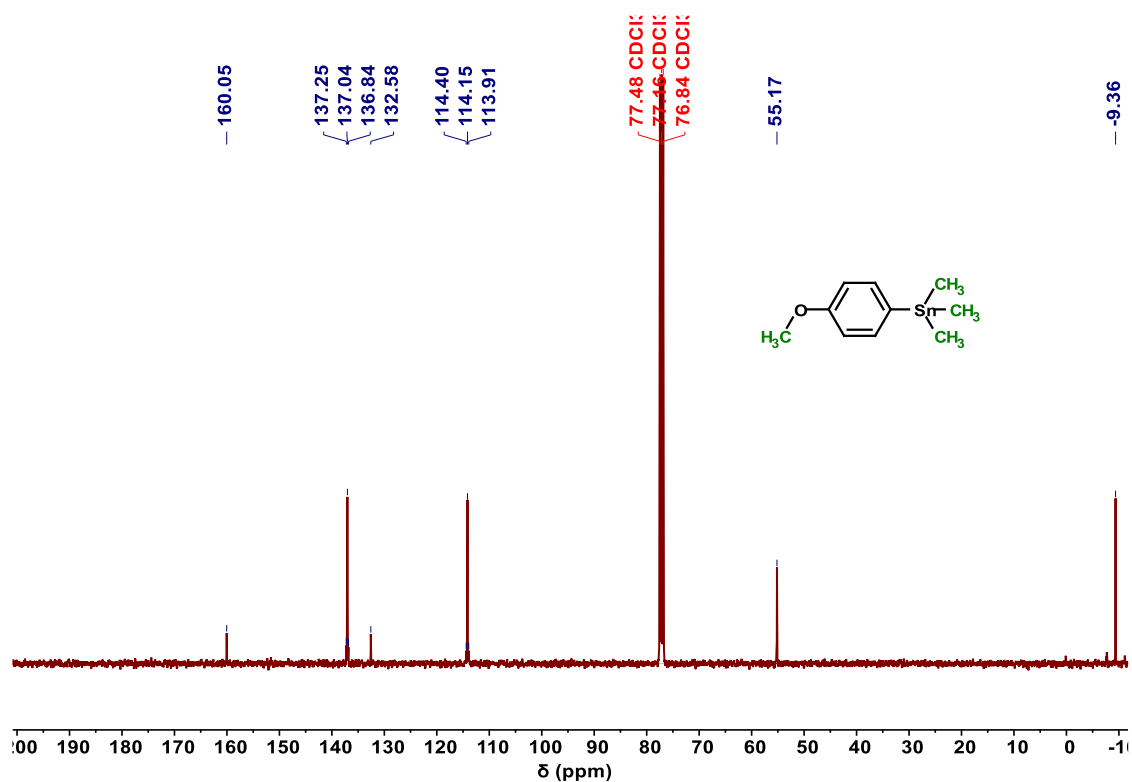


Figure S33. $^{13}\text{C}\{^1\text{H}\}$ -NMR spectrum (101 MHz, 298 K, CDCl_3) of (4-methoxyphenyl)trimethylstannane.

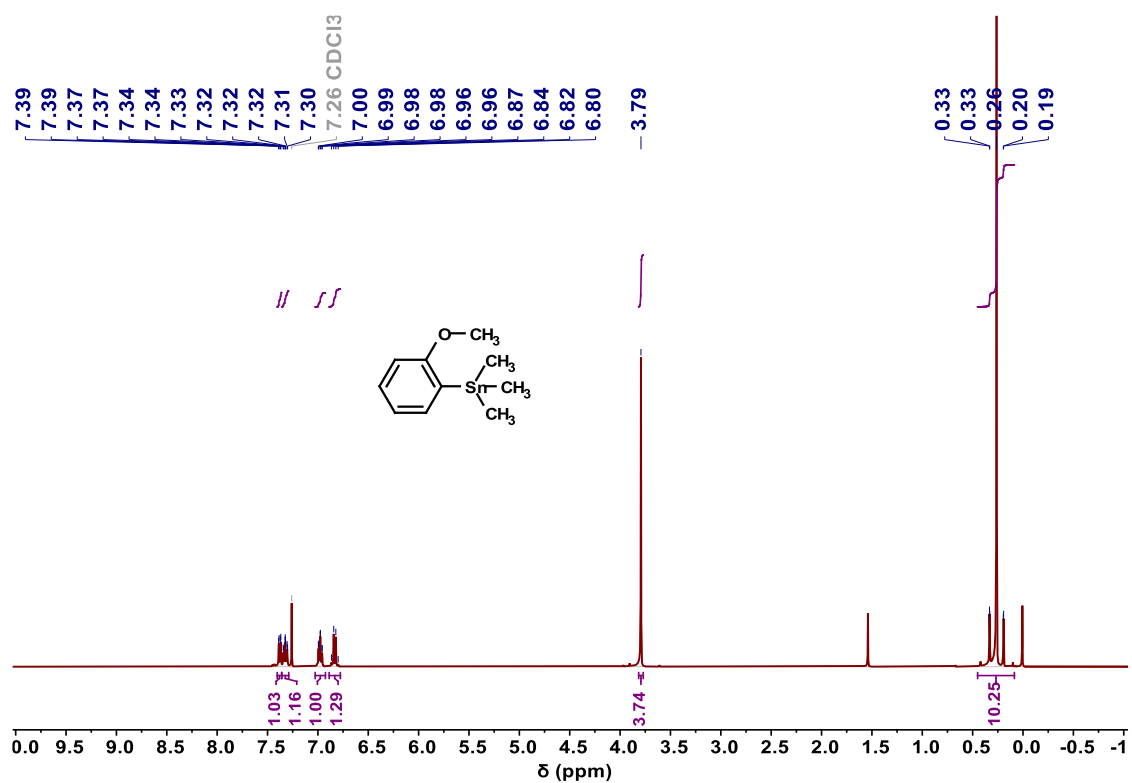


Figure S34. ^1H -NMR spectrum (400 MHz, 298 K, CDCl_3) of (2-methoxyphenyl)trimethylstannane.

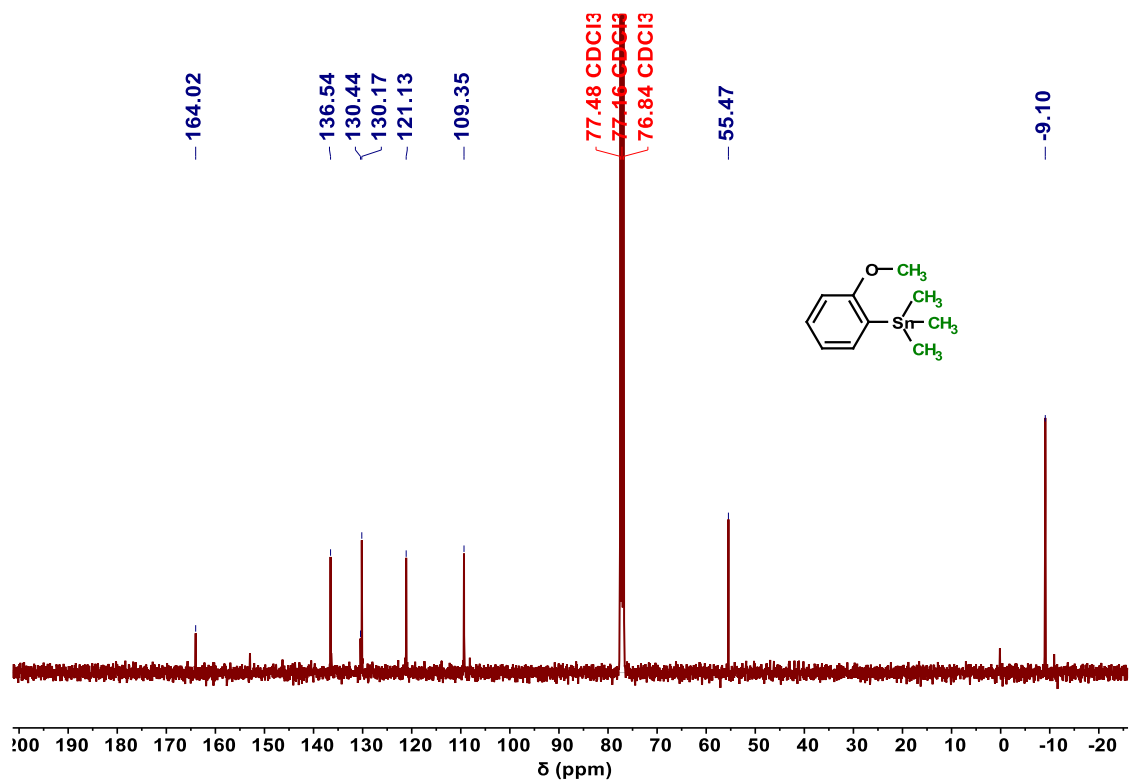


Figure S35. $^{13}\text{C}\{^1\text{H}\}$ -NMR spectrum (101 MHz, 298 K, CDCl_3) of (2-methoxyphenyl)trimethylstannane.

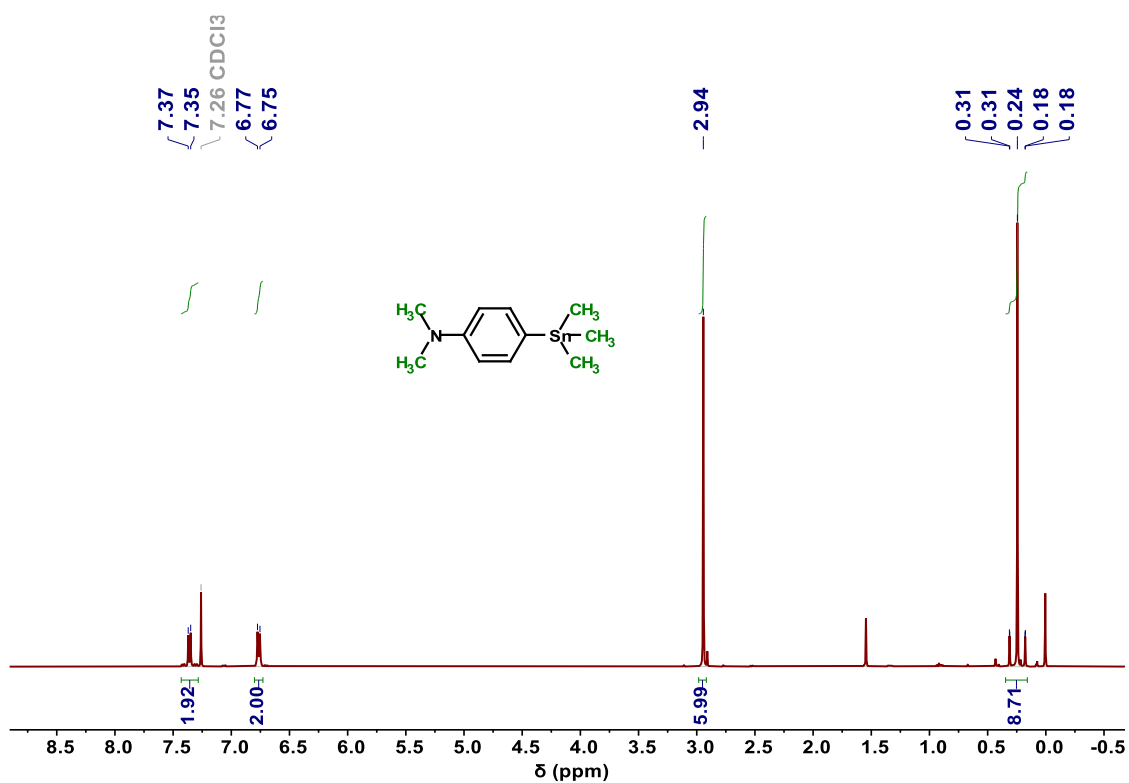


Figure S36. ^1H -NMR spectrum (400 MHz, 298 K, CDCl_3) of N,N-dimethyl-4-(trimethylstannyl)aniline.

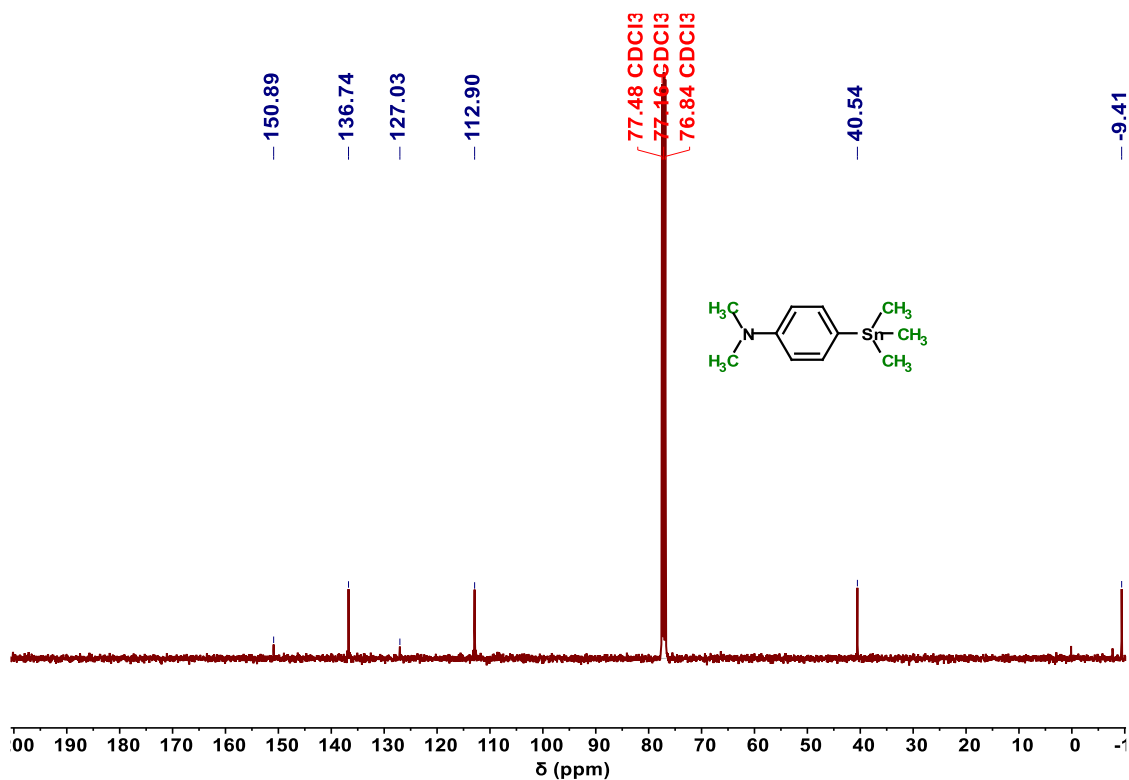


Figure S37. $^{13}\text{C}\{^1\text{H}\}$ -NMR spectrum (101 MHz, 298 K, CDCl_3) of N,N-dimethyl-4-(trimethylstannyl)aniline.

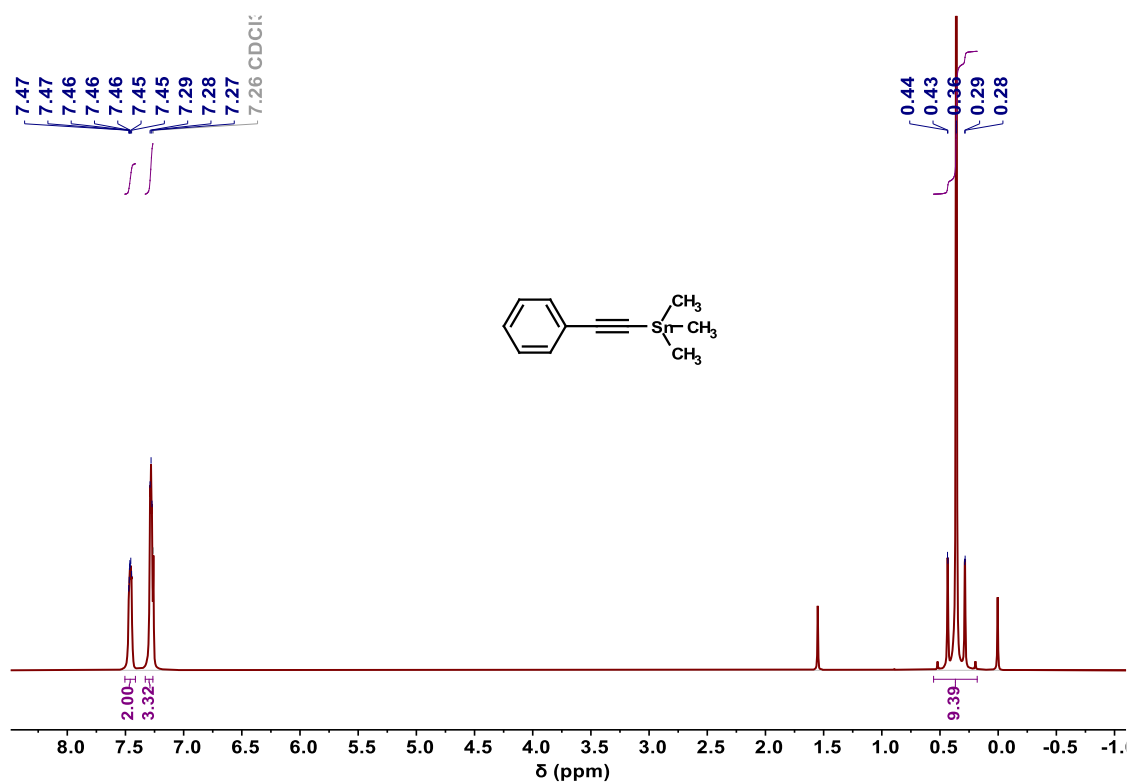


Figure S38. ^1H -NMR spectrum (400 MHz, 298 K, CDCl_3) of trimethyl(phenylethynyl)stannane.

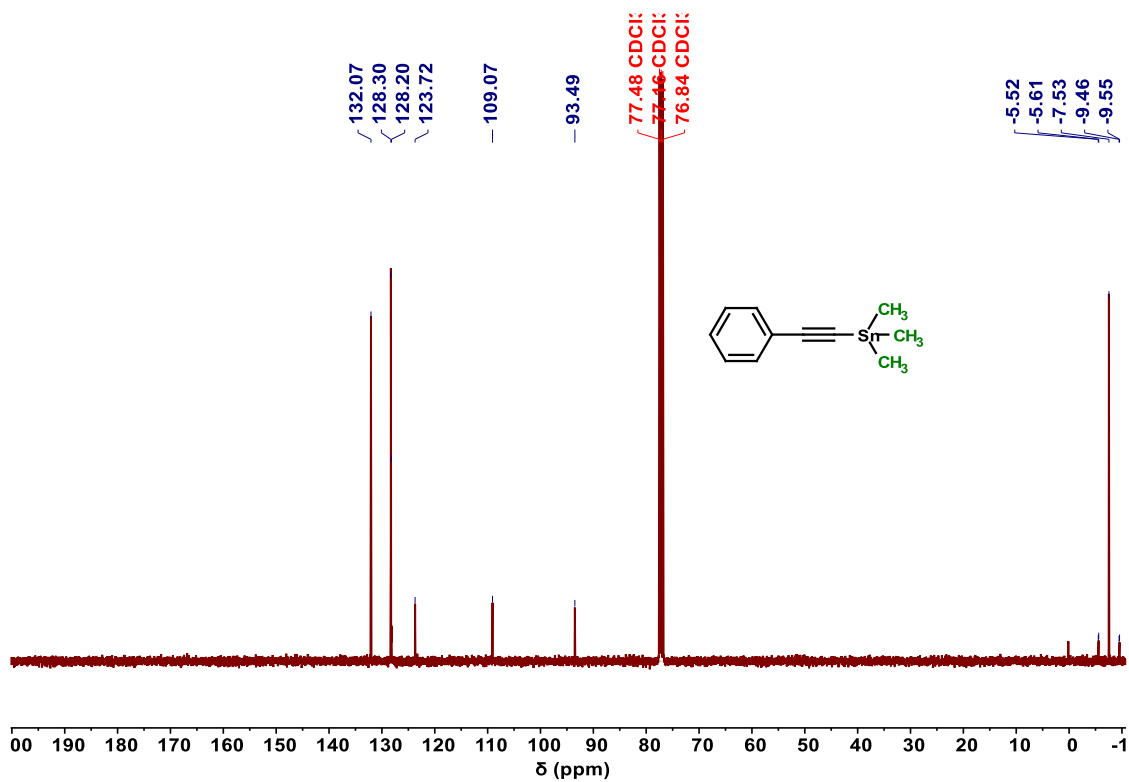


Figure S6. $^{13}\text{C}\{^1\text{H}\}$ -NMR spectrum (101 MHz, 298 K, CDCl_3) of trimethyl(phenylethynyl)stannane.

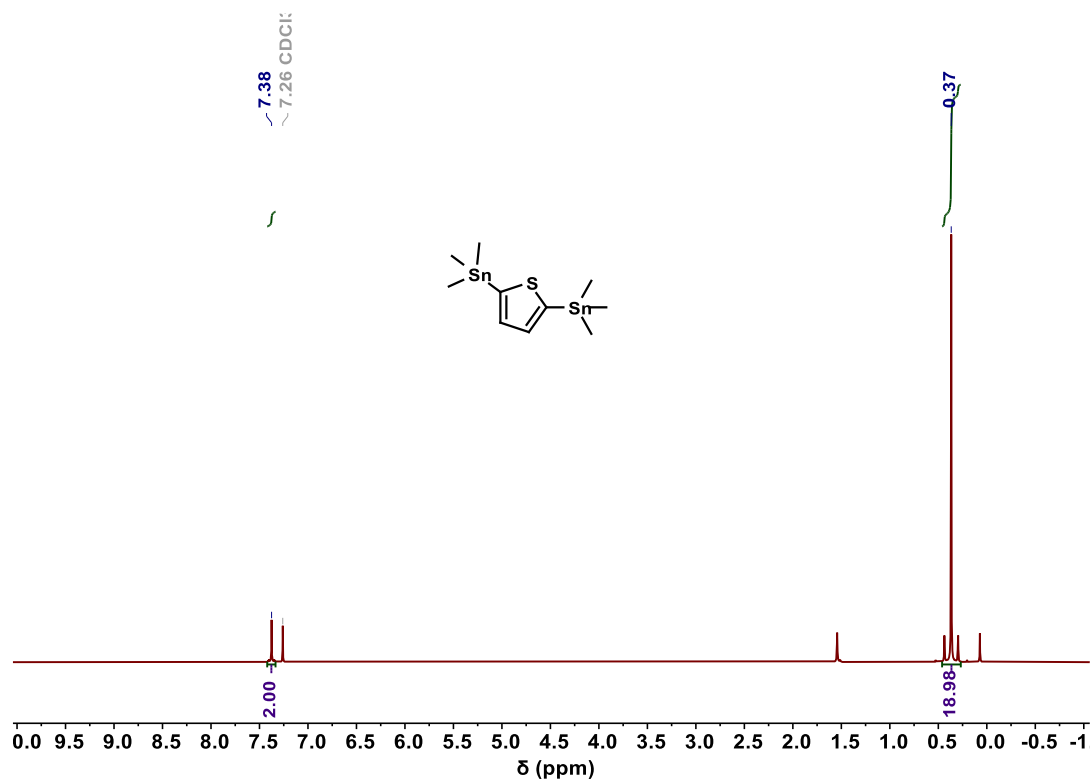


Figure S40. ^1H -NMR spectrum (400 MHz, 298 K, CDCl_3) of **B1**.

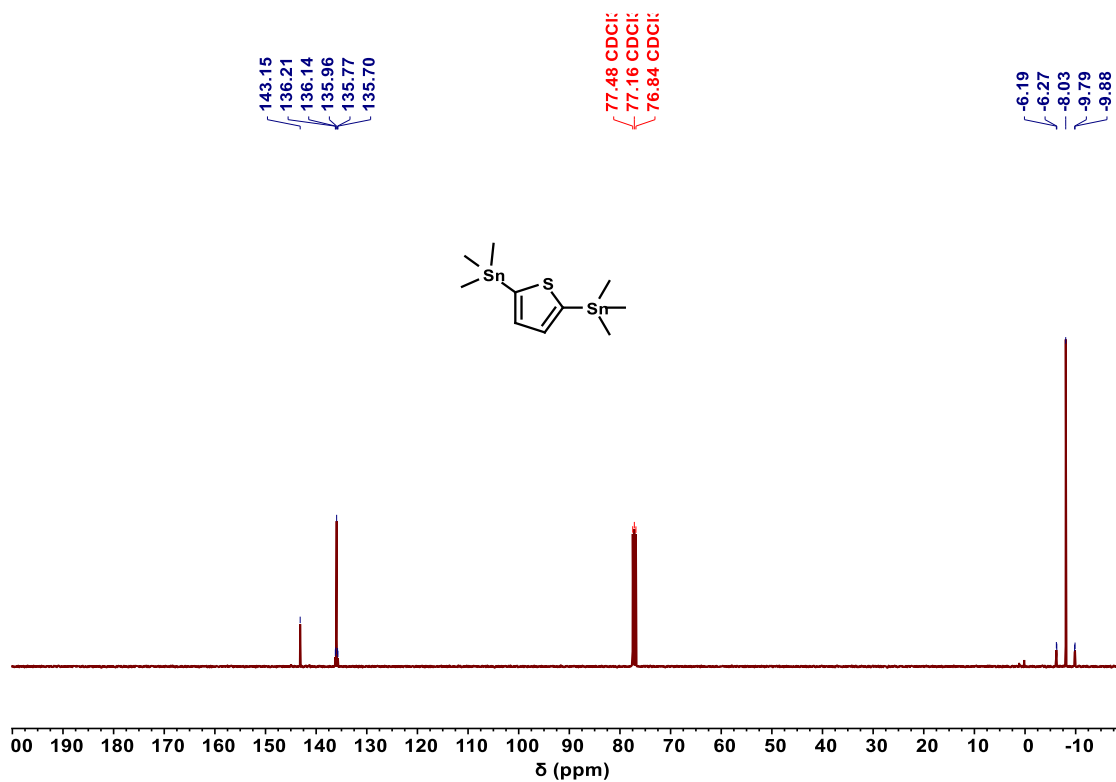


Figure S41. $^{13}\text{C}\{^1\text{H}\}$ -NMR spectrum (101 MHz, 298 K, CDCl_3) of **B1**.

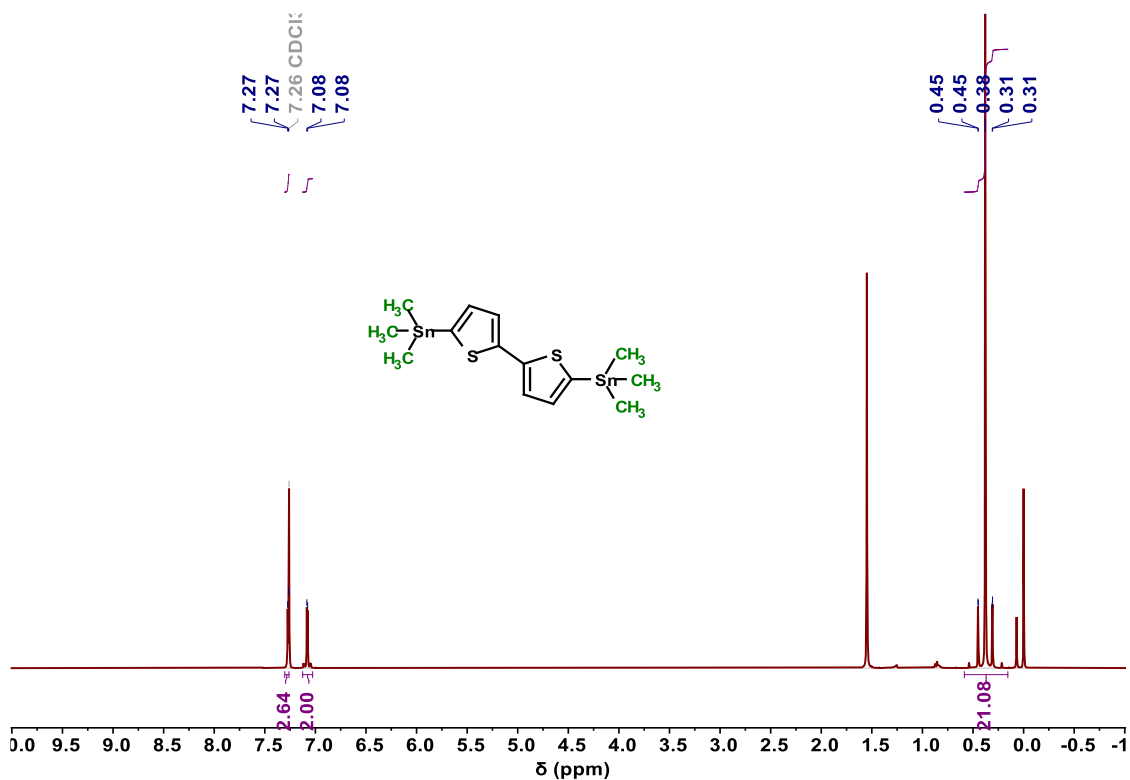


Figure S42. ^1H -NMR spectrum (400 MHz, 298 K, CDCl_3) of **B2**.

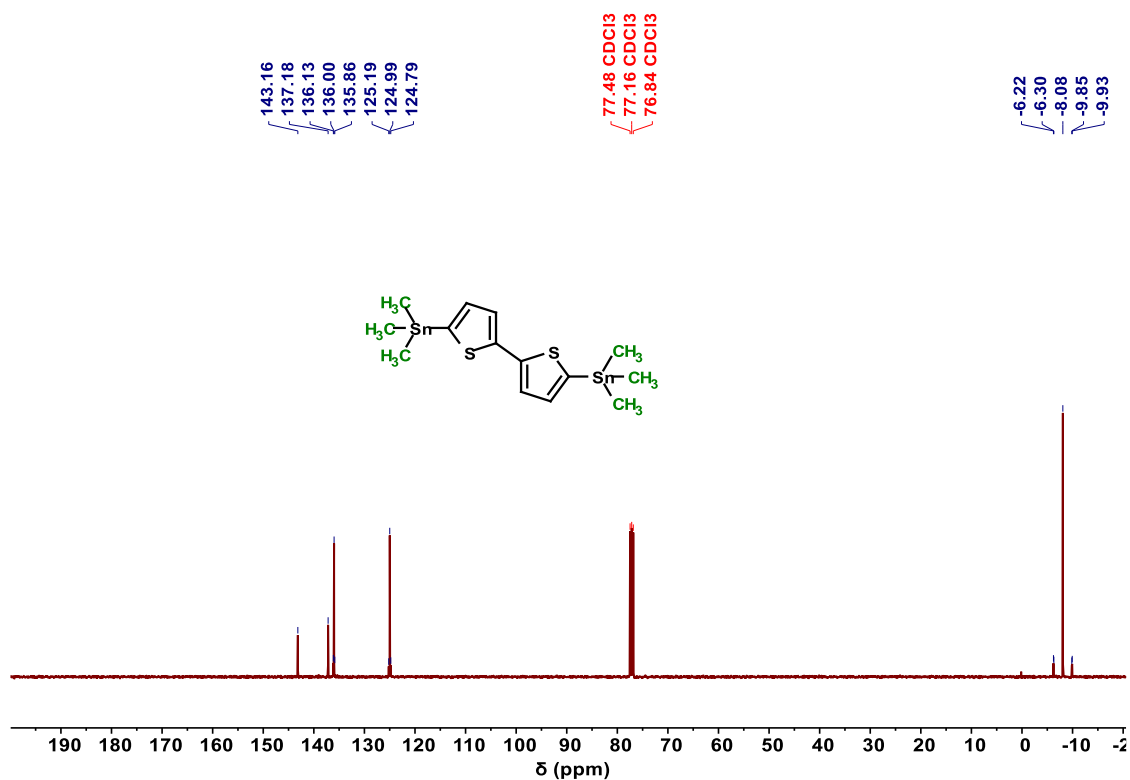


Figure S43. $^{13}\text{C}\{^1\text{H}\}$ -NMR spectrum (101 MHz, 298 K, CDCl_3) of **B2**.

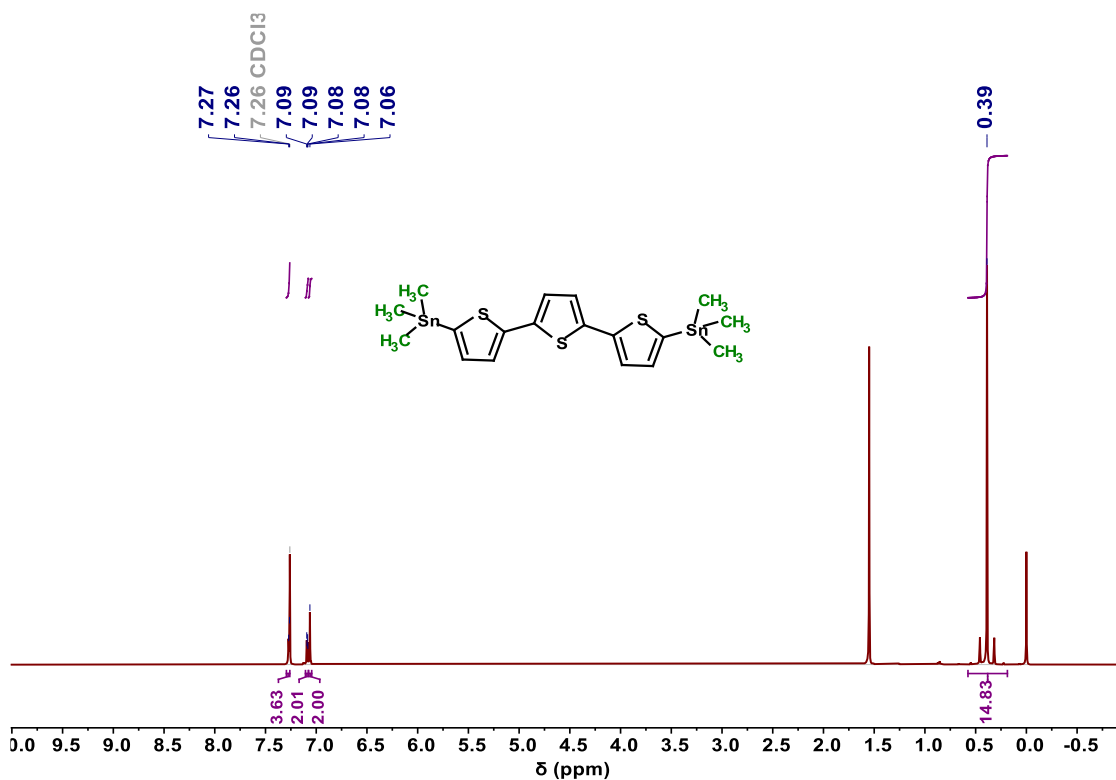


Figure S44. ^1H -NMR spectrum (400 MHz, 298 K, CDCl_3) of **B3**.

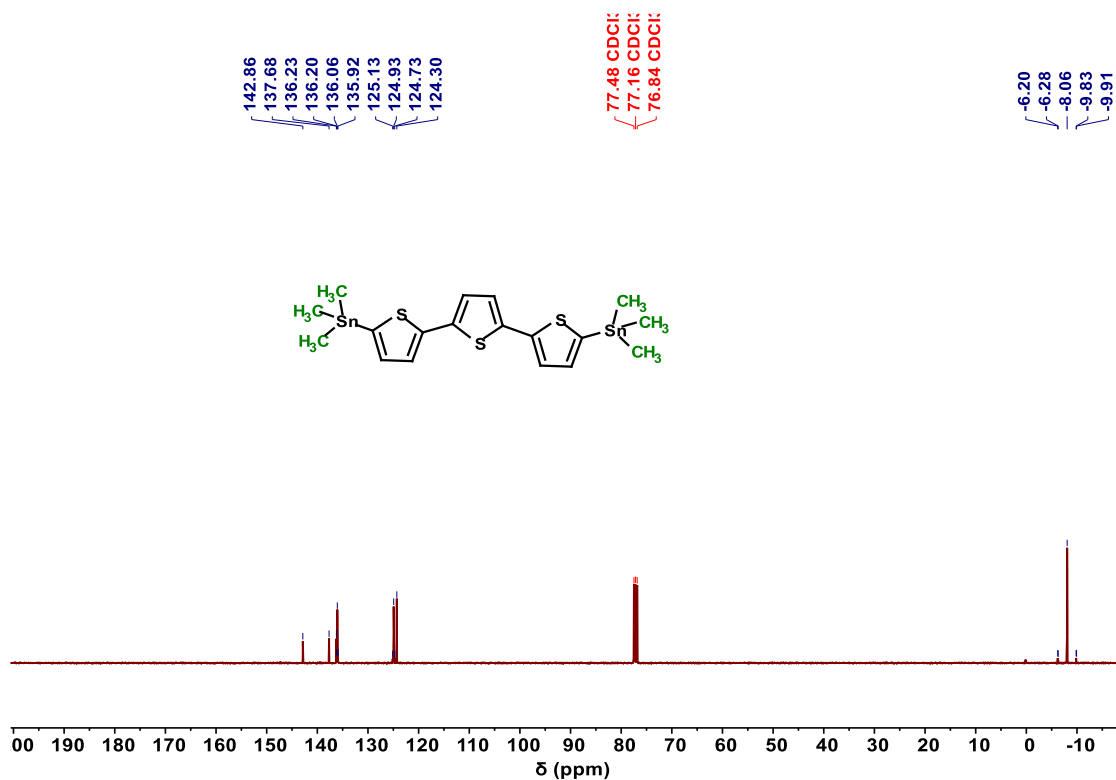


Figure S45. $^{13}\text{C}\{^1\text{H}\}$ -NMR spectrum (101 MHz, 298 K, CDCl_3) of **B3**.

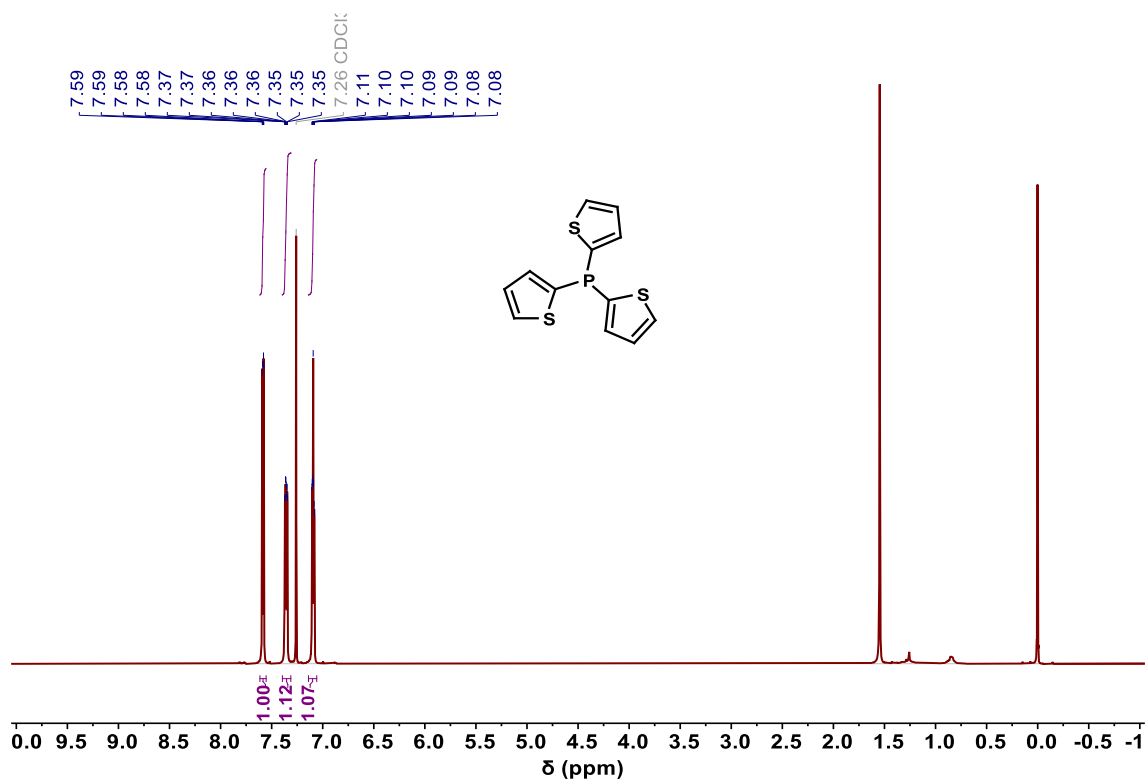


Figure S46. ^1H -NMR spectrum (400 MHz, 298 K, CDCl_3) of **1**.

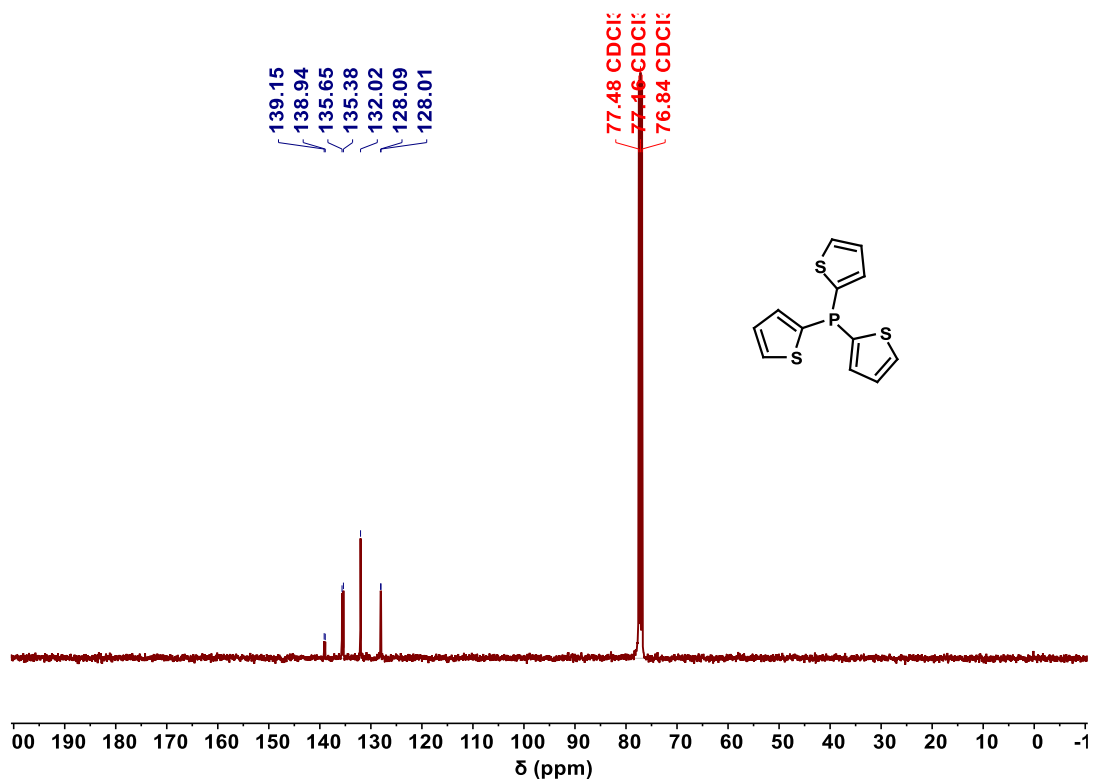


Figure S47. $^{13}\text{C}\{^1\text{H}\}$ -NMR spectrum (101 MHz, 298 K, CDCl_3) of **1**.

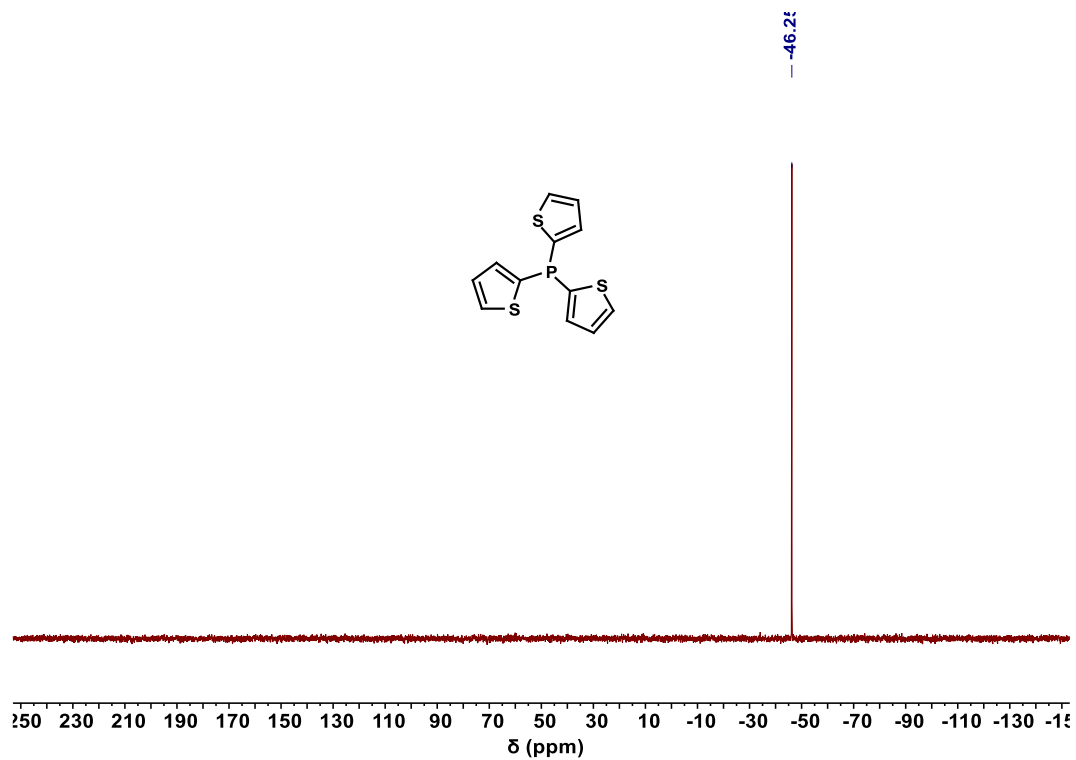


Figure S48. $^{31}\text{P}\{^1\text{H}\}$ -NMR spectrum (162 MHz, 298 K, CDCl_3) of **1**.

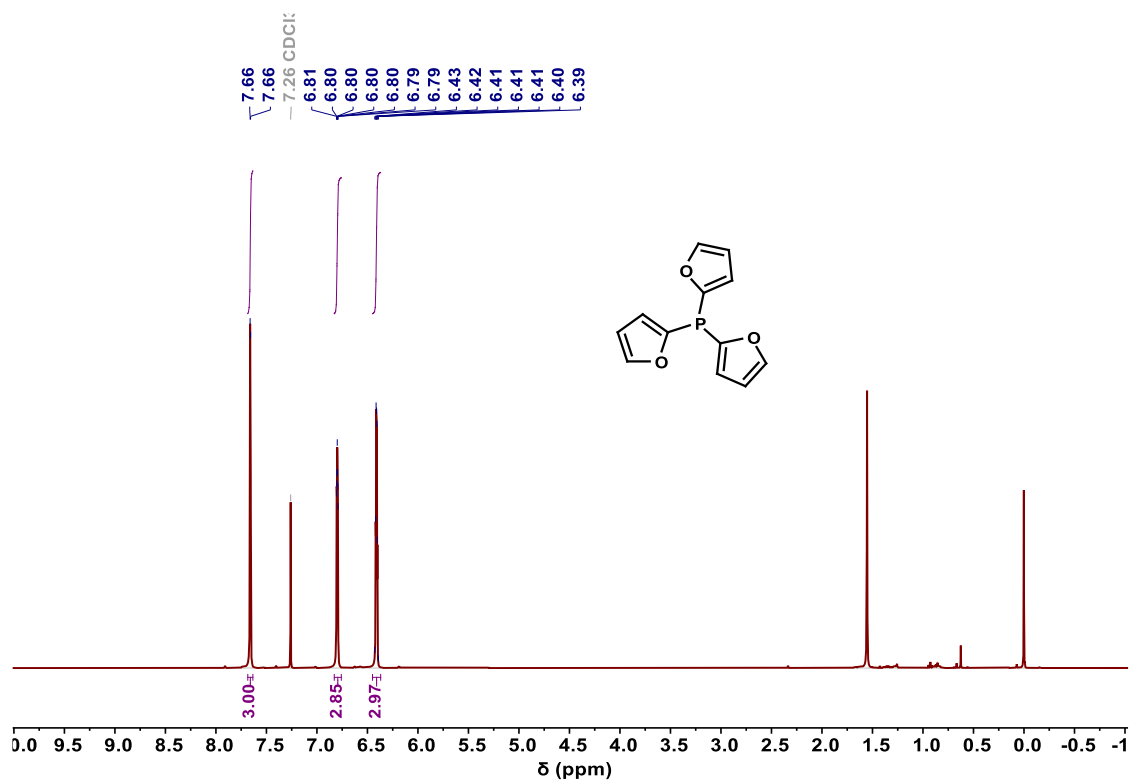


Figure S49. $^1\text{H-NMR}$ spectrum (400 MHz, 298 K, CDCl_3) of **2**.

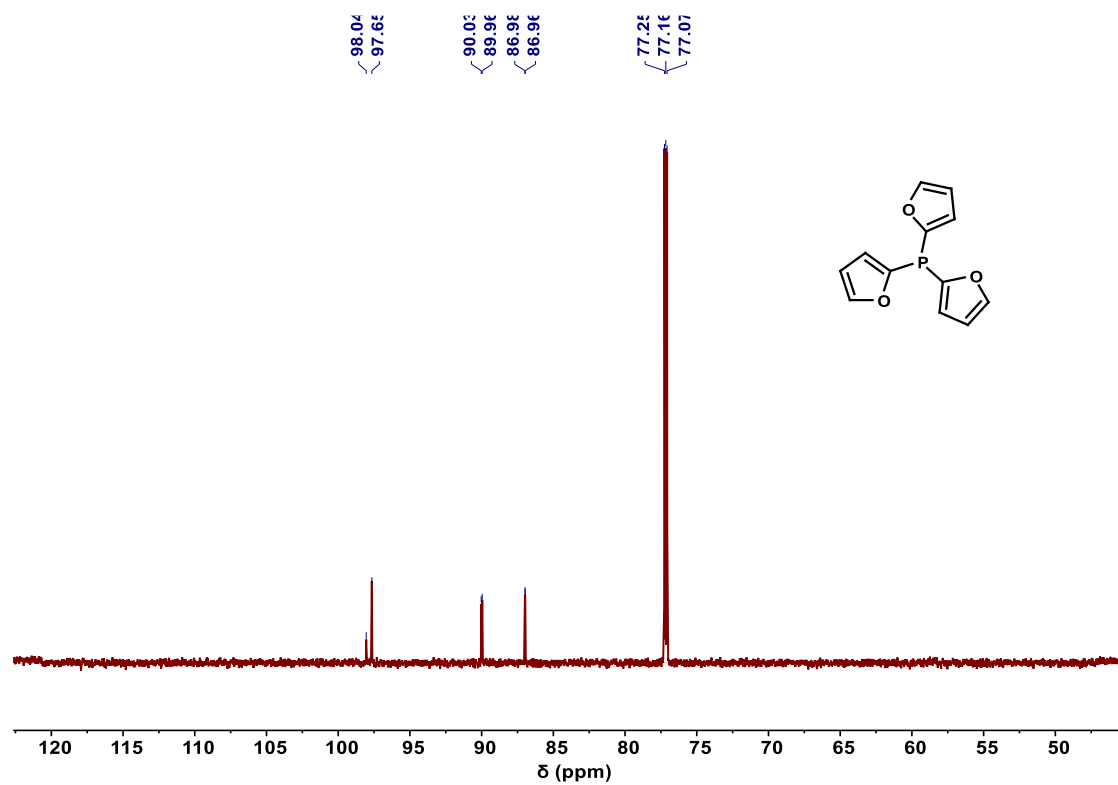


Figure S50. $^{13}\text{C}\{^1\text{H}\}$ -NMR spectrum (101 MHz, 298 K, CDCl_3) of **2**.

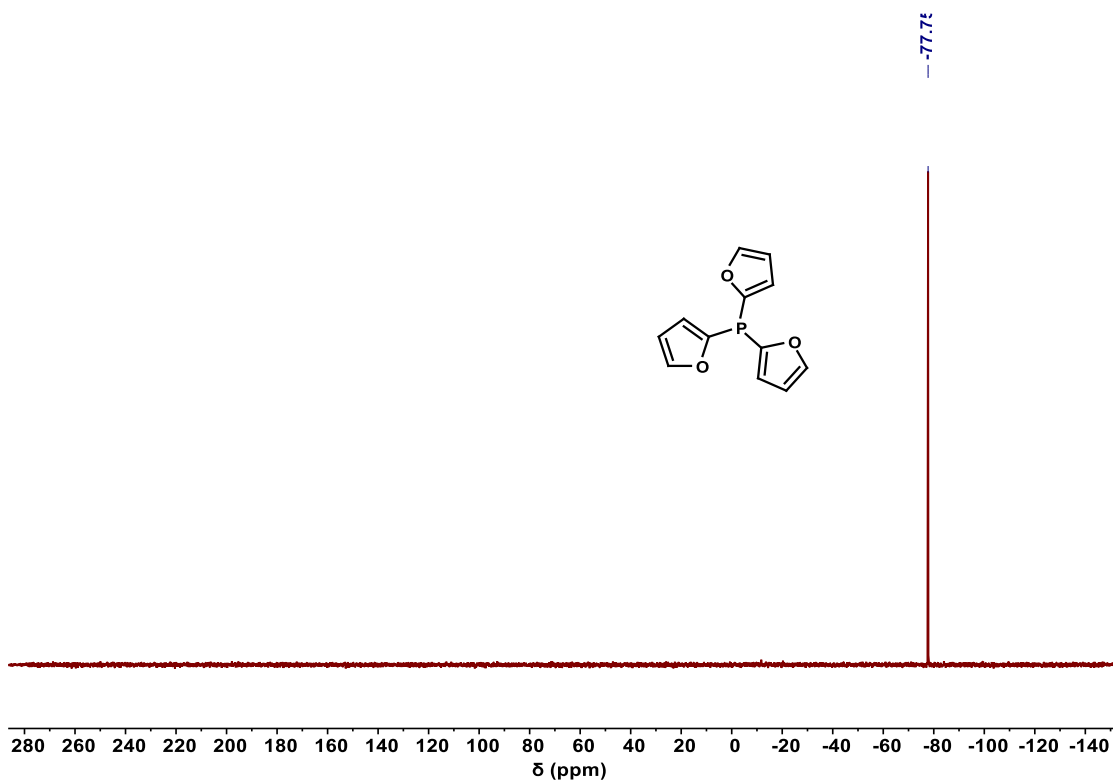


Figure S51. $^{31}\text{P}\{^1\text{H}\}$ -NMR spectrum (162 MHz, 298 K, CDCl_3) of 2.

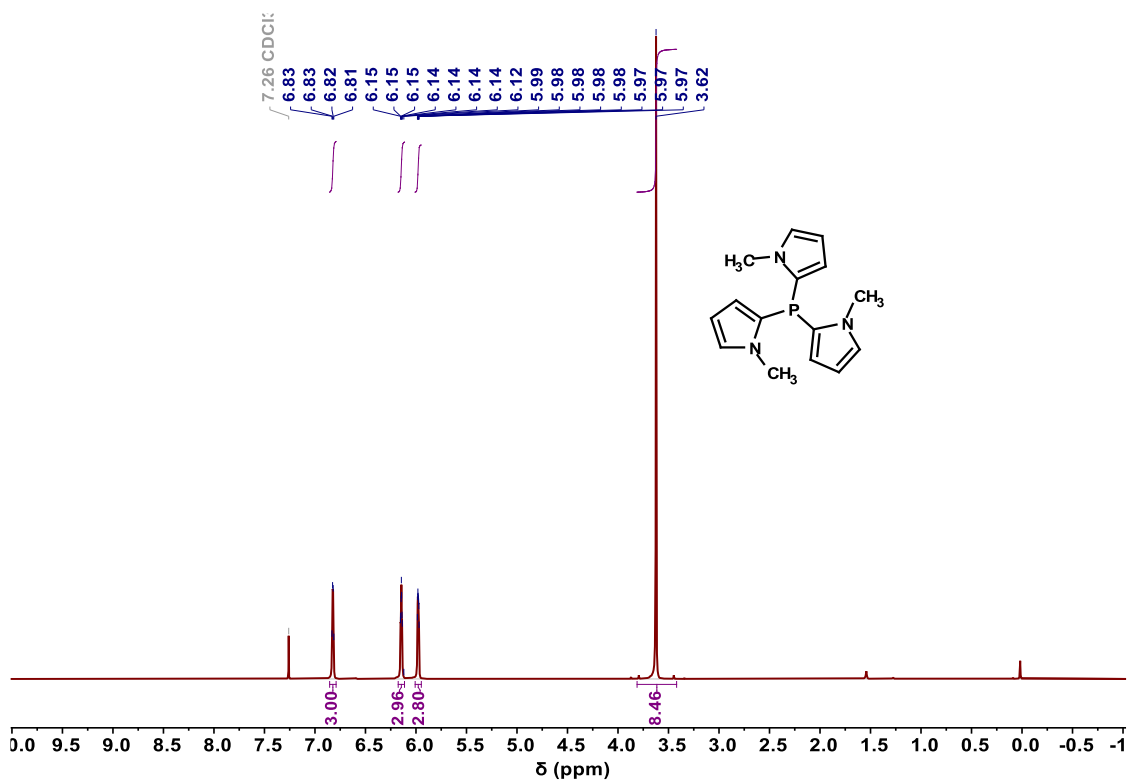


Figure S52. ^1H -NMR spectrum (400 MHz, 298 K, CDCl_3) of 3.

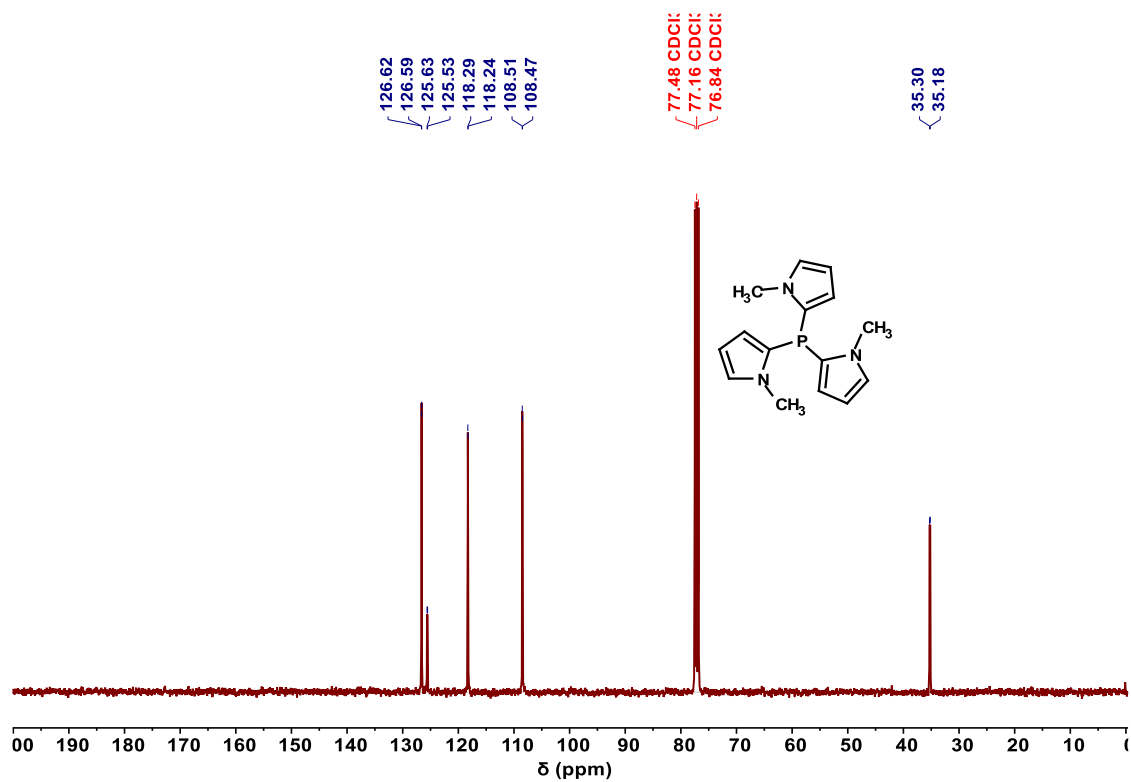


Figure S53. $^{13}\text{C}\{^1\text{H}\}$ -NMR spectrum (101 MHz, 298 K, CDCl_3) of **3**.

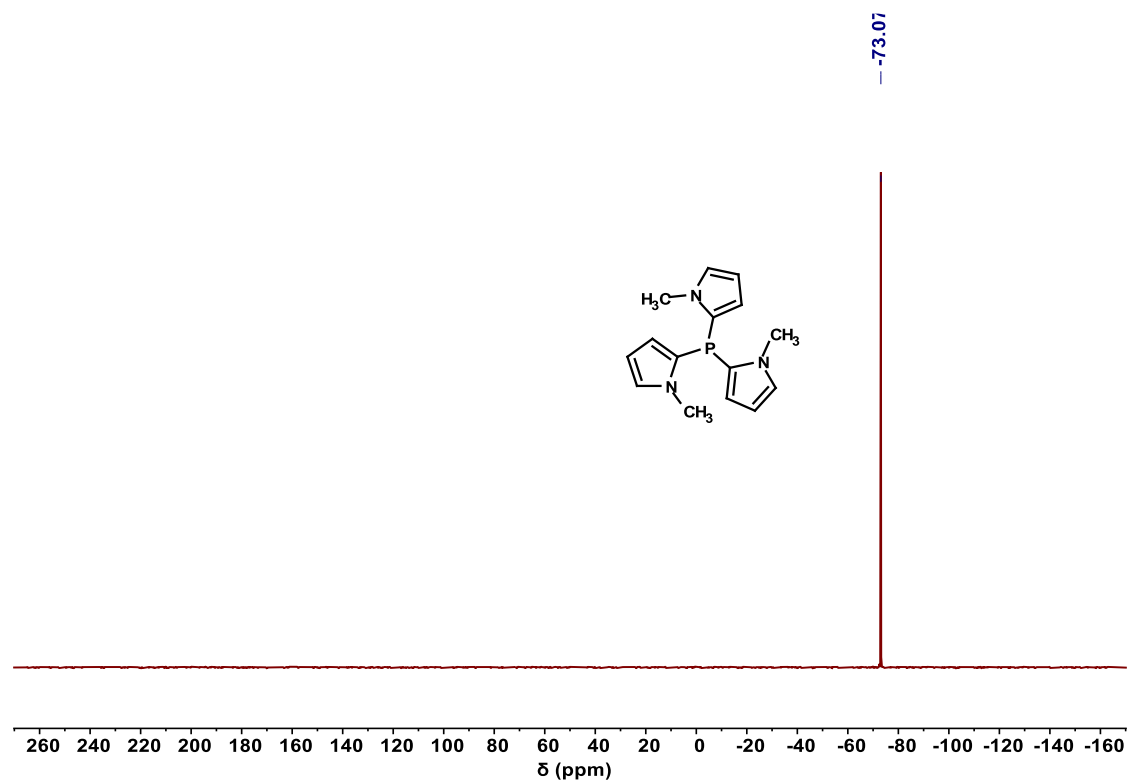


Figure S54. $^{31}\text{P}\{^1\text{H}\}$ -NMR spectrum (162 MHz, 298 K, CDCl_3) of **3**.

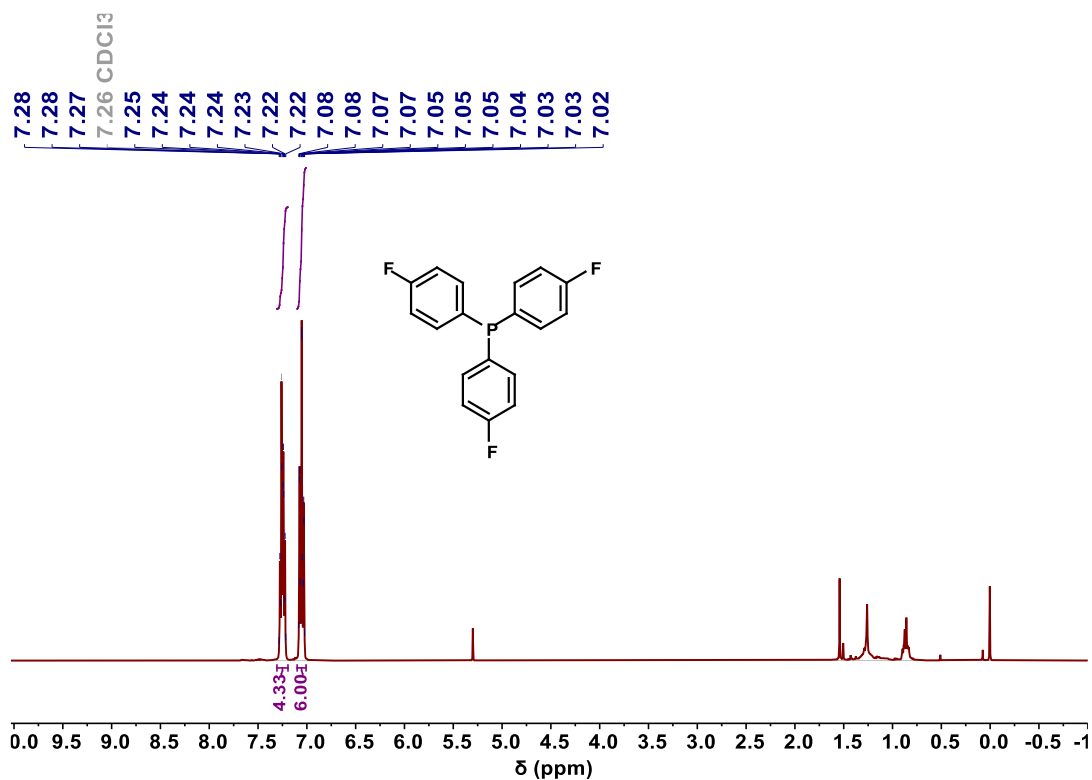


Figure S55. ¹H-NMR spectrum (400 MHz, 298 K, CDCl₃) of **5**.

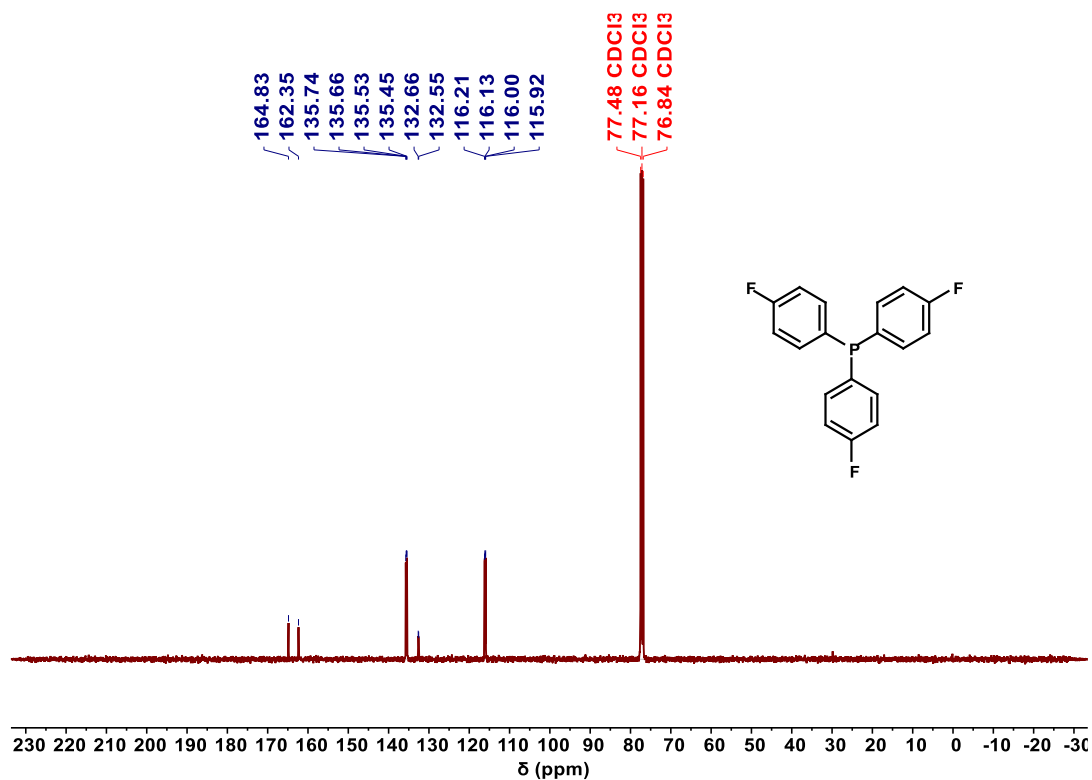


Figure S56. ¹³C{¹H}-NMR spectrum (101 MHz, 298 K, CDCl₃) of **5**.

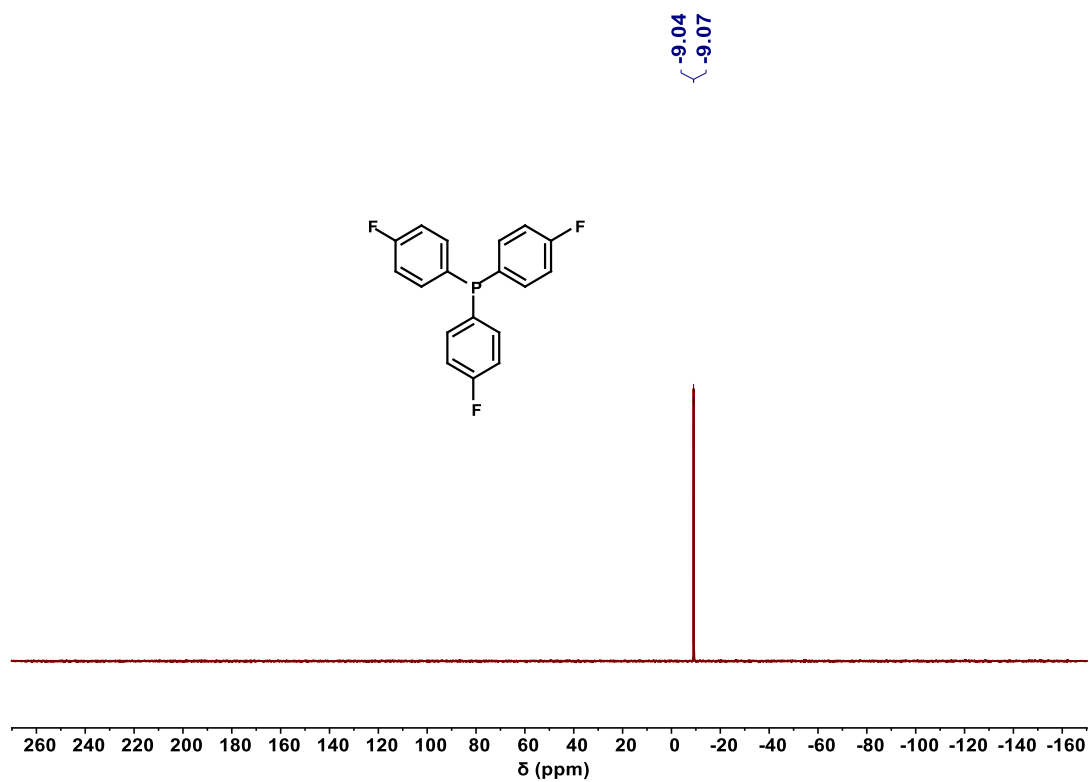


Figure S7. $^{31}\text{P}\{^1\text{H}\}$ -NMR spectrum (162 MHz, 298 K, CDCl_3) of **5**.

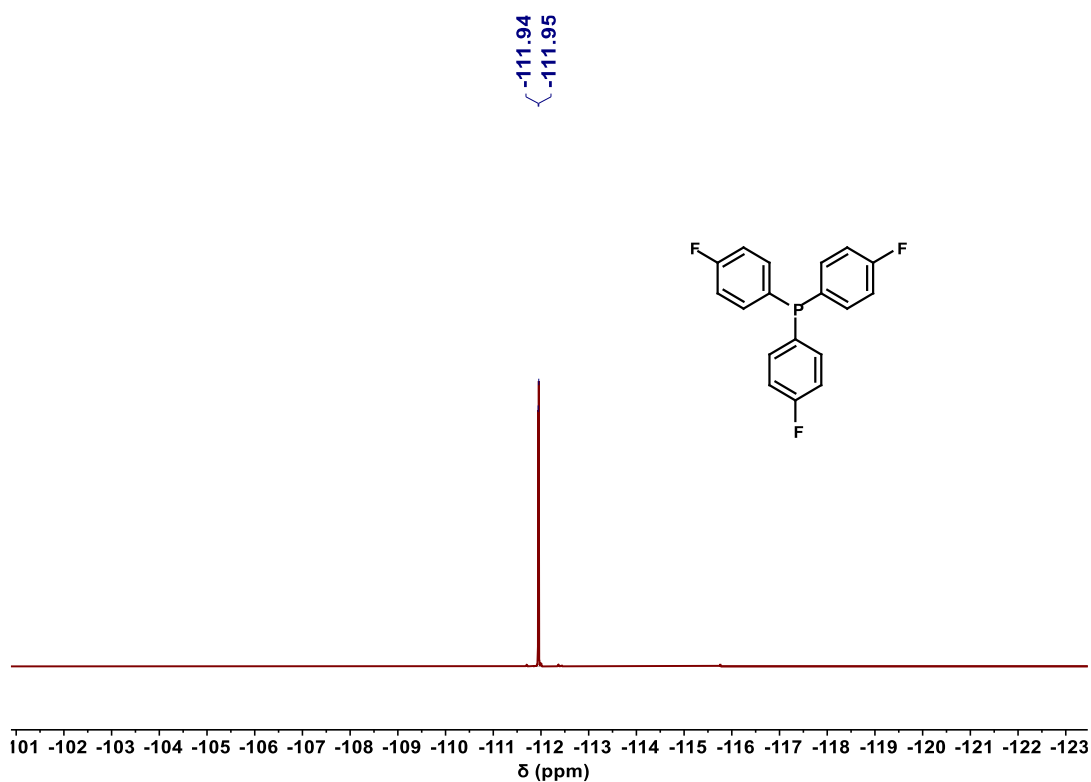


Figure S58. $^{19}\text{F}\{^1\text{H}\}$ -NMR spectrum (376 MHz, 298 K, CDCl_3) of **5**.

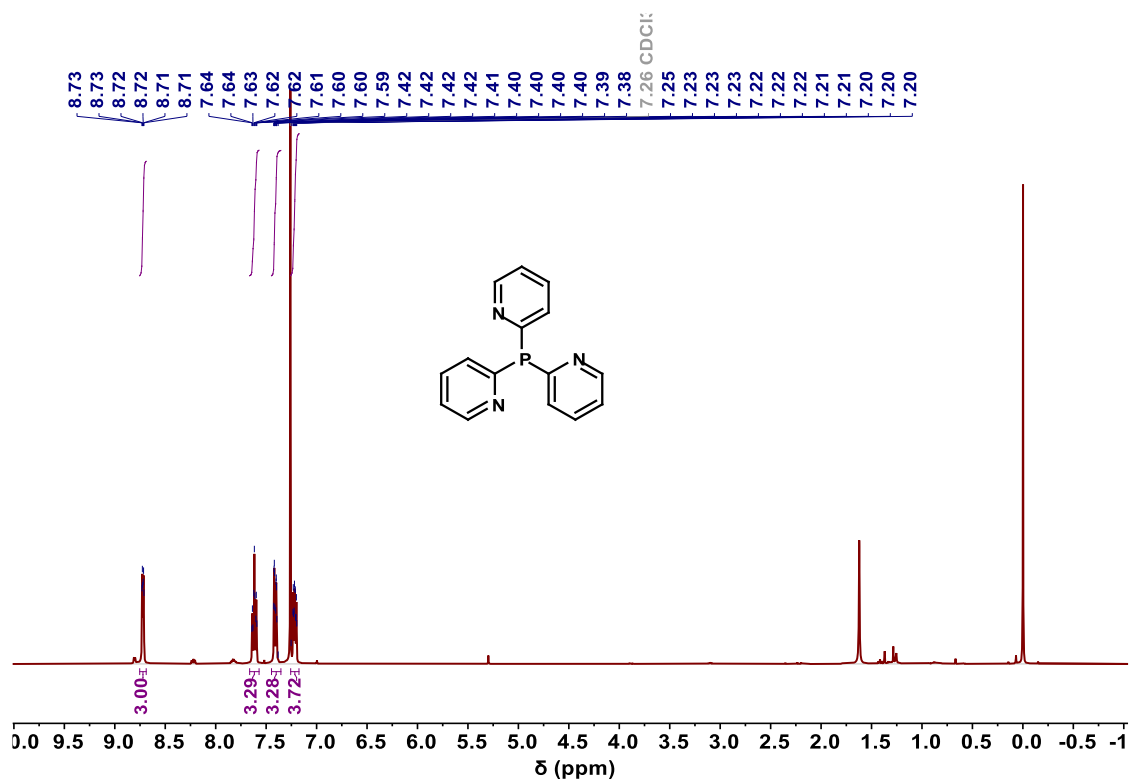


Figure S59. ^1H -NMR spectrum (400 MHz, 298 K, CDCl_3) of **6**.

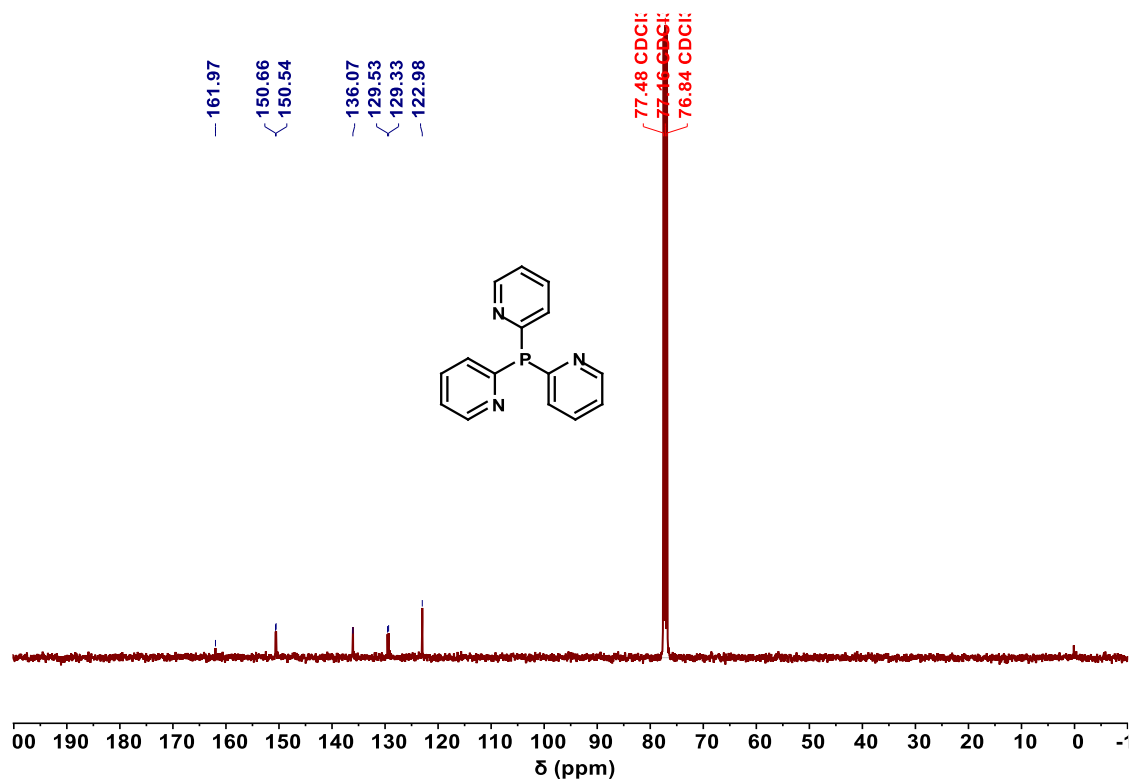


Figure S60. $^{13}\text{C}\{^1\text{H}\}$ -NMR spectrum (101 MHz, 298 K, CDCl_3) of **6**.

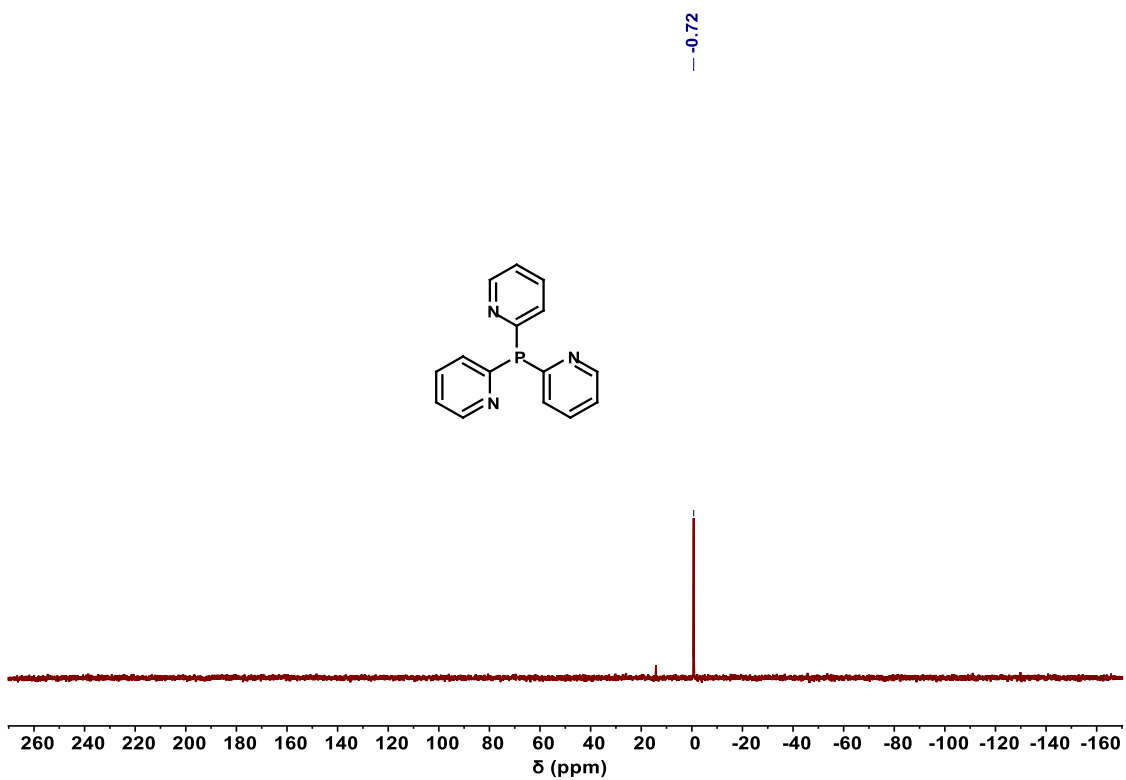


Figure S61. $^{31}\text{P}\{^1\text{H}\}$ -NMR spectrum (162 MHz, 298 K, CDCl_3) of 6.

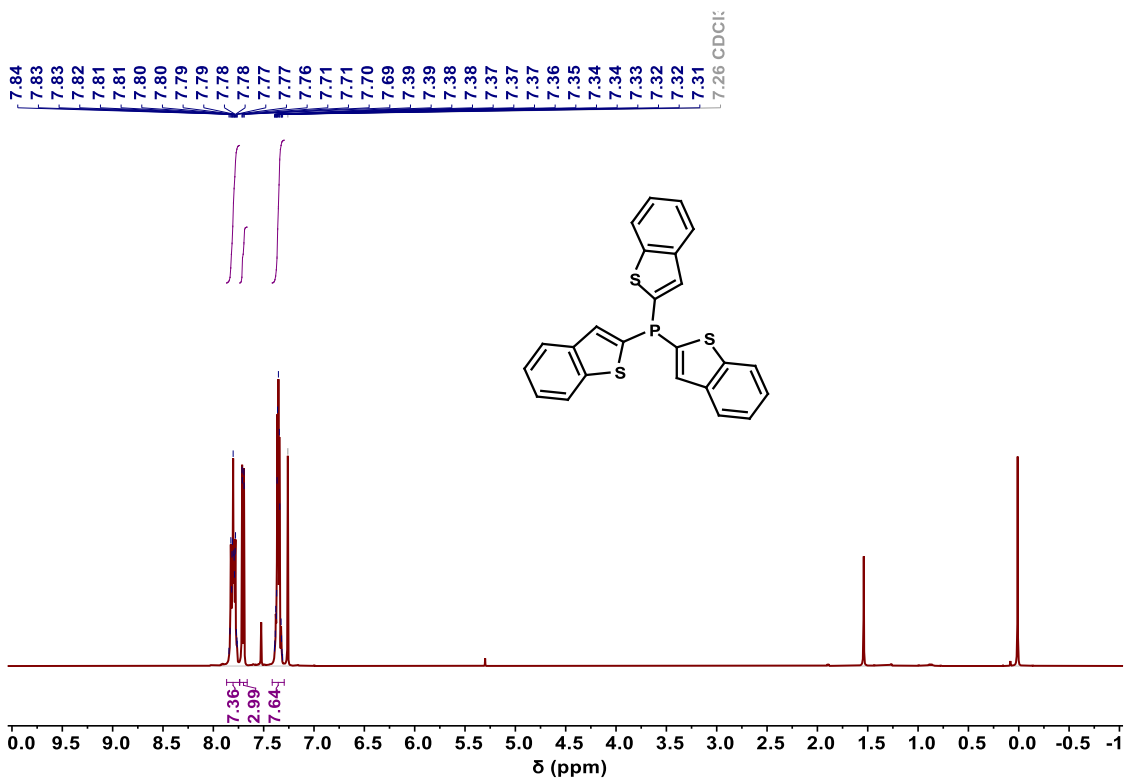


Figure S62. ^1H -NMR spectrum (400 MHz, 298 K, CDCl_3) of 7.

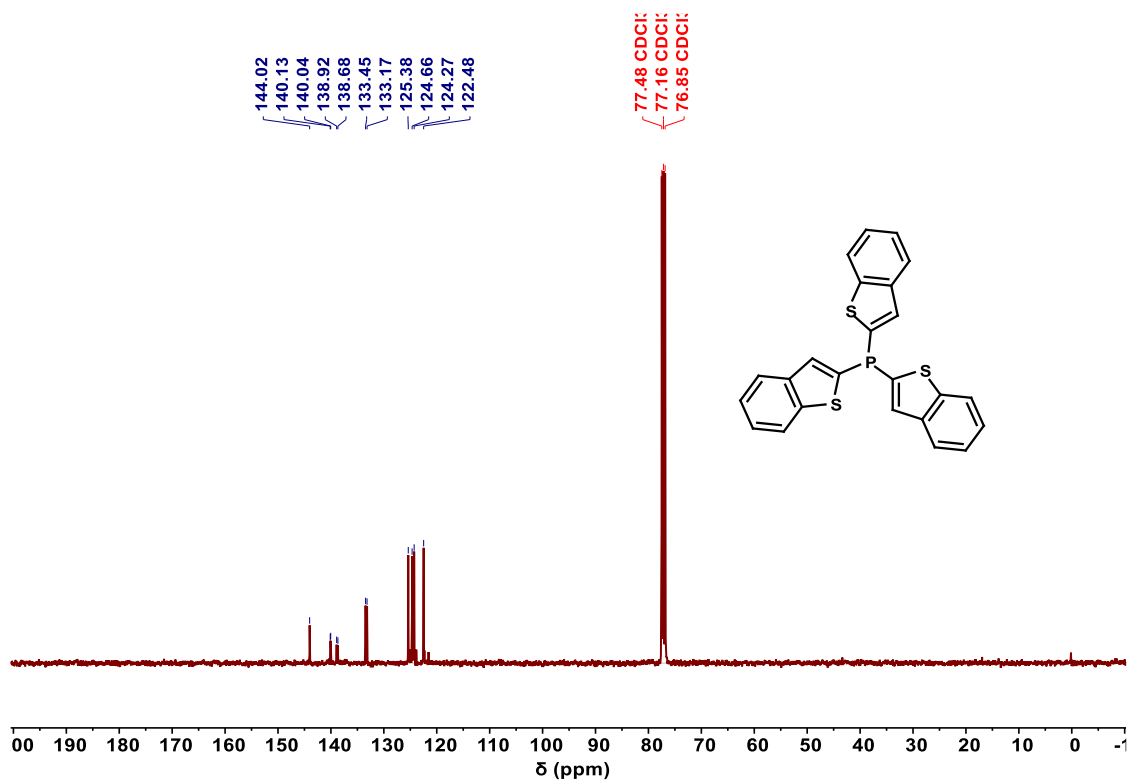


Figure S63. $^{13}\text{C}\{^1\text{H}\}$ -NMR spectrum (101 MHz, 298 K, CDCl_3) of 7.

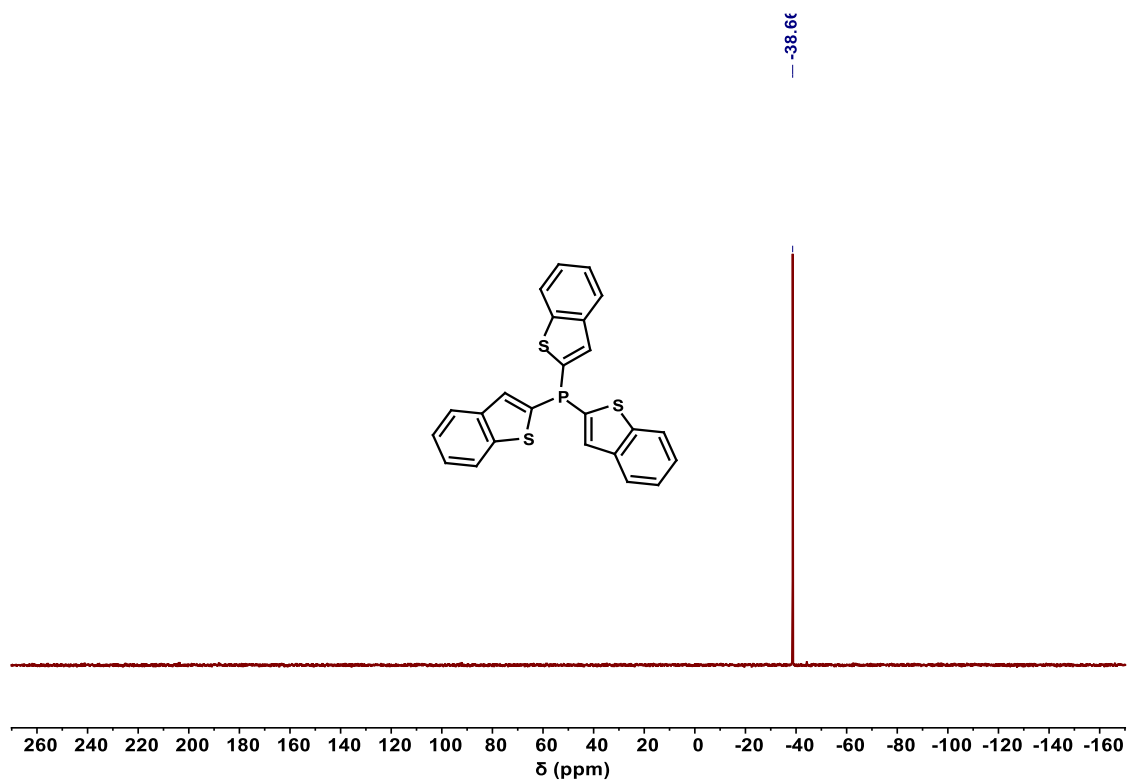


Figure S64. $^{31}\text{P}\{^1\text{H}\}$ -NMR spectrum (162 MHz, 298 K, CDCl_3) of 7.

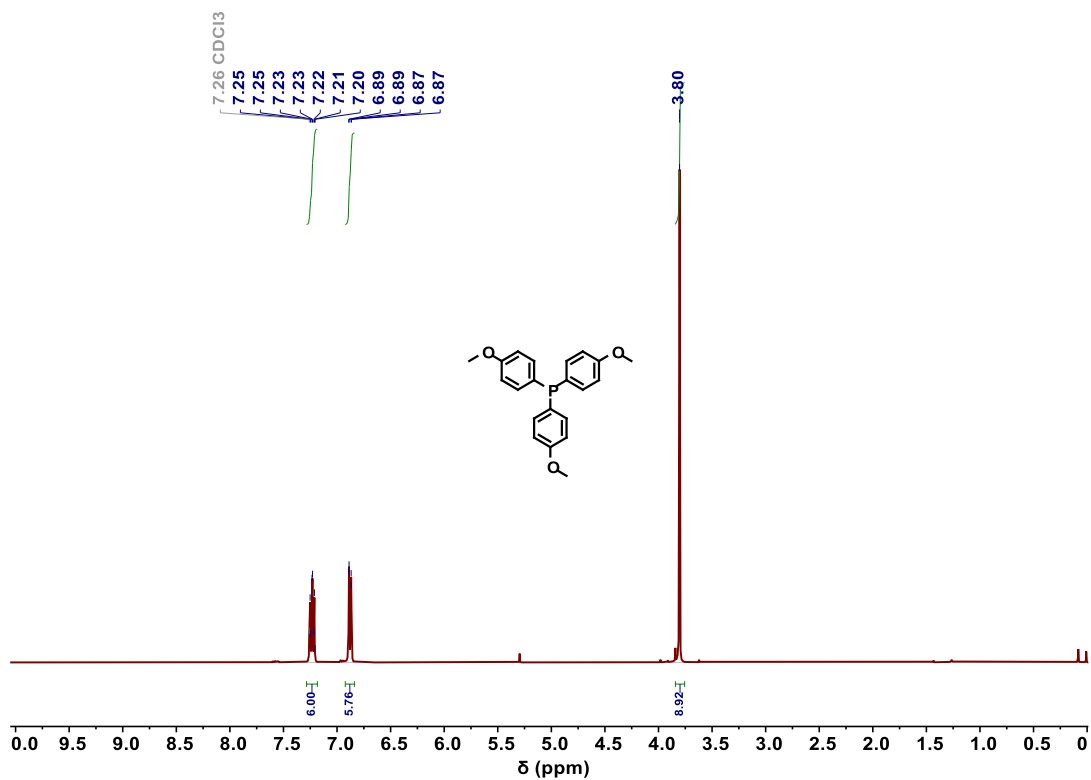


Figure S65. ¹H-NMR spectrum (400 MHz, 298 K, CDCl₃) of **8**.

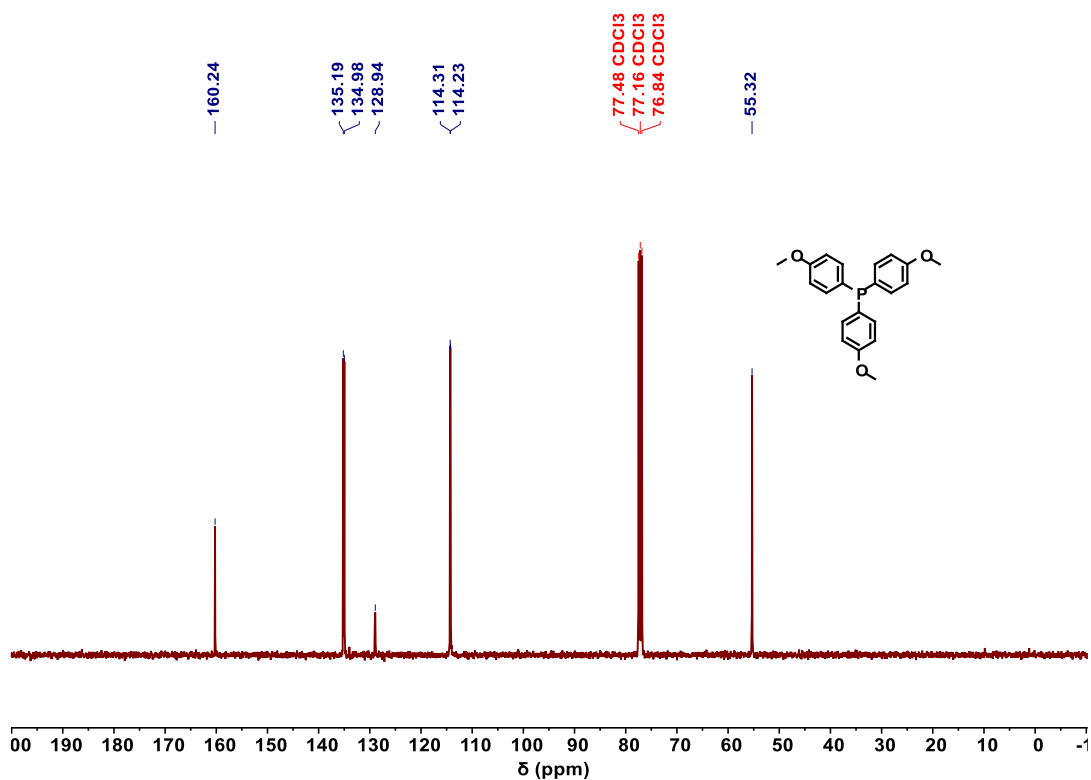


Figure S8. ¹³C{¹H}-NMR spectrum (101 MHz, 298 K, CDCl₃) of **8**.

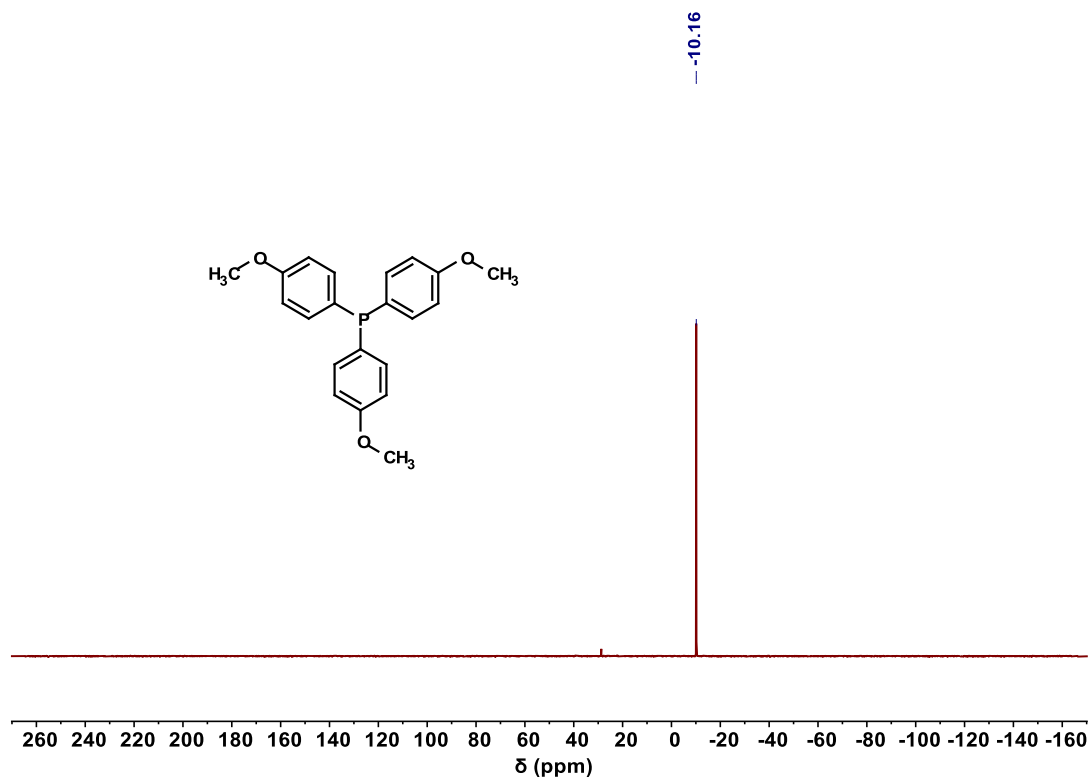


Figure S67. $^{31}\text{P}\{^1\text{H}\}$ -NMR spectrum (162 MHz, 298 K, CDCl_3) of **8**.

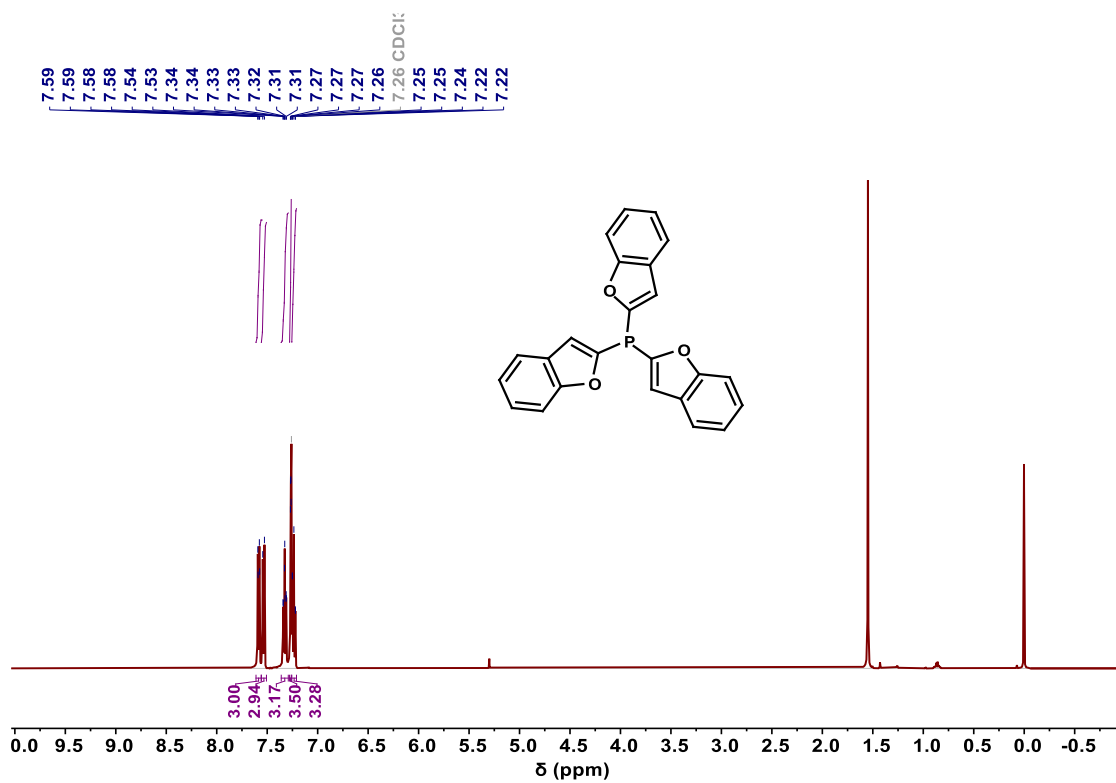


Figure S68. ^1H -NMR spectrum (400 MHz, 298 K, CDCl_3) of **10**.

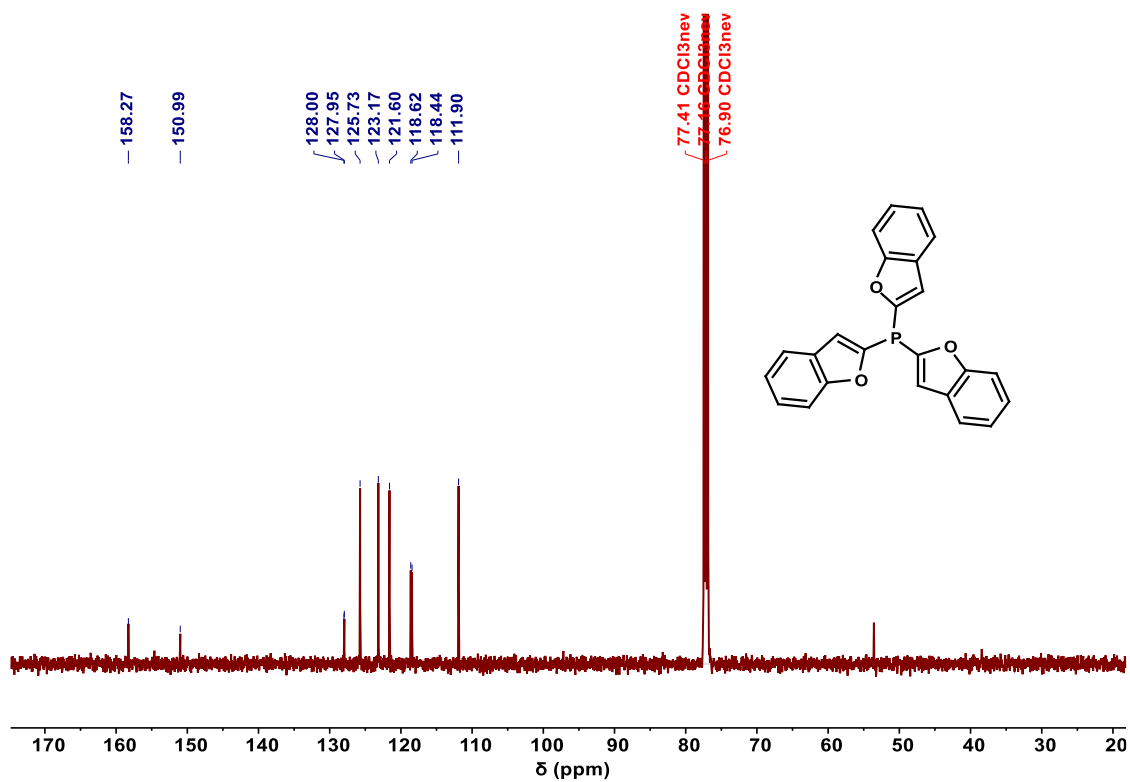


Figure S9. $^{13}\text{C}\{^1\text{H}\}$ -NMR spectrum of **10**.

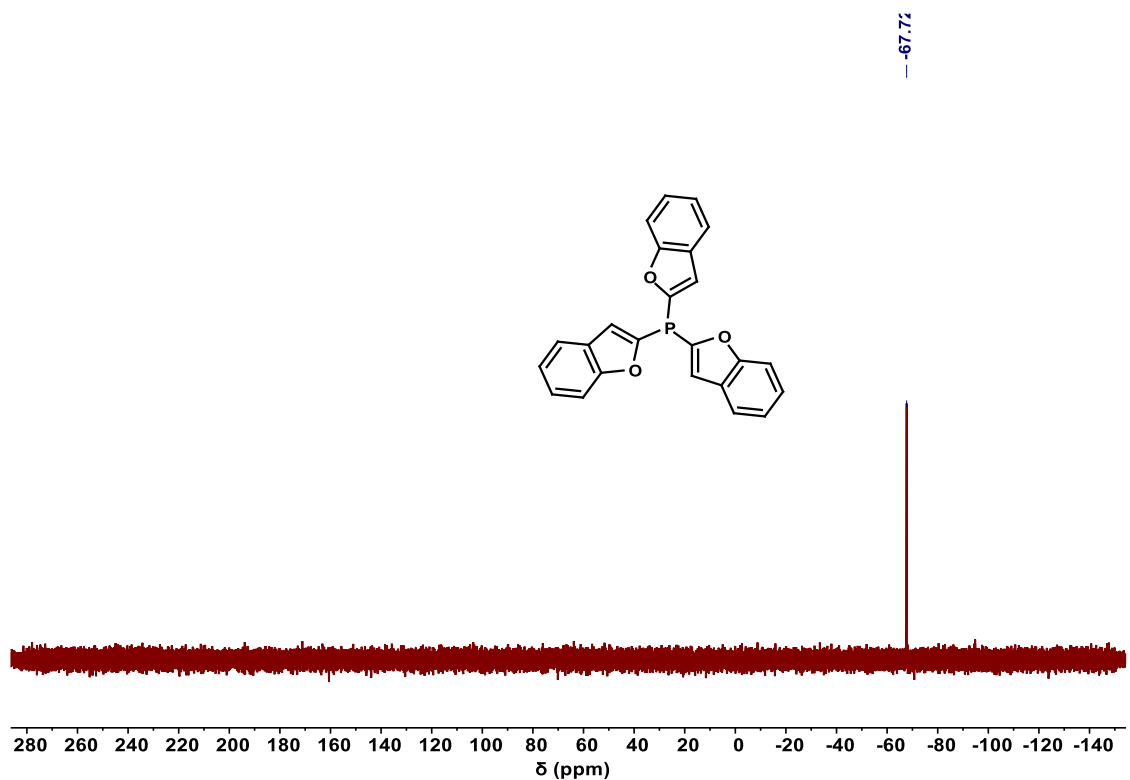


Figure S70. $^{31}\text{P}\{^1\text{H}\}$ -NMR spectrum (162 MHz, 298 K, CDCl₃) of **10**.

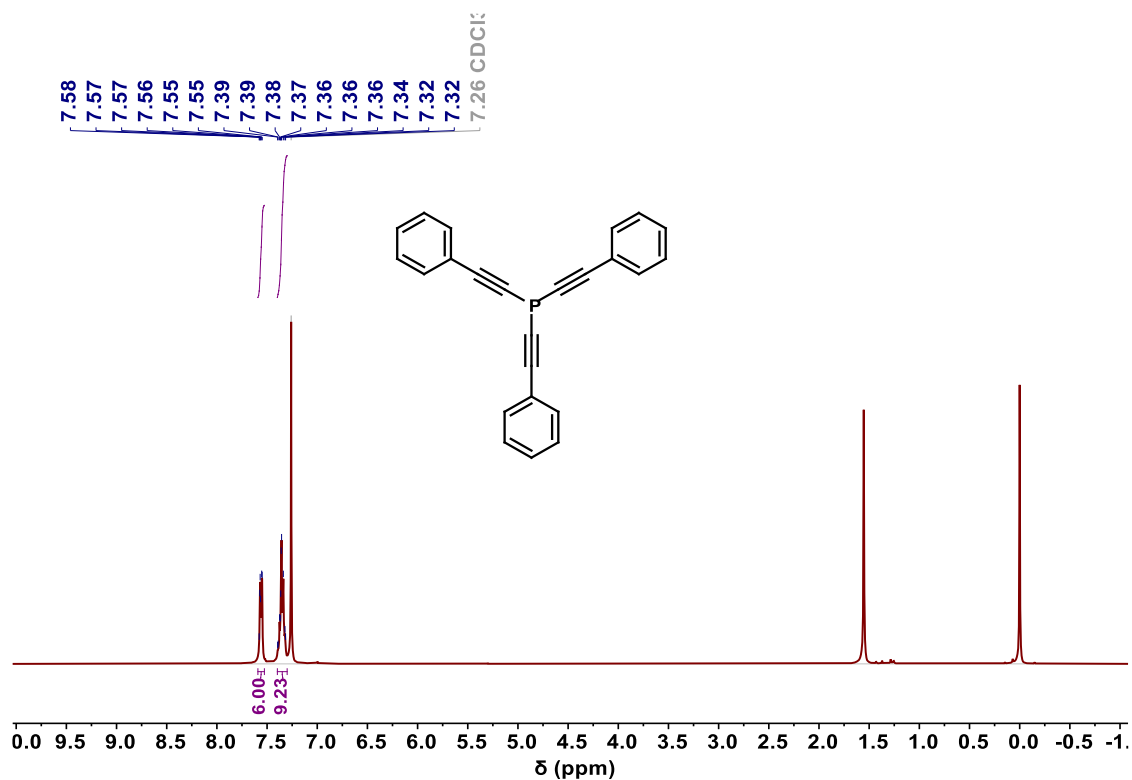


Figure S10. $^1\text{H-NMR}$ spectrum (400 MHz, 298 K, CDCl_3) of **11**.

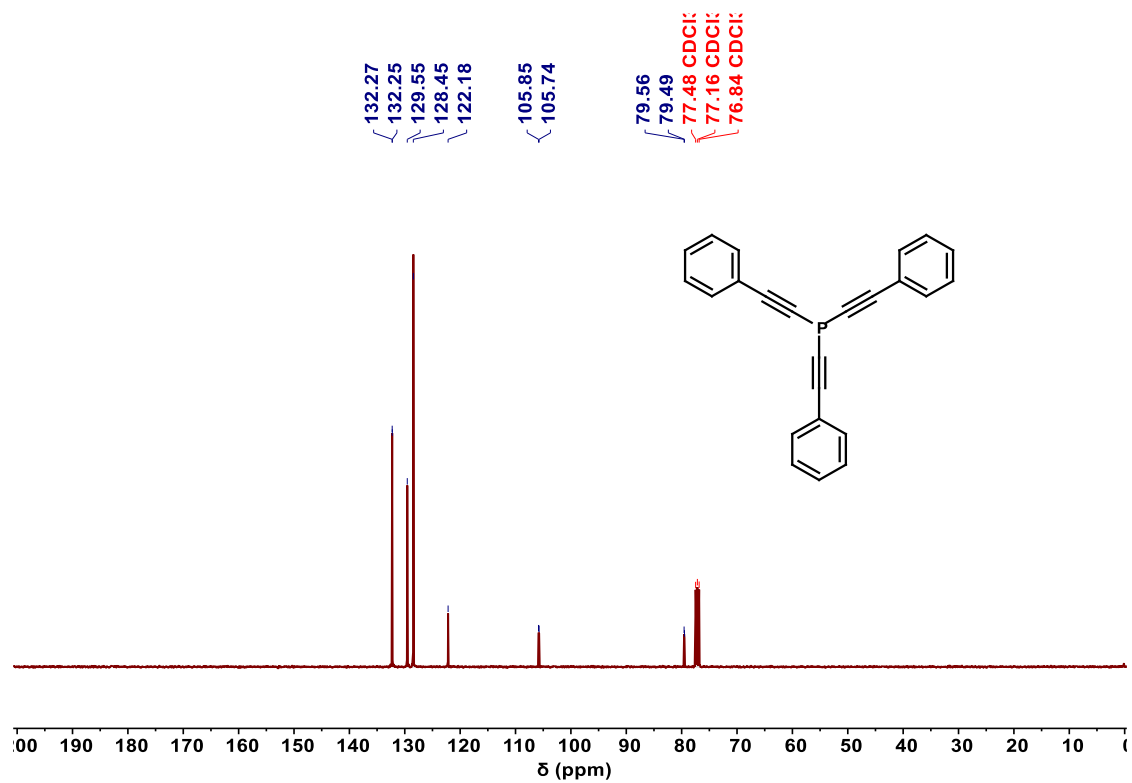


Figure S72. $^{13}\text{C}\{^1\text{H}\}$ -NMR spectrum (101 MHz, 298 K, CDCl_3) of **11**.

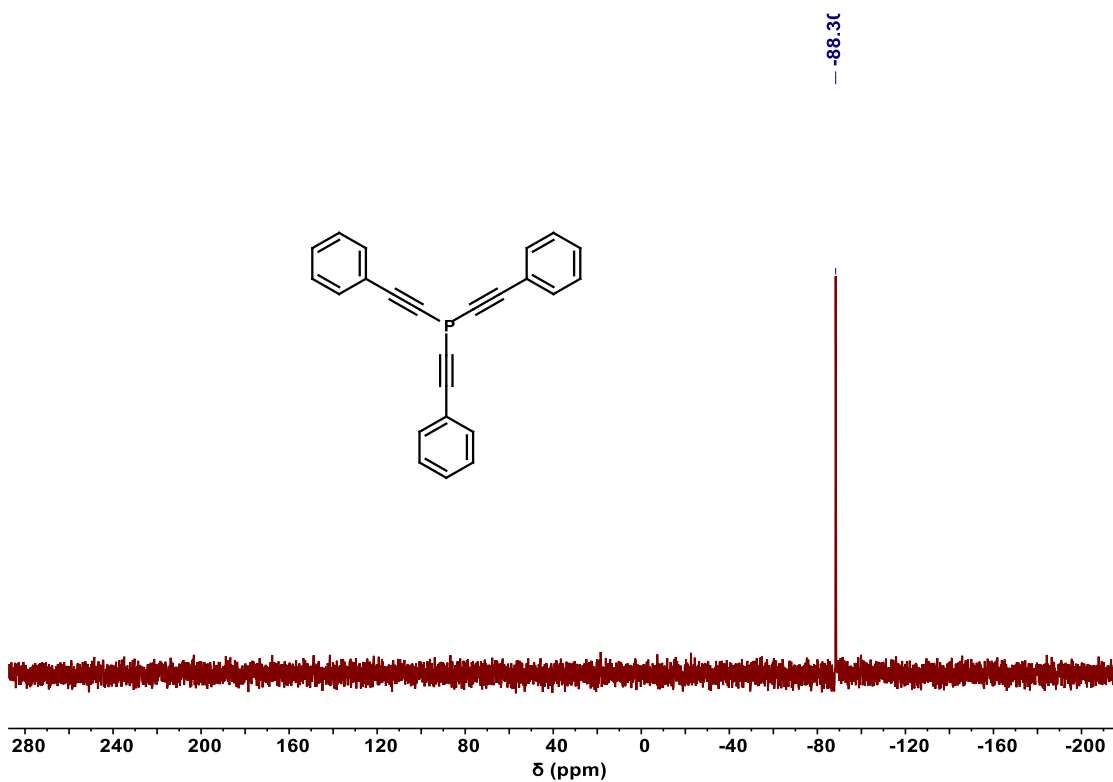


Figure S11. $^{31}\text{P}\{^1\text{H}\}$ -NMR spectrum (162 MHz, 298 K, CDCl_3) of **11**.

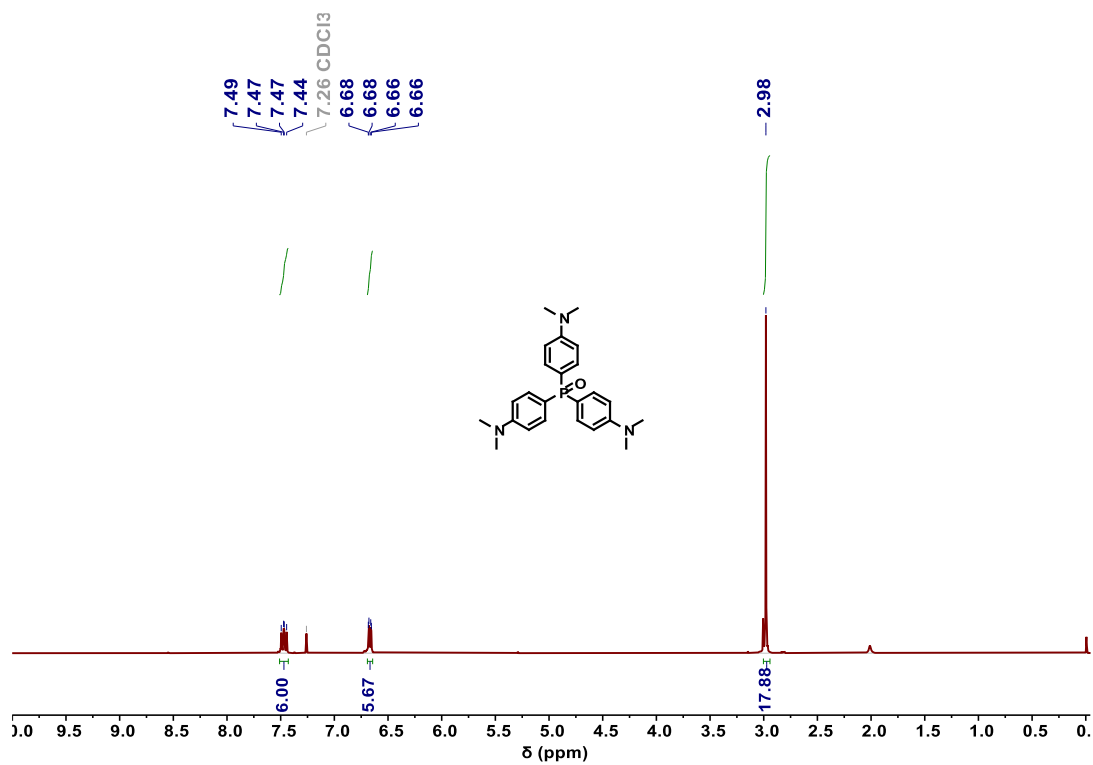


Figure S74. ^1H -NMR spectrum (400 MHz, 298 K, CDCl_3) of **12 oxide**.

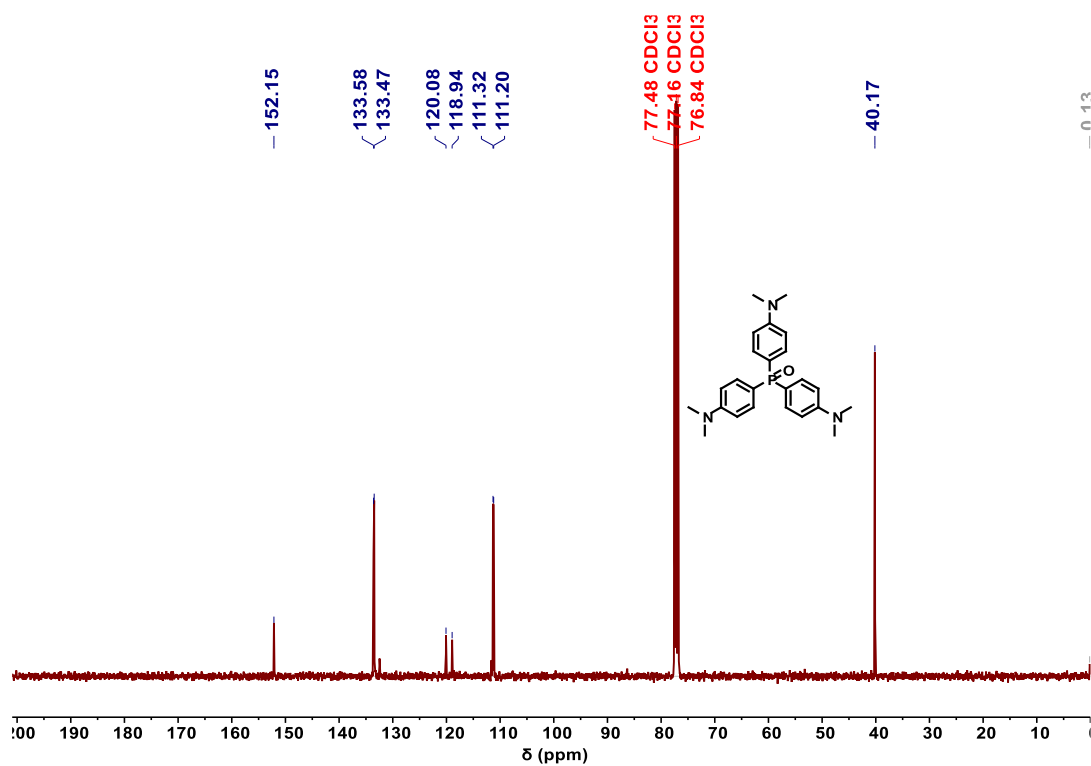


Figure S75. $^{13}\text{C}\{^1\text{H}\}$ -NMR spectrum (101 MHz, 298 K, CDCl_3) of **12** oxide.

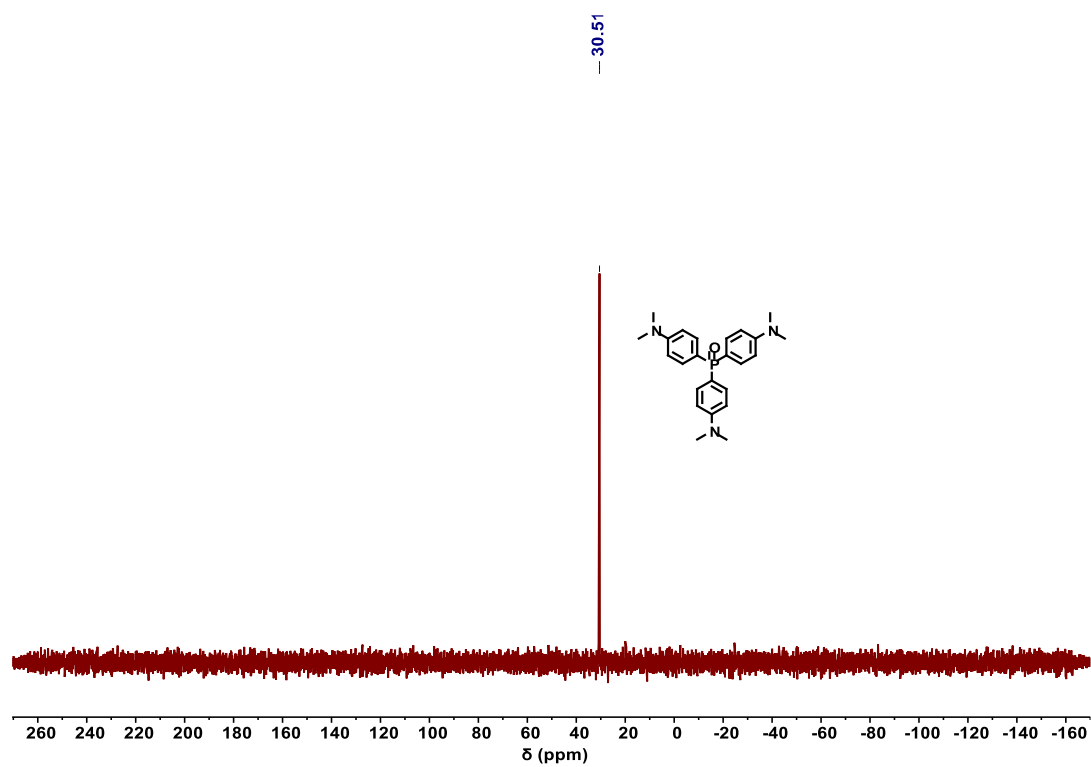


Figure S 76. $^{31}\text{P}\{^1\text{H}\}$ -NMR spectrum (162 MHz, 298 K, CDCl_3) of **12** oxide.

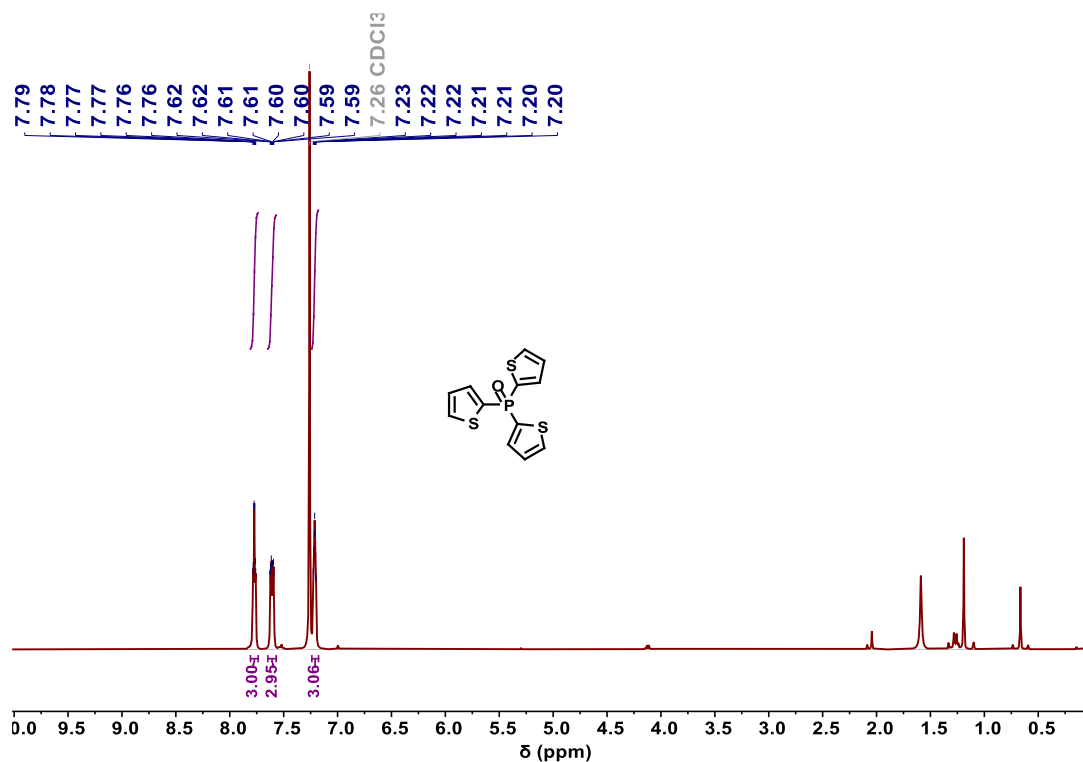


Figure S77. ^1H -NMR spectrum (400 MHz, 298 K, CDCl_3) of tri(thiophen-2-yl)phosphine oxide.

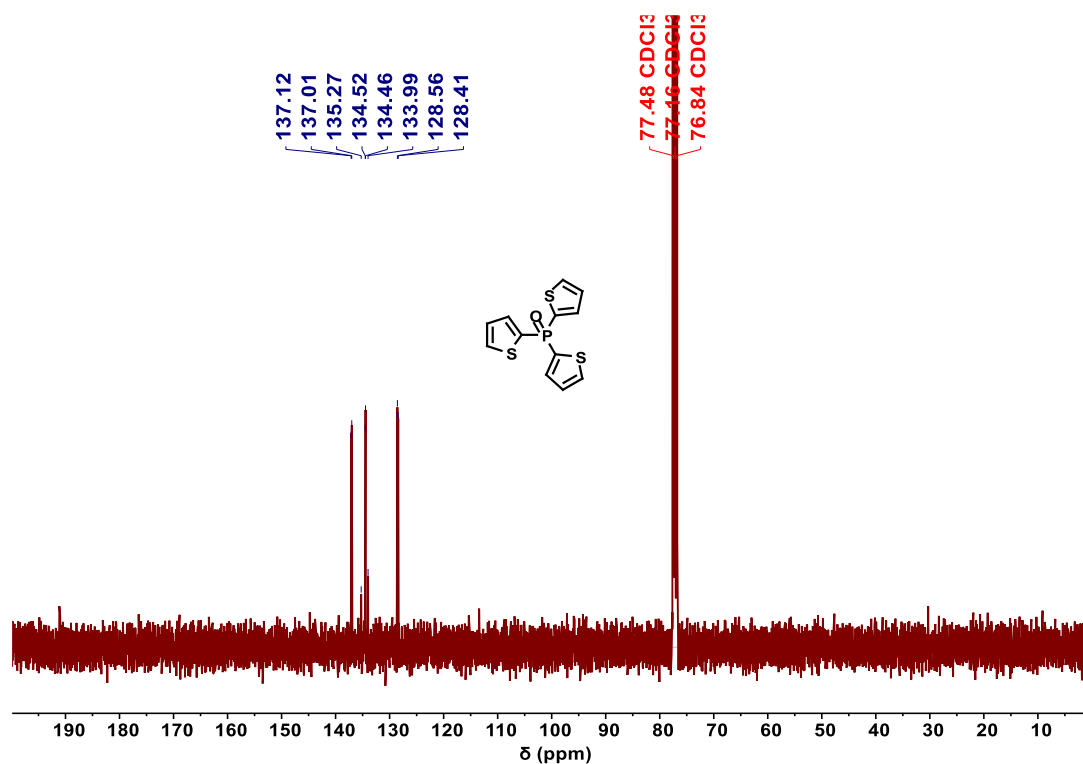


Figure S78. $^{13}\text{C}\{^1\text{H}\}$ -NMR spectrum (101 MHz, 298 K, CDCl_3) of tri(thiophen-2-yl)phosphine oxide.

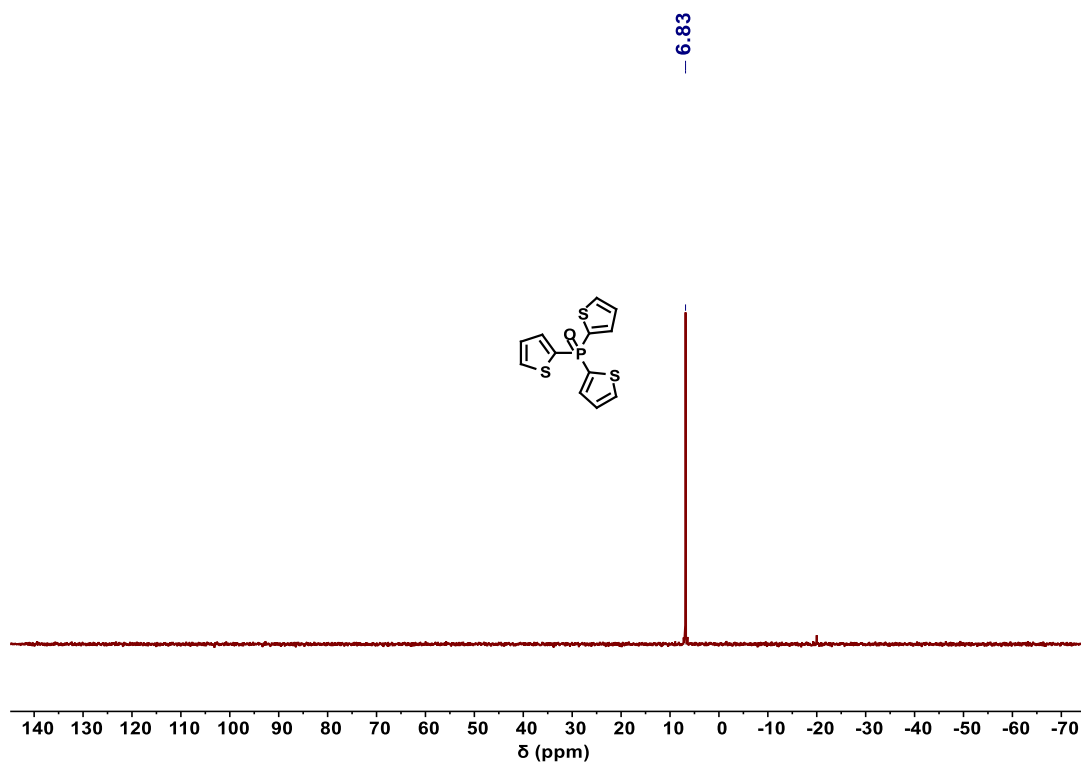


Figure S79. $^{31}\text{P}\{^1\text{H}\}$ -NMR spectrum (162 MHz, 298 K, CDCl_3) of tri(thiophen-2-yl)phosphine oxide.

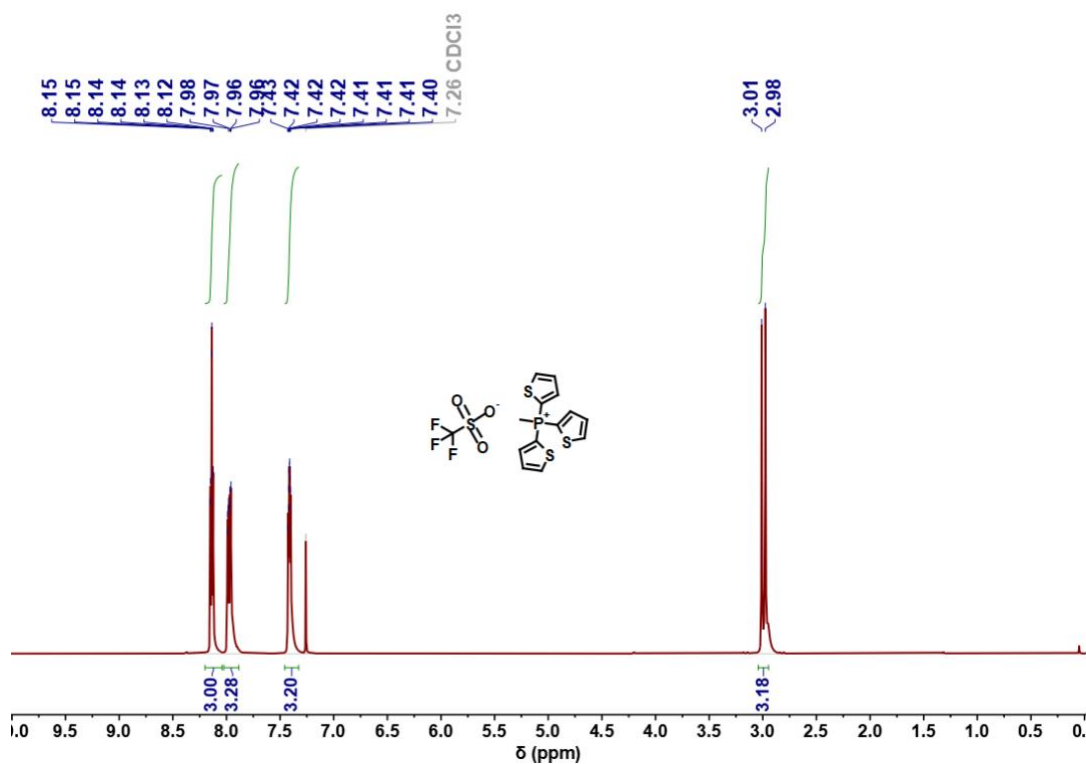


Figure S80. ^1H -NMR spectrum (400 MHz, 298 K, CDCl_3) of methyl-tri(2-thienyl)phosphonium triflate.

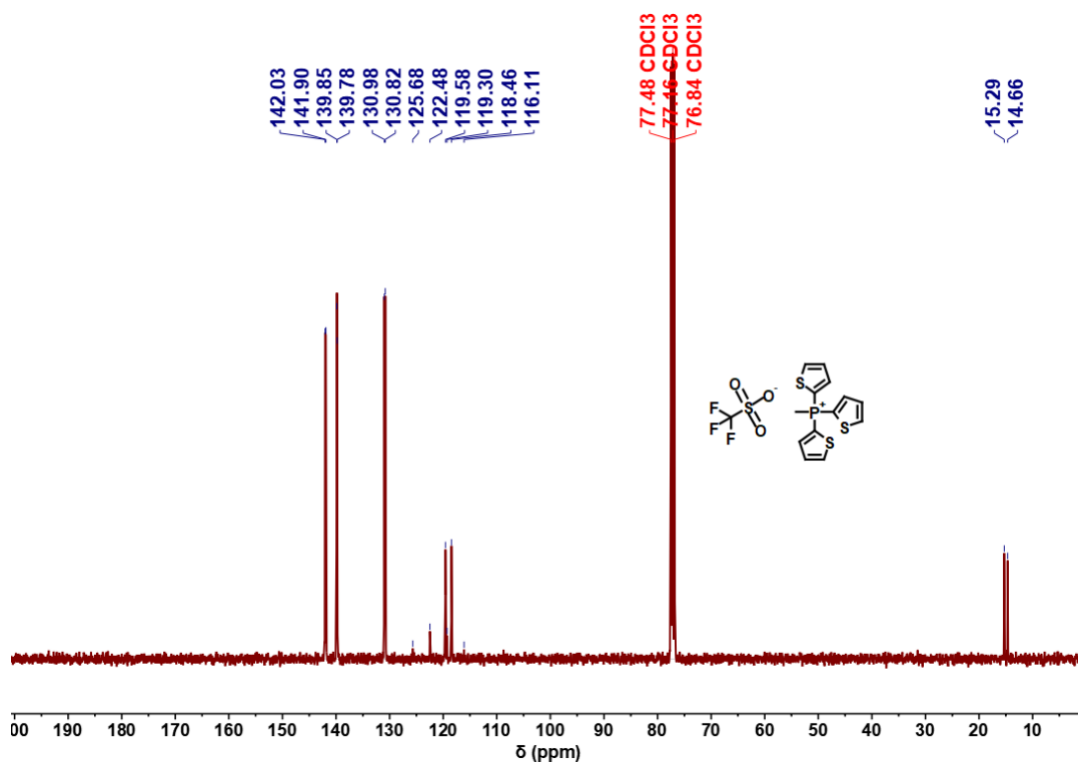


Figure S81. $^{13}\text{C}\{^1\text{H}\}$ -NMR spectrum (101 MHz, 298 K, CDCl_3) of methyl-tri(2-thienyl)phosphonium triflate.

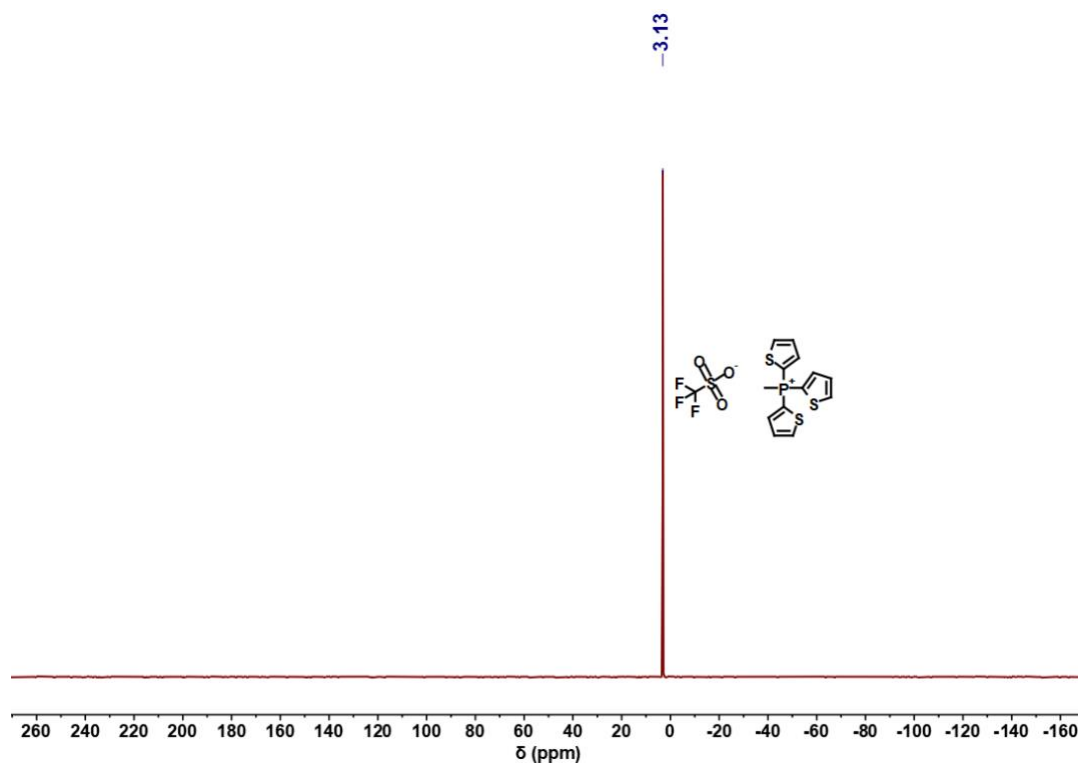


Figure S82. $^{31}\text{P}\{^1\text{H}\}$ -NMR spectrum (162 MHz, 298 K, CDCl_3) of methyl-tri(2-thienyl)phosphonium triflate.

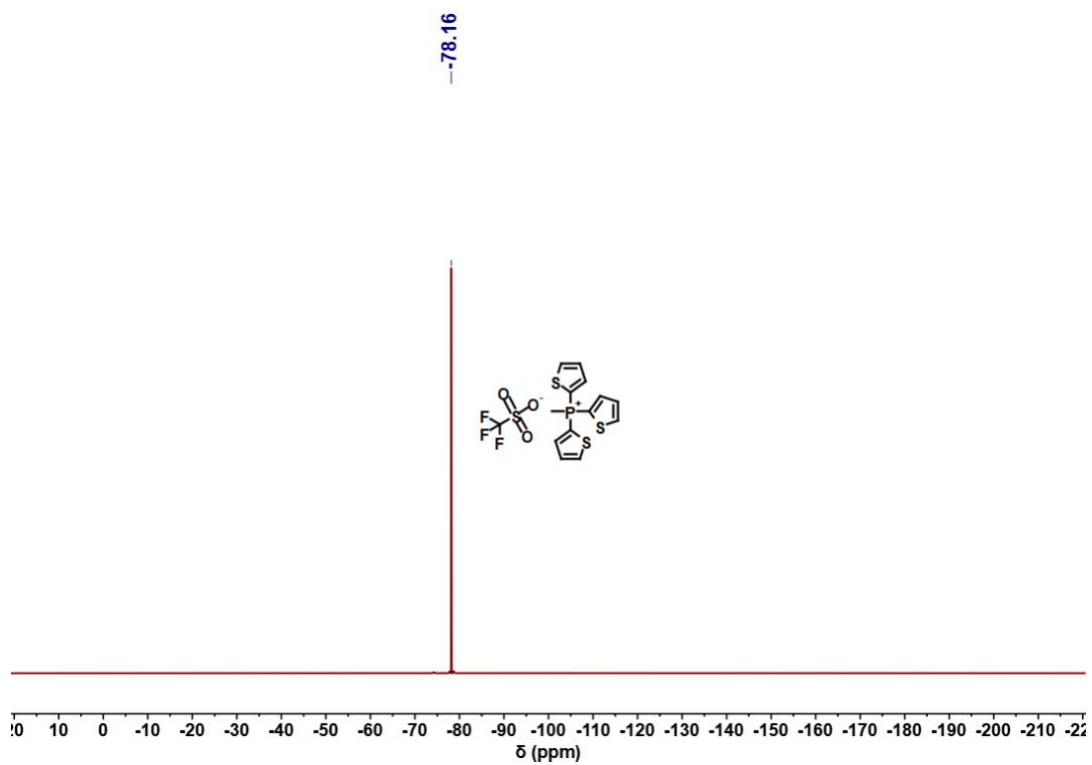


Figure S83. ^{19}F $\{^1\text{H}\}$ -NMR spectrum (376 MHz, 298 K, CDCl_3) of methyl-tri(2-thienyl)phosphonium triflate.

13. References

- (S1) Armarego, W. L. F., Chapter 3 - Purification of Organic Chemicals. In *Purification of Laboratory Chemicals (Eighth Edition)*, Armarego, W. L. F., Ed. Butterworth-Heinemann: **2017**, 95–634.
- (S2) Bura, T.; Leclerc, N.; Fall, S.; Lévêque, P.; Heiser, T.; Retailleau, P.; Rihn, S.; Mirloup, A.; Ziessel, R. High-Performance Solution-Processed Solar Cells and Ambipolar Behavior in Organic Field-Effect Transistors with Thienyl-BODIPY Scaffoldings. *J. Am. Chem.Soc.* **2012**, *134*, 17404–17407.
- (S3) Pinhey, J. T.; Roche, E. G. The chemistry of organolead(IV) tricarboxylates. Synthesis and electrophilic heteroarylation reactions of 2- and 3-thienyl-, and 2- and 3-furyl-lead tricarboxylates. *J. Chem. Soc., Perkin Trans.* **1988**, 2415–2421.
- (S4) Denat, F.; Gaspard-Illoughmane, H.; Dubac, J. Pyrrolyl compounds of main group elements. Synthesis of group 14 5-metallated pyrrole-2-carbaldehydes. *J. Organometallic Chem.* **1992**, *423*, 173–182.
- (S5) Mallet, C.; Didane, Y.; Watanabe, T.; Yoshimoto, N.; Allain, M.; Videlot-Ackermann, C.; Frère, P. Electronic Properties and Field-Effect Transistors of Oligomers End-Capped with Benzofuran Moieties. *ChemPlusChem* **2013**, *78*, 459–466.
- (S6) Mao, S.; Chen, Z.; Wang, L.; Khadka, D. B.; Xin, M.; Li, P.; Zhang, S. Q. Synthesis of Aryl Trimethylstannane via BF₃.OEt₂-Mediated Cross-Coupling of Hexaalkyl Distannane Reagent with Aryl Triazine at Room Temperature. *J. Org. Chem.* **2019**, *84*, 463–471.
- (S7) Tsai, C. H.; Chirdon, D. N.; Maurer, A. B.; Bernhard, S.; Noonan, K. J. Synthesis of thiophene 1,1-dioxides and tuning their optoelectronic properties. *Org. Lett.* **2013**, *15*, 5230–5233.
- (S8) Rudebusch, G. E.; Zakharov, L. N.; Liu, S. Y. Rhodium-catalyzed boron arylation of 1,2-azaborines. *Angew Chem Int. Ed.* **2013**, *52*, 9316–9319.
- (S9) Banwell, M. G.; Collis, M. P.; Crisp, G. T.; Lambert, J. N.; Reum, M. E.; Scoble, J. A. The palladium-mediated cross-coupling of bromotropolones with organostannanes; application to concise syntheses of β -dolabrin, β -thujaplicin, 7-methoxy-4-isopropyltropolone, and β -thujaplicinol. *J. Chem. Soc., Chem. Commun.* **1989**, 616–617.
- (S10) Anderson, G. K.; Lumetta, G. J. Reactions of diphosphineplatinum(II) oxalate complexes with phenylacetylene. Formation of phenylalkynylplatinum complexes. *J. Organometallic Chem.* **1985**, *295*, 257–264.
- (S11) Kotani, S.; Shiina, K.; Sonogashira, K. Synthesis and properties of 2- or 2,5-substituted thiophene and 2- or 2,5'-substituted dithiophene derivatives of platinum. *J. Organometallic Chem.* **1992**, *429*, 403–413.
- (S12) Zhang, X.; Yao, J.; Zhan, C., Synthesis and photovoltaic properties of low bandgap dimeric perylene diimide based non-fullerene acceptors. *Science China Chemistry* **2016**, *59*, 209–217.
- (S13) Tolmachev, A. A.; Ivonin, S. P.; Pinchuk, A. M. Phosphorylation of five-membered aromatic heterocycles with phosphorus tribromide. *Heteroatom Chem.* **1995**, *6*, 407–412.
- (S14) Du, T.; Wang, B.; Wang, C.; Xiao, J.; Tang, W. Cobalt-catalyzed asymmetric hydrogenation of ketones: A remarkable additive effect on enantioselectivity. *Chinese Chemical Letters* **2021**, *32*, 1241–1244.
- (S15) Allen, D. W.; Hutley, B. G.; Mellor, M. T. J., The chemistry of heteroarylphosphorus compounds. Part VI. Alkaline hydrolysis of 1-methylpyrrol-2-yl- and 1-methylpyrrol-2-yl-methyl-phosphonium salts. A comparison with 2-furyl, 2-thienyl, phenyl, and related heteroarylmethyl and benzyl derivatives. Relative stabilities of forming carbanions. *J. Chem. Soc., Perkin Trans.* **1974**, *2*, 1690–1694.

- (S16) Rommel, S.; Belger, C.; Begouin, J.-M.; Plietker, B. Dual [Fe+Phosphine] Catalysis: Application in Catalytic Wittig Olefination. *ChemCatChem* **2015**, *7*, 1292–1301.
- (S17) Trofimov, B. A.; Artem'ev, A. V.; Malysheva, S. F.; Gusarova, N. K.; Belogorlova, N. A.; Korocheva, A. O.; Gatilov, Y. V.; Mamatyuk, V. I. Expedient one-pot organometallics-free synthesis of tris(2-pyridyl)phosphine from 2-bromopyridine and elemental phosphorus. *Tetrahedron Lett.* **2012**, *53*, 2424–2427.
- (S18) Lloret, J.; Estevan, F.; Lahuerta, P.; Hirva, P.; Perez-Prieto, J.; Sanau, M. Dirhodium(II) compounds with bridging thienylphosphines: studies on reversible P,C/P,S coordination. *Chemistry* **2009**, *15*, 7706–7716.
- (S19) Arockiam, P. B.; Lennert, U.; Graf, C.; Rothfelder, R.; Scott, D. J.; Fischer, T. G.; Zeitler, K.; Wolf, R. Versatile Visible-Light-Driven Synthesis of Asymmetrical Phosphines and Phosphonium Salts. *Chemistry* **2020**, *26*, 16374–16382.
- (S20) Beletskaya, I. P.; Afanasiev, V. V.; Kazankova, M. A.; Efimova, I. V. New approach to phosphinoalkynes based on Pd- and Ni-catalyzed cross-coupling of terminal alkynes with chlorophosphanes. *Org. Lett.* **2003**, *5*, 4309–4311.
- (S21) Morosaki, T.; Wang, W.-W.; Nagase, S.; Fujii, T. Synthesis, Structure, and Reactivities of Iminosulfane- and Phosphane-Stabilized Carbenes Exhibiting Four-Electron Donor Ability. *Chemistry – A European Journal* **2015**, *21*, 15405–15411.
- (S22) Vicente, V.; Fruchier, A.; Taillefer, M.; Combes-Chamalet, C.; Scowen, I. J.; Plénat, F.; Cristau, H.-J. Synthesis and structural studies (¹H,¹³C,³¹P NMR and X-ray) of new C-bonded cyclotriphosphazenes with heterocyclic substituents from novel phosphinic acid derivatives. *New J. Chem.* **2004**, *28*, 418–424.
- (S23) M. J. Frisch, G. W. T., H. B. Schlegel, G. E. Scuseria, M. A. Robb, J. R. Cheeseman, G. Scalmani, V. Barone, B. Mennucci, G. A. Petersson, H. Nakatsuji, M. Caricato, X. Li, H. P. Hratchian, A. F. Izmaylov, J. Bloino, G. Zheng, J. L. Sonnenberg, M. Hada, M. Ehara, K. Toyota, R. Fukuda, J. Hasegawa, M. Ishida, T. Nakajima, Y. Honda, O. Kitao, H. Nakai, T. Vreven, J. A. Montgomery, Jr., J. E. Peralta, F. Ogliaro, M. Bearpark, J. J. Heyd, E. Brothers, K. N. Kudin, V. N. Staroverov, R. Kobayashi, J. Normand, K. Raghavachari, A. Rendell, J. C. Burant, S. S. Iyengar, J. Tomasi, M. Cossi, N. Rega, J. M. Millam, M. Klene, J. E. Knox, J. B. Cross, V. Bakken, C. Adamo, J. Jaramillo, R. Gomperts, R. E. Stratmann, O. Yazyev, A. J. Austin, R. Cammi, C. Pomelli, J. W. Ochterski, R. L. Martin, K. Morokuma, V. G. Zakrzewski, G. A. Voth, P. Salvador, J. J. Dannenberg, S. Dapprich, A. D. Daniels, Ö. Farkas, J. B. Foresman, J. V. Ortiz, J. Cioslowski, and D. J. Fox *Gaussian 09*, Gaussian, Inc.: Wallingford, CT, **2009**.
- (S24) Lee, C. T.; Yang, W. T.; Parr, R. G. Development of the Colle-Salvetti correlation-energy formula into a functional of the electron density, *Phys. Rev. B* **1988**, *37*, 785–789.

- (S25) Becke, A. D. Density-functional thermochemistry. III. The role of exact exchange *J. Chem. Phys.* **1993**, *98*, 5648–5652.
- (S26) Miehlich, B.; Savin, A.; Stoll, H.; Preuss, H. Results obtained with the correlation energy density functionals of Becke and Lee, Yang and Parr, *Chem. Phys. Lett.* **1989**, *157*, 200–206.
- (S27) Dunning, T. H., Jr.; Hay, P. J. In *Modern Theoretical Chemistry*; Schaefer, H. F., III, Ed.; Plenum: New York, **1976**; Vol. 3.
- (S28) Leininger, T.; Nicklass, A.; Stoll, H.; Dolg, M.; Schwerdtfeger, P. J. The accuracy of the pseudopotential approximation. II. A comparison of various core sizes for indium pseudopotentials in calculations for spectroscopic constants of InH, InF, and InCl, *Chem. Phys.* **1996**, *105*, 1052–1059.
- (S29) Lu, T.; Chen, Q. Shermo: A general code for calculating molecular thermochemistry properties *Comput. Theor. Chem.* **2021**, *1200*, 113249.
- (S30) Roy Dennington, T. A. K., and John M. Millam *GaussView*, 6; Semichem Inc: Shawnee Mission, KS, **2016**.